UNIVERSITA' DEGLI STUDI DI NAPOLI

"FEDERICO II"

DOTTORATO DI RICERCA IN "SCIENZA DEL FARMACO"

XXII CICLO 2006-2009

ANTIMALARIAL MARINE ENDOPEROXIDES. ISOLATION, SYNTHESIS, AND INVESTIGATION ON THE MECHANISM OF ACTION

Dott. Fernando Scala

Tutor

Prof. O. Taglialatela-Scafati

Coordinatore

Prof.ssa M. V. D'Auria

INDEX

CHAPTER 1 – THE MARINE POTENTIAL

1.1. Chemistry in the oceans

More than 60% of the earth's biosphere is made up by oceans, which represent an endless source of compounds with interesting pharmacological activity.[1] The remarkable biodiversity within the marine environment is guaranteed by the coexistence of an enormous number of species, which interact with each other and with the environment in different ways. In this process, chemistry plays an essential role: all the marine organisms synthesize or obtain from symbiotic microorganisms "secondary metabolites", molecules with even very complex structures, which are characteristic of specific species or specific taxa. Many secondary metabolites are involved in the interactions within or between species. Considering the number of different species and their immeasurable possible interactions, it's not a surprise that a wide variety of secondary metabolites are produced to preserve and improve the life of the producing organisms.

It's very well known that plants are particularly rich in secondary metabolites, and their properties have been long exploited for the treatment of diseases. In the last decades, the progress in some technologies and the wider availability of diving equipment made it possible to extend this research to marine organisms.

A larger number of organisms and less genetic homogeneity between separate populations of the same species exist in the marine compared to the terrestrial environment. This results in a higher structural diversity at the molecular level. Among

marine organisms, the chance of finding bioactive compounds is remarkably higher in some invertebrates, like corals, tunicates, and sponges. Many of these compounds are involved in the chemical defence of these organisms, essential for their survival since they are sessile organisms often lacking any physical defence from the predators.

Even when showing interesting and specific pharmacological activities, natural compounds isolated from marine organisms rarely raise the interest of pharmaceuticals companies, because they are difficult to obtain in sufficient amounts for clinical use. Total synthesis is a possible way to overcome this problem, but this option is usually prevented by the complex structure of many natural products, often including many chiral centers, which make the chemical synthesis particularly challenging and this option economically unfeasible.

In this case, tapping the natural source is the best option. The problem is to conciliate development dynamics necessary for man and protection of the marine environment and biodiversity. Oceans are showing increasing signs of overexploitation and degradation, resulting in loss of both productivity and biodiversity. In this context, a massive collection of marine organisms producing compounds of industrial interest appears unrealistic. Alternative approaches have therefore been proposed, such as the cultivation of the organism of interest under controlled conditions (aquaculture), and the laboratory production of metabolites in bioreactors from cell cultures. A more recent approach, which, in the light of the explosive development of molecular biotechnologies is rapidly gaining a prominent position worldwide, is the study of the metabolic processes leading to the synthesis of secondary metabolites. The understanding of these processes at the genetic level is paving the way to the possibility to control them, and eventually to

produce the desired metabolites in large scale using a "green technology" such as gene cloning.

The research work described in this PhD Thesis was performed at the Dipartimento di Chimica delle Sostanze Naturali of Università di Napoli "Federico II", and was addressed to different aspects of the research on marine natural products. On one hand, part of the research was directed to the "core activity" of natural product chemistry, i.e. isolation and structure elucidation of new compounds from marine organisms (produced by their symbiotic microorganisms?). In this respect, particular attention was paid to metabolites isolated from the marine sponges *Plakortis simplex,*[1,2] *Plakortis sp.* and *Theonella swinhoei*.[3]

On the other hand, a new research project was started up and focused on the synthesis of endoperoxide derivatives based on the plakortin scaffold. Plakortin is an endoperoxide polyketide with interesting antimalarial properties which was isolated from the marine sponge *Plakortis simplex* and is probably produced by an uncultivable symbiotic microorganism of the sponge.

1.2. Porifera

Marine sponges (Porifera) have been the only object of the chemical investigation carried out during my Ph.D., and described in this thesis.

Porifera constitute the simplest and most ancient phylum among metazoans. They are ubiquitous animals and live permanently attached to a location in the water. There are from 5,000 to 10,000 known species of sponges. Most sponges live in salt water; only about 150 species live in fresh water. Their body consists of specialized tube-like cells called porocytes which control channels leading to the interior of mesohyl (ostia).

Mesohyl is the gelatinous matrix within the sponge made of collagen and covered by choanocytes, cylindrical flagellated cells. The outer layer is formed by pinacocytes, plate-like cells which digest food particles too large to enter the ostia.

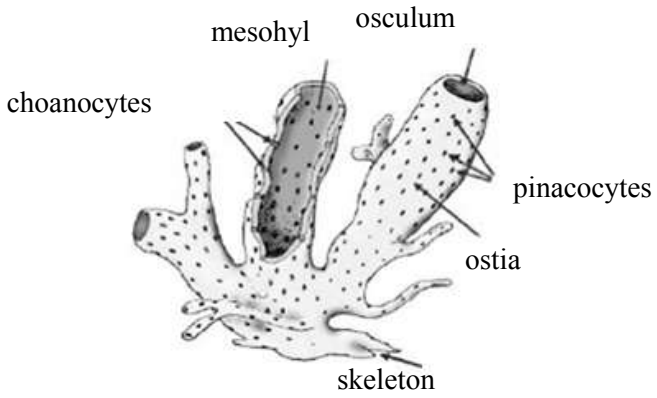

Figure 1.1. A sponge body structure

The body is reinforced by the skeleton, collagen fibers and spicules: Calcareous sponges produce spicules made of silica calcium carbonate while the larger class (90%) of Demonspongiae produce a special form of collagen called spongin besides silica spicules; glass sponges, common in polar water and in the depths of temperate and tropical seas contain synctia in their structure which enable them to extract food from these resource-poor waters with the minimum of effort. Sponges are filters feeders; they obtain nourishment, tiny and floating organic particles, plankton and oxygen from flowing water that they filter through their body. Water flows into a sponge through porocytes and flows out of it through large opening called oscula. The flowing water also carries out waste products.

The simplest body structure in sponges is a tube or vase shape known as asconoid; in siconoids the body wall is pleated and the pumping capacity is increased; leuconoids

contain a network of chambers lined with choanocytes and connected to each other and to the water intakes and outlet by tubes.

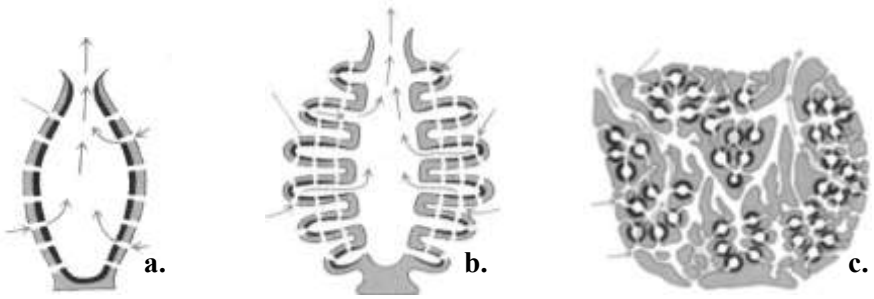

Figure 1.2: Sponge classification: **a.** asconoid; **b**. siconoids; **c.** leuconoids

Most sponges are hermaphrodites (each adult can act as either the female or the male in reproduction). Fertilization is internal in most species; some released sperm randomly float to another sponge with the water current. If a sperm is caught by another sponge's collar cells (choanocytes), fertilization of an egg by the travelling sperm takes place inside the sponge. The resulting tiny larva is released and is free-swimming; it uses tiny cilia (hairs) to propel itself through the water. The larva eventually settles on the sea floor, becomes sessile and grows into an adult.

Some sponges also reproduce asexually; fragments of their body (buds) are broken off by water currents and carried to another location, where the sponge will grow into a clone of the parent sponge (its DNA is identical to the parent's DNA).

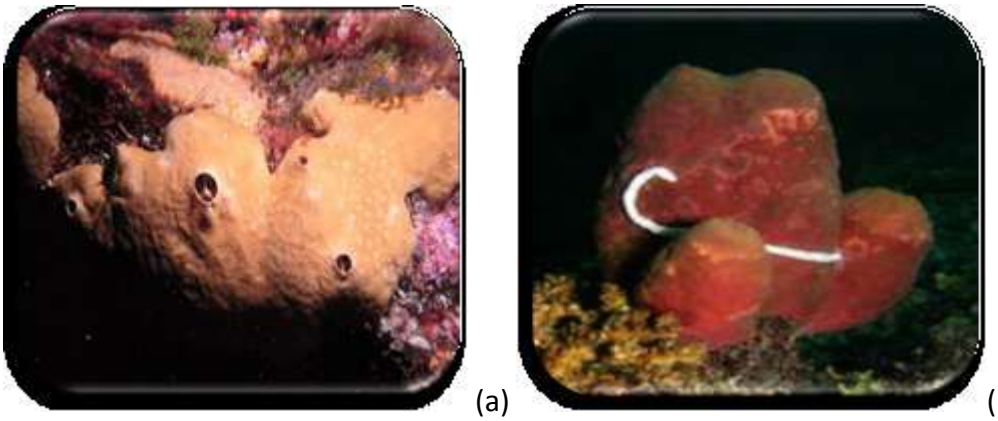

(a) (b)

Figure 1.3: Two **s**ponges analyzed in my PhD: (a) *Plakortis simplex* (b) *Theonella swinhoei*

The research work carried out during my Ph.D. followed three different projects:

1. **Study of mechanism and antimalarial activity of plakortin**
2. **Isolation and structure elucidation of secondary metabolites from the marine sponges *Plakortis* sp., *Plakortis simplex* and *Theonella swinhoei***
3. **Synthesis of simplified endoperoxide derivates based on the plakortin scaffold**

The obtained results have been reported in three papers (cited in the reference chapter) already published or sent for publication, while two additional papers are in preparation.

CHAPTER 2 - STEREOSTRUCTURAL ELUCIDATION METHODS

Until some decades ago, structural determination of new organic compounds was only pursued through the use of chemical techniques (degradation and interconversion of functional groups). The development of spectroscopic techniques dramatically changed this approach. Today, it is possible to determine complex organic structures, including stereochemical details, completely and in a non-destructive way, with submilligram samples. Structural determination described in this thesis is largely based on spectroscopic techniques, mostly mass spectrometry (MS) and nuclear magnetic resonance (NMR), even if in some cases some chemical interconversions were necessary.

2.1 Mass Spectrometry

The first step in the study of a new bioactive compound is the determination of the molecular formula through the high resolution mass spectrometry. Mass spectrometry is an analytical technique used to determine the molecular mass of a compound on the basis of the mass-to-charge ratio (*m*/*z* ratio) of ions produced from the molecules. A very accurate measurement of the molecular mass (high resolution mass spectrometry) can upgrade the knowledge of the molecule under investigation providing its molecular formula. The *source* is the component of the mass spectrometer which produces ions from the molecule, while the *analyzer* measures the mass-to-charge ratio of the ions. There are many different types of sources, as well as of analyzers. During or after ionization, the molecule may fragment, and the mass of the fragments can provide additional

information about the structure of the molecule. If the ions do not fragment by themselves, they may be induced to fragment by letting them to collide with gas molecules. In this case, a second analyzer is used to measure the mass of the fragments. This is known as tandem mass spectrometry or MS/MS.

Most of compounds described in the following sections were analyzed by ESI mass spectrometry. The ESI source is technique developed for polar and/or charged macromolecules but now it is widely used for a number of molecules, also with not marked polarity. The sample is dissolved in a volatile solvent like H_2O, MeOH, and CH_3CN; volatile acids, bases or buffers are often added to the solution. This solution is pumped through a charged metal capillary and, in coming out of the capillary, forms a spray. Because of the electric potential of the capillary, each droplet of the spray carries an excess positive or negative charge, and this causes extensive protonation or deprotonation of the molecules of the sample, which become ions. An uncharged carrier gas such as nitrogen is used to help the liquid to nebulize and the neutral solvent in the droplets to evaporate.

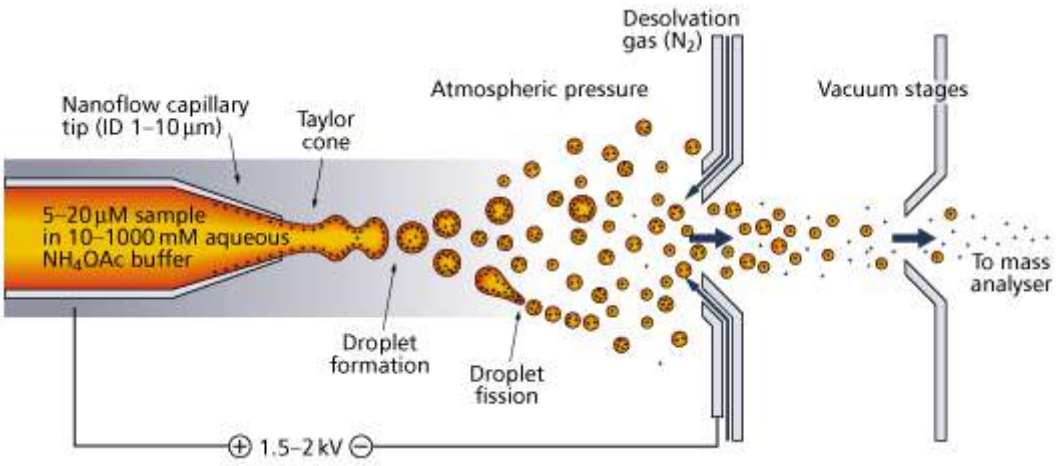

Figure 2.1. A schematic view of electrospray ionization

As the solvent evaporates, the ionized analyte molecules become closer and closer, until they can escape from the droplet by electrostatic repulsion. For molecules with a high molecular weight, the ions may take more than one proton (up to some tens), and therefore may have multiple charge. Formation of multiply charged ions allows the analysis of high molecular weight molecules such as proteins, because it reduces the *m/z* ratio of the ions, which is therefore easier to measure.

2.2 Nuclear Magnetic Resonance

The most important spectroscopic technique used for structure elucidation of the isolated secondary metabolites has been nuclear magnetic resonance (NMR). In addition to standard ^{1}H- and ^{13}C-NMR spectra, a large use of 2D NMR experiments was necessary. They provide an important tool for the interpretation of their 1D NMR counterparts and are characterized by reasonably long acquisition times (often shorter than the time needed to acquire a ^{13}C NMR spectrum), and for the easy assignment of nuclei resonating in crowded regions of the spectra (signal overlapping is much less likely in two dimensions than in one).

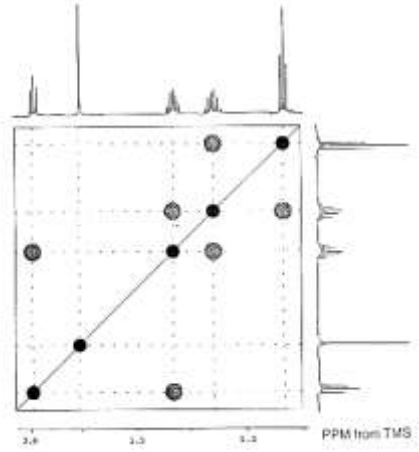

Figure 2.2. A typical COSY spectrum

The COSY (Correlation SpectroscopY) experiment is one of the simplest and yet most useful 2D NMR experiment. It allows determination of the connectivity of a molecule by identifying which protons show scalar couplings. In spite of the many modifications which have been proposed along the years, the very basic sequence composed of two π/2 pulses separated by the evolution period t_1 is still the best choice if one is simply dealing with the presence or the absence of a given coupling, but not with the value of the relevant coupling constant.

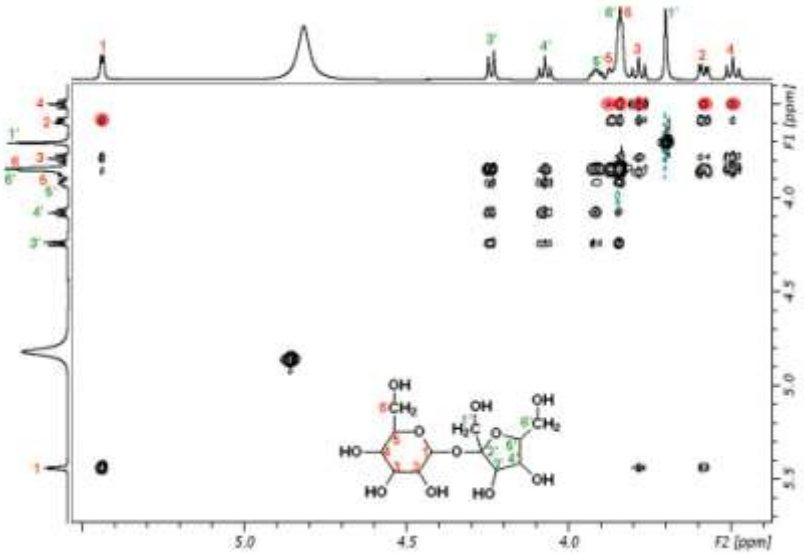

Figure 2.3. The TOCSY spectrum of sucrose

The TOCSY (Total Correlation SpectroscopY) experiment is a 2D NMR experiment very useful in the analysis of molecules composed of many separate spin systems, such as oligosaccharides (the TOCSY spectrum of sucrose is shown in Fig. 2.3) or peptides. The TOCSY spectrum shows correlation peaks between nuclei that may be not directly coupled, but are still within the same spin system. The appearance of a TOCSY spectrum resembles in all aspects a COSY; the difference is that the cross peaks in a COSY result from coupled spins, whereas in the TOCSY spectra they arise from coherence transfer through a chain of spin-spin couplings, and therefore any pair of protons within a spin

system may give rise to a peak. The range of the coherence transfer (i.e. through how many couplings the coherence may be transferred) increases with increasing mixing times (Δ), but a mixing time too long may reduce sensitivity.

The HSQC (Heteronuclear Single Quantum Correlation) and HMQC (Heteronuclear Multiple Quantum Correlation) experiment are 2D NMR heteronuclear correlation experiments, in which only one-bond proton-carbon couplings ($^{1}J_{CH}$) are observed. In principle, the HSQC experiment is superior to HMQC in terms of selectivity and additionally allows DEPT-style spectral editing. However, the sequence is longer and contains a larger number of π pulses, and is therefore much more sensitive to instrumental imperfections than HMQC.

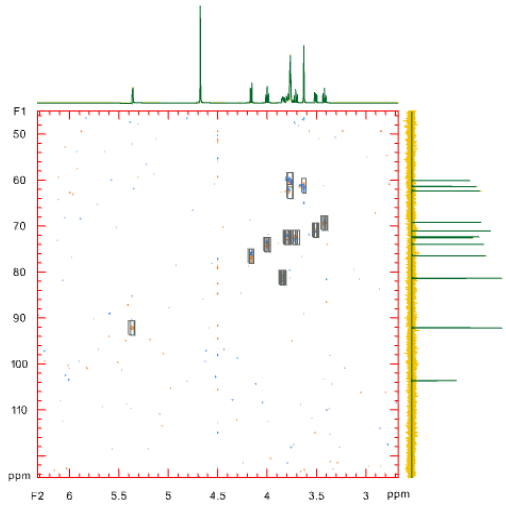

Figure 2.4. The HSQC spectrum of sucrose

The HMBC (Heteronuclear Multiple Bond Correlation) experiment is a heteronuclear two- and three-bond ^{1}H-^{13}C correlation experiment; its sequence is less efficient than HSQC because the involved $^{2,3}J_{CH}$ couplings are smaller (3-10Hz). Moreover, while $^{1}J_{CH}$ are all quite close to each other, $^{2,3}J_{CH}$ can be very different, making necessary the optimization of the experiment for each type of coupling. As a consequence, in many HMBC spectra not all

of the correlation peaks which could be expected from the structure of the molecule are present.

The ROESY (Rotating-frame Overhauser SpectroscopY) experiment is a chemical shift homonuclear correlation which can detect ROEs (Rotating-frame Overhauser Effect). ROE is similar to NOE, being related to dipolar coupling between nuclei, and depending on the geometric distance between the nuclei. While NOE is positive for small molecules and negative for macromolecules, ROE is always positive. Therefore, the ROESY experiment is particularly useful for mid-size molecules, which would show a NOE close to zero.

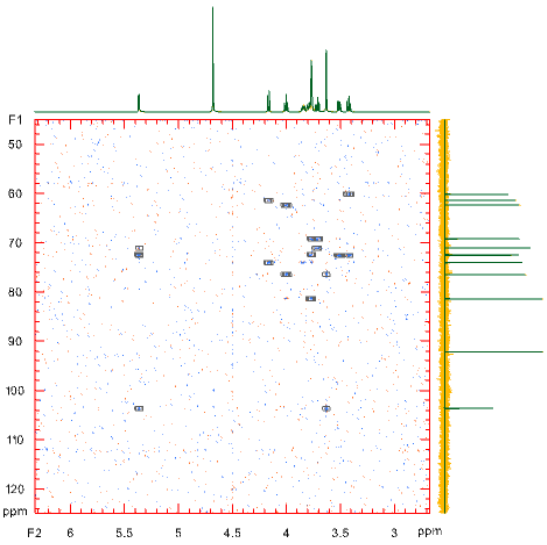

Figure 2.5. The HMBC spectrum of sucrose

The ROESY sequence is similar to the TOCSY sequence, and unwanted TOCSY correlation peaks may be present in the ROESY spectra. Fortunately, these unwanted peaks can be easily recognized, because their phase is opposite compared to ROESY correlation peaks. It is important to acquire ROESY spectrum in phase-sensitive mode for a correct interpretation of the spectrum.

2.3 Stereochemistry determination

The determination of the relative and absolute configuration of natural products represents one the most important goals of the structural characterization. The detailed knowledge of the tridimensional arrangement of natural products is essential to understand the biological activity, the relationships drug-receptor, and to synthesize the natural products or its optimized analogues.

The structure of many natural compounds includes a number of different stereogenic centers. Usually, in a step-by-step structural elucidation, the first goal is the identification of relative stereochemistry of chiral centers. Then, after the elucidation of absolute stereochemistry even at a single stereogenic carbon, it will be possible to deduce the absolute configuration of the total structure. Unluckily, when the relative stereochemistry of different chiral centers cannot be correlated, the absolute configuration must be assigned independently.

2.3.1 Scalar and spatial NMR couplings

Through the use of NMR spectroscopy it is possible to obtain information about the tridimensional structure of molecules. Evaluation of coupling constants (*J*) and NOE effects are of key importance to this aim.

The Karplus's law[4] describes the influence of relative arrangements of protons in a molecules on the values of coupling constants (J_{H-H}).

$$^{3}J = A\cos\theta^{2} + B\cos\theta + C$$

This equation evidences that the values of homonuclear ($^{3}J_{H-H}$) and heteronuclear ($^{3}J_{C-H}$) coupling constants are related to the value of the dihedral angle θ between atoms.

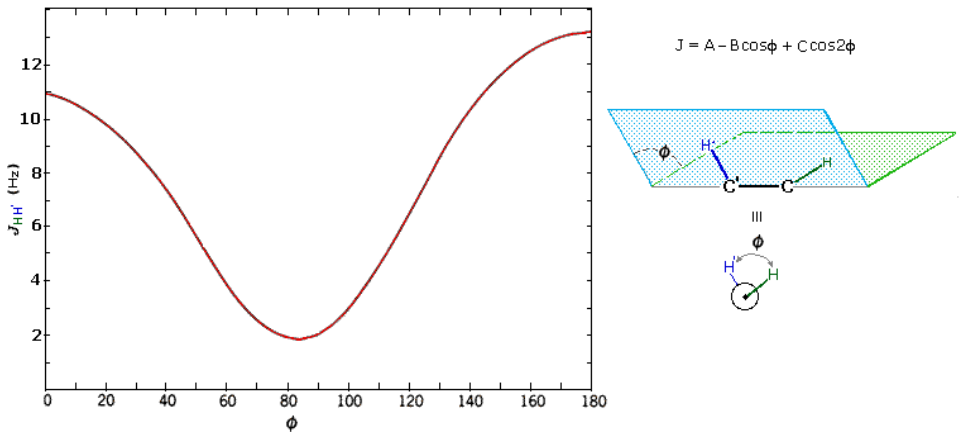

Figure 2.6. The Karplus rule

Usually the $^3J_{H\text{-}H}$ values are about 0-1,5 Hz, when θ is 90°, while the greatest are observed when θ is about 0° or 180°, generally $J_{180°}$ is hioghest than $J_{0°}$. Thus, for example, it is very easy to discriminate between an axial-axial correlation within a six-membered ring ($^3J_{a\text{-}a}$~7-9 Hz), and an axial-equatorial or equatorial-equatorial correlations ($^3J_{a\text{-}e}$~$^3J_{e\text{-}e}$~2,5 Hz). Furthermore, it is very easy to discriminate between a *cis* or a *trans* relationship of two double bond protons, $^3J_{cis}$~6-12 Hz, $^3J_{trans}$ ~14-20 Hz.

Additional information about relative configuration of stereogenic centers can be obtained from the so-called NOE effect (**N.O.E**.: "Nuclear Overhauser Enhancement"). This effect can be observed upon irradiation, during the acquisition of the spectra, on a specific signal. In this way, the relaxation times of all the protons surrounding the irradiated proton (distance ≤ 2.5 A°), even though not belonging to the same spin system, are influenced and thus, their height changes. The NOE effect establishes a spatial relationship between substituents of fixed molecules, but this effect is dependent from the dimensions of the molecule. Indeed, NOE effects cannot be evidenced for large molecules. To overcome this limitation, a two-dimensional omonuclear experiment, the ROESY experiment (Rotating-frame Overhauser Effect SpettroscopY), can be used (see above).

2.3.2 Murata's method

Generally, the use of coupling constants $^{3}J_{H\text{-}H}$ and ROESY correlations is limited to rigid o cyclic systems, where the large number of weak interactions limits the possibility of conformational motions, and consequently the dihedral angles and interatomic distances between the protons are rigidly fixed. However, many biologically active natural products, often have linear or flexible macrocyclic structures. Recently, Murata et al. proposed a simple method[7] based on the evaluation of homo- and heteronuclear coupling constants, which may be used to determine the relative stereochemistry of flexible systems, especially in those cases where the chiral centers are composed of oxygen-linking methines.

This method is based on the assumption that the conformation of the adjacent asymmetric centers, in acyclic systems, is mainly represented by staggered rotamers, and their relative stereochemistry can be determined using proton-carbon coupling constants, $^{2,3}J_{H\text{-}C}$, and vicinal proton coupling constants, $^{3}J_{H\text{-}H}$. The combined use of the values of these constants makes possible the identification of the predominant rotamer. An accurate measurement of heteronuclear coupling constants can be realized with two-dimensional NMR experiments. In many cases it is sufficient a qualitative assessment of the constants, achieved through phase-sensitive HMBC experiments, which allow to discriminate between large constants (large), and small constants (small).

2.3.3 Circular Dichroism

Circular dichroism (CD) spectroscopy of optically active compounds is a powerful method for studying the three-dimensional structure o molecules, and can provide information on absolute configurations, conformations, etc.

The CD spectroscopy takes advantage of the different absorption shown by chiral compounds of left and right circularly polarized UV/Vis light. In circularly polarized light, the electric field vector rotates about its propagation direction forming a helix in the space while propagating. This helix can be left-handed or right-handed, hence the names left and right circularly polarized light.

At a given wavelength, circular dichroism of a substance is the difference between absorbance of left circularly polarized and right circularly polarized light:

$$\Delta A = A_L - A_R$$

Since circular dichroism uses asymmetric electromagnetic radiations, it can distinguish between enantiomers. Two enantiomers have the same CD spectra, but with reversed sign.

Of course, in order to show a *differential* absorbance, the molecules needs to absorb the UV/Vis light, and therefore must possess at least one chromophore. If the molecule does not have a chromophore, this can be introduced using a derivatization reaction. This is why methyl glycosides are benzoylated to determine their absolute configuration.

One of the most important methods to establish the absolute configuration of a molecule is the exciton chirality method. This method is based on the interaction between two chromophores. When two or more strongly absorbing chromophores are located around a chiral system, their electric transition moments interact spatially (exciton coupling) and generate a circular dichroism. Because the theoretical basis of exciton coupling are well understood, it is possible to correlate the CD spectrum of an exciton-coupled chromophore system with the spatial orientation of the chromophores, which in turn can be related to the absolute configuration of the molecule. It is important to point out that,

unlike for example optical rotation, the exciton chirality method does not require any reference nearby in space and constitute of organic compound to provide the absolute configuration of the molecule under study (if its conformation is known).

2.3.4 Mosher's method

Several methods are available for the determination of absolute stereochemistry of compounds, however, the most extensively used is undoubtedly the Mosher's method. This method utilizes the preparation of diastereomeric acyl derivatives with the two enantiomers of 2-methoxy-2-(trifluoromethyl) phenylacetic acid (MTPA) and evaluation of the ^{1}H NMR resonances of the protons surrounding the stereogenic center. In particular, the chemical shift differences $\Delta\delta_{S-R}$ must be calculated, after a detailed assignment of proton resonances for the two diastereomers obtained. This method has been proposed for determination of the absolute configuration of secondary alcohols. The application of the Mosher model is based on the existence, in the reaction solution, of a preferential conformation, in which the proton at the stereogenic center, the carbonyl of the ester group and the trifluoromethylic group reside on the same plane.[5] This preferential conformation is shown in Fig. 2.8.

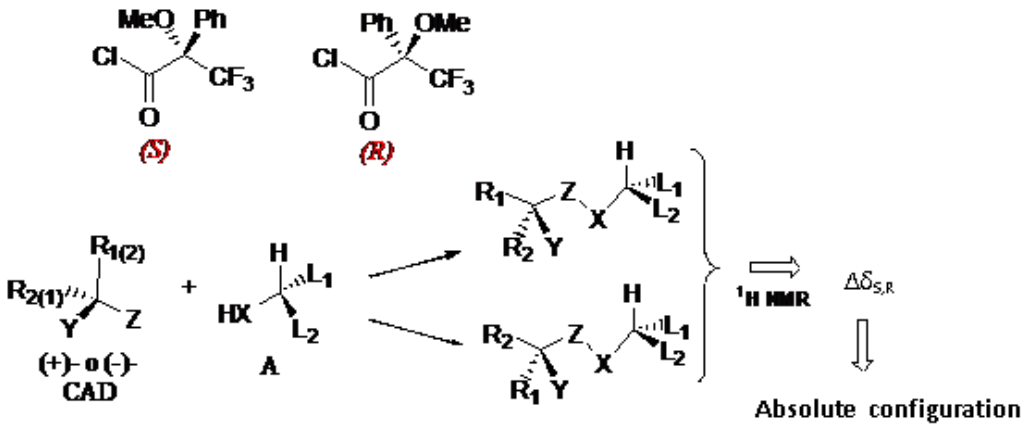

Figure. 2.7 A schematic view of the Mosher's method

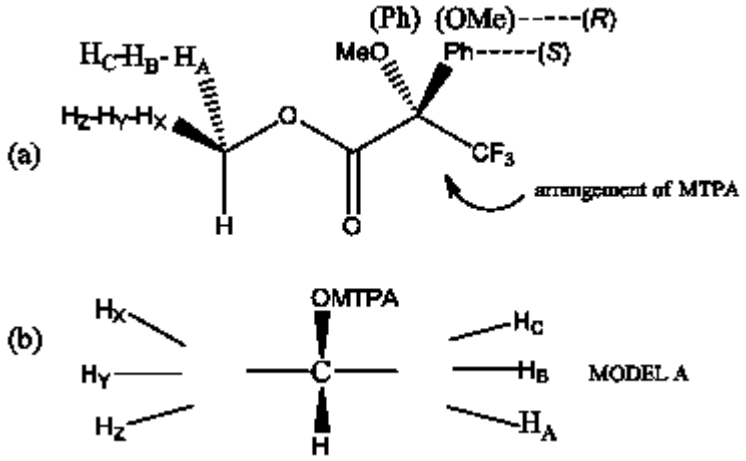

Figure 2.8. (a) Preferential conformation of Mosher's model. (b) Mosher's empiric rule for the absolute configuration of secondary alcohols. The groups on the right are characterized by $\Delta\delta>0$ while the groups on the left by $\Delta\delta<0$

Kakisawa and Kashman proposed some changes to the Mosher's method including the evaluation of $\Delta\delta_{S-R}$ values not only of proton chemical shifts for carbons directly linked to the stereogenic center, but also for other protons on the two sides.

CHAPTER 3 – ANTIMALARIAL ENDOPEROXIDES. ISOLATION AND SYNTHESIS OF NEW COMPOUNDS

3.1. The malaria threat

Malaria is an infectious disease caused by several protozoans belonging to the genus *Plasmodium* (*P. falciparum*, *P. ovale*, *P. vivax*, *P. malariae*) but *P. falciparum* is the parasite that causes most severe diseases and most fatal cases. The protozoan comes in contact with humans through the vector contribution of female mosquitoes of the genus *Anopheles*. The bite of infected mosquitoes injects protozoans in the sporozoite form, that invade selectively the parenchymal cells of the human liver. In this stage, the patient remains asymptomatic and, after an average incubation period of 5-7 days (in the case of *P. falciparum*), protozoa reach the merozoite stage and are released from the liver. The merozoites invade the erythrocytes and start feeding on the haemoglobin. After proliferation, the rupture of the erythrocyte membrane and the consequent liberation of other merozoites, that invade other erythrocytes, cause the massive infection and the symptoms. A small portion of merozoites develops into the sexual stage of gametocytes, a form that is able to re-start the life cycle of the malaria parasite when a mosquito takes a blood meal from an infected person.[8]

The clinical symptoms of malaria infections are exclusively attributable to parasites in the erythrocytic stage. The rupture of infected erythrocytes is associated with the release into the blood stream of cell debris responsible for the characteristic fever spike patterns. In the lethal cases, a specific protein produced by the protozoan is embedded into the cell

membrane of the infected erythrocyte and, as a consequence of this modification, the erythrocyte sticks to the walls of capillaries causing obstruction of vessels. When this mechanism operates at the level of brain vessels, the loss of consciousness is the first symptom, but, if this form of cerebral malaria is not treated immediately, it is soon followed by death.

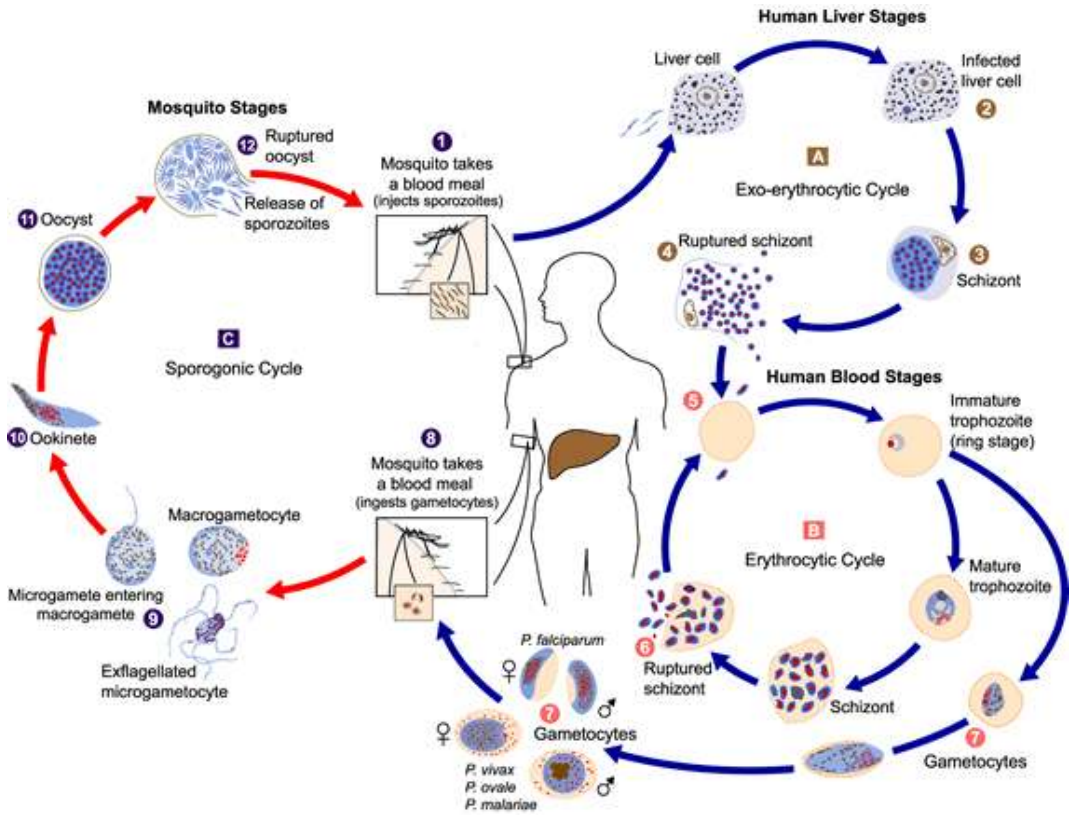

Figure 3.1 The malaria cell cycle

The treatment of malaria infections holds a venerable place in the history of medicinal chemistry and of natural product chemistry. As commonly well-known, the first specific treatment for malaria dates back to the 17th century when the bark of Cinchona trees was used as the best tool to face infections of malaria, that was endemic in Africa, Asia but also in several parts of Europe and North America. Later, malaria was the first disease to be treated with an active principle isolated from a natural source, quinine isolated from the

Cinchona bark in 1820, and, later again, the first human disease to be treated with a synthetic drug (methylene blue in 1891).

In the course of 20th century, especially during World War II, a series of effective synthetic antimalarial drugs have been developed. Among them, chloroquine (**2**), mefloquine (**3**), and pyrimethamine (**4**) (Fig. 3.2), became the drugs of choice in several programs and contributed to the almost complete eradication of malaria from Europe and North America.

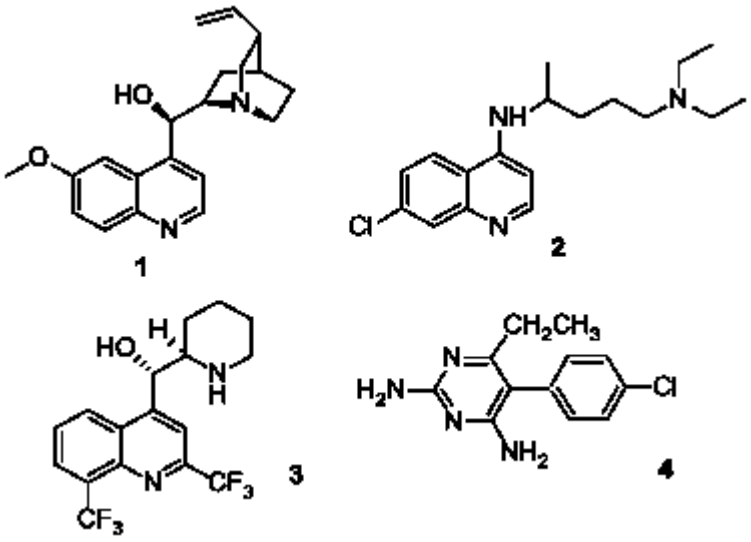

Figure 3.2. First-line antimalarial drugs: quinine (**1**), choloquine (**2**), mefloquine (**3**), pyrimetamine (**4**)

Unfortunately, in our days malaria still continues to be an extremely important threat to the health and economic prosperity of the human race, constituting a major cause of morbidity and mortality in tropical countries of Asia, Africa and South America. The reality is probably worse than that commonly conceived: a recent analysis estimates, at a minimum, between 700,000 and 2.7 million deaths each year from malaria (over 75% of them are African children) and between 400 and 900 million acute febrile episodes per year in African children under the age of 5 living in malaria-endemic regions . Part of the

reason for the failure to control malaria in these areas is the emergence and spread of resistance to first-line antimalarial drugs, cross-resistance between the members of the limited number of drug families available, and in some areas, multi-drug resistance. In addition, the prevalent spreading of the disease to poor countries has suggested to many pharmaceutical companies to categorize malaria as a low priority. In this context, funds provided by public agencies, as European Community, are the good news of recent years. Their specific aim is to encourage the antimalarial research in spite of the poor economic interest.

Two major breakthroughs of the past few decades have renewed the assault of scientists to this infective disease. The first is the complete sequencing of the genome of *Plasmodium falciparum* that is expected to provide useful information for the identification of new drug targets. The second is the discovery by Chinese researchers of artemisinin (qinghaosu), an endoperoxide sesquiterpene lactone, as the active principle of the sweet wormwood, *Artemisia annua*, an herbal remedy used in folk Chinese medicine for 2000 years. This molecule and its oil soluble (e.g. artemether and arteether) and water soluble (e.g. artesunate and artelinate) semi-synthetic derivatives have shown excellent efficacy against chloroquine-resistant *Plasmodium* strains and are becoming increasingly used, especially in combination with traditional antimalarials (e.g. mefloquine).

However, these important discoveries should be considered only as stimulating starting points in the continuing fight against malaria. As commonly believed, in spite of several efforts, an effective vaccine against all the forms malaria probably will never be introduced, and the complete removal of the vector of the transmission is practically impossible. Therefore, the need for rapid development and introduction of safe and affordable drugs against malaria continues to be urgent.

3.2. The efficacy of endoperoxide derivatives

The sweet wormwood *Artemisia annua* (Compositae), also named qinghao, has been used in Chinese folk medicine for 2000 years, originally as a treatment for haemorrhoids, but starting from the III century also to treat fevers. In 1972, after activity-guided fractionation, the sesquiterpene derivative artemisinin (in China named qinghaosu: "the active principle of qinghao") was isolated; later its structure was elucidated and it was shown to possess a potent antimalarial activity. This molecule soon appeared to constitute a major breakthrough in the antimalarial therapy because of: 1) its nanomolar activity on chloroquine-resistant *P. falciparum* strains (higher than the activity on chloroquine-sensitive ones) even on cerebral malaria; 2) its fast action; 3) the absence of detectable toxicity at therapeutic doses.

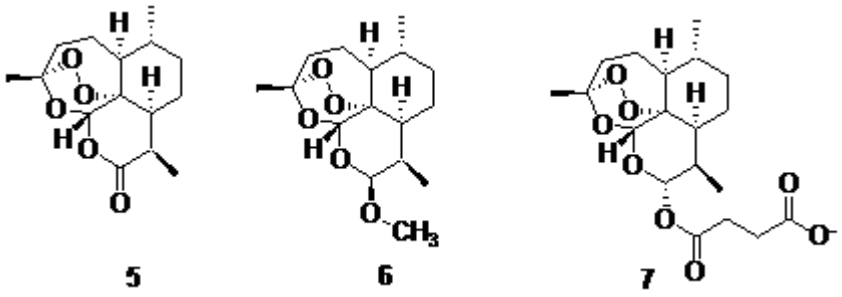

Figure 3.3. Chemical structures of artemisinin (**5**) and of its semisynthetic derivatives artemether (**6**) and artesunate (**7**)

Artemisinin (**5**) is a structurally complex cadinane sesquiterpene lactone bearing an endoperoxide group embedded in a 1,2,4-trioxane ring. With its unique juxtaposition of peracetal, acetal and lactone functionalities, it has very much to interest organic chemists.

Since the relatively efficient totally synthetic routes developed[9] will very unlikely supplant the natural source, an intense scientific activity has been carried out entailed to the chemical derivatization of artemisinin. The aim was to obtain compounds with better solubility, higher stability, and thus with increased formulation characteristics, and, possibly devoid of the neurotoxic side effects detected for the natural molecule.

These efforts soon resulted in the recognition that the endoperoxide linkage is an essential feature for antimalarial activity, given that the acyclic diol and the ether (1,3-dioxolane) analogues of artemisinin were completely devoid of activity. Consequently, the lactone group became the main site for chemical variations that bore the preparation of the oil-soluble artemether (**6**) (Fig. 3.3), and the water-soluble artesunate (**7**). Although these molecules are now used for treatment of severe malaria with the support of the World Health Organization, unfortunately, they still possess neurotoxic activity. As a result of the continuing synthetic studies, several artemisinin derivatives, some of which surpass the parent compound in antimalarial potency, have been prepared but many of them show toxicity or have unfavourable pharmacokinetic features. An essential requirement to design optimized artemisinin derivatives would be a perfect knowledge of the mechanism of its antimalarial activity. Unfortunately, still today our knowledge appears incomplete. While the crucial importance of the endoperoxide pharmacophore is no longer questioned, the detailed mechanism of action of this molecule is still not unanimously accepted. According to a first hypothesis, artemisinin (or its analogues) would interact, within the parasite food vacuole, with the iron center of the heme unit released during the digestion of hemoglobin. The interaction of artemisinin with the heme ferrous iron would cause the cleavage of the peroxide bridge and the formation of alkoxy radicals that, after several rearrangements, would result in the formation of free C-centered radicals (see

below, Figure 3.11). These should be toxic to the parasite because they should alkylate not better defined "sensitive" macromolecular targets. This hypothesis is based on the evidence that, in several experimental models, artemisinin reacts with iron ions and in particular it interacts strongly with hemin (ferriprotoporphyrin IX) and its ferrous form (ferroprotoporphyrin IX) to give covalent adducts.

Some researchers have proposed for artemisinin the interaction with a specific target. This has been identified as a Ca^{2+}-dependent ATPase specific of *P. falciparum* (PfATP6), a trans-membrane protein associated with the parasite endoplasmic reticulum. However, it is still not clear whether artemisinin reacts with this target as it is (and, therefore, the peroxide bridge exerts its key role concomitantly with the binding), or it needs a foregoing reaction with an iron-containing molecule.

Further experiments would be required to gain more insights into the mechanism of action of the endoperoxide-containing antimalarial agents. The isolation of different antimalarial endoperoxides from natural sources can evidently help in this task. Indeed, it could provide additional information about the structural features required to the carbon backbone of a endoperoxide-containing antimalarial agent. With luck, this research could afford new natural compounds whose antimalarial activity is higher than that of artemisinin. In this context, with the inspiration of artemisinin, several research groups are currently engaged in the isolation of endoperoxide-containing compounds from terrestrial plants and marine organisms.

3.2.1. Marine Endoperoxides

A large number of cyclic peroxides have been isolated from marine organisms and some of them have been tested for antimalarial activity. Marine sponges belonging to the family

Plakinidae contain a series of simple endoperoxide derivatives that have been identified as polyketide metabolites possessing six- or five-membered 1,2-dioxygenated rings (1,2-dioxane or 1,2-dioxolane, respectively). A further variation is represented, in some cases, by the presence of a 3-methoxy substitution, building a peroxyketal group.

The parent compound of this group of secondary metabolites is plakortin (**8**) (Fig. 3.4), that was isolated more than 25 years ago from *Plakortis halichondroides*. This interesting secondary metabolite, whose polyketide skeleton suggests the involvement of butyrate units in the biogenesis, has been recently re-isolated in remarkable amounts from the Caribbean sponge *Plakortis simplex*.[10] In the same study the absolute configuration of the four stereogenic carbons of plakortin has been determined by means of chemical derivatization and reaction with chiral auxiliaries; in addition, a closely related analogue, named dihydroplakortin (**9**), (Fig. 3.3), has been obtained.[10]

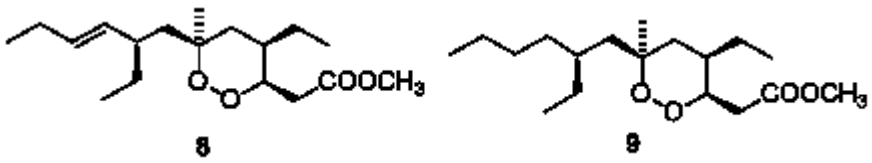

Figure 3.4. Chemical structures of plakortin (**8**) and dihydroplakortin (**9**)

At the time of its first isolation, plakortin was found to be a weak antibacterial agent, but a recent study has finally disclosed the antimalarial potential of this molecule.[11] Using the pLDH assay, plakortin (**8**) and dihydroplakortin (**9**) were assayed against D10, chloroquine-sensitive strain, and W2, chloroquine-resistant strain of *P. falciparum.* The two compounds showed a good activity, that was more potent on the W2 strain (IC_{50} = ab. 250 ng/mL on D10; ab. 180 ng/mL on W2). In addition, the two compounds proved to be non-cytotoxic in

vitro.[10] Interestingly, in the same investigation[11] the structurally related, even more sterically hindered, five-membered endoperoxide plakortide E (**10**) (Fig. 3.4) was found to be inactive

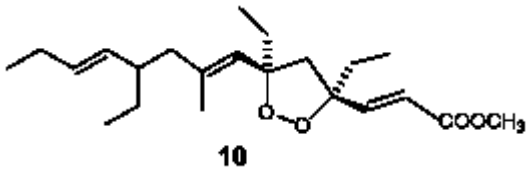

10

Figure 3.5. Chemical structure of the inactive plakortide E (**10**)

The chemical structure of these two antimalarial leads is remarkably simple and thus they could constitute a good probe to establish structure-activity relationships, to check the currently postulated mechanisms of action for antimalarial peroxides and to prepare semi-synthetic or totally synthetic derivatives. In this regard, a synthetic study toward this class of cyclic peroxides has recently appeared.[12]

Some 1,2-dioxane derivatives structurally related to plakortin have been isolated from Plakinidae sponges and tested for their antimalarial activity. Plakortide F (**11**) (Fig. 3.6) has been isolated from a *Plakortis sp.*[13] and it has been shown to possess an antimalarial activity that is slightly lower (about one half) compared to that of plakortin: IC_{50} = 480 ng/mL on D10; ab. 390 ng/mL on W2; however, unless plakortin, this molecule was found to be consistently cytotoxic since the IC_{50} of toxicity against human colon carcinoma and mouse lymphoma cells is only about double (IC_{50} = 1.25 μg/mL) than the concentration of the antimalarial activity.

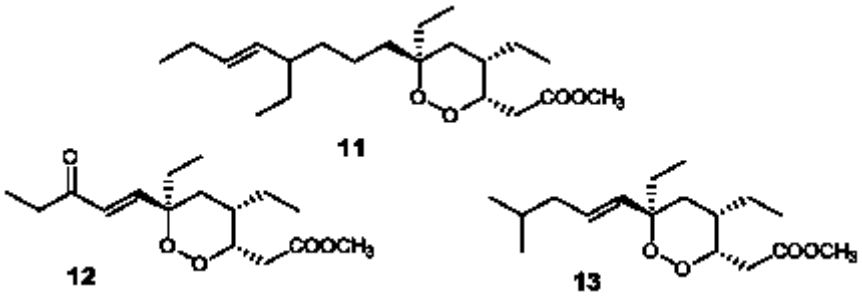

Figure 3.6. Chemical structures of plakortides F (**11**), K (**12**) and L (**13**)

A very moderate antimalarial activity was also recently reported for plakortide K (**12**) (Fig. 3.6), an 1,2-dioxane derivative substituted at position 3 with an unsaturated ketone, isolated from a Jamaican sponge *Plakortis* sp.[14]. This molecule showed activity against W2 *P. falciparum* strain with IC_{50} = 570 ng/mL and a selectivity index > 8.4. Interestingly, plakortide L (**13**) (Fig. 3.6), a closely related analogue lacking the carbonyl function, was completely inactive. Two additional plakortides, named plakortide O (**14**) (Fig. 3.7) and plakortide P (**15**) (Fig. 3.7), have been isolated from *Plakortis halichondrioides* and tested for antimalarial activity against *P. falciparum*.[15] These compounds showed a very low activity with an IC_{50} = 8 µg/mL for plakortide O and an $IC_{50} \geq 50$ µg/mL for plakortide P. In addition, these molecules showed toxicity in vitro toward several cell lines at lower concentrations.

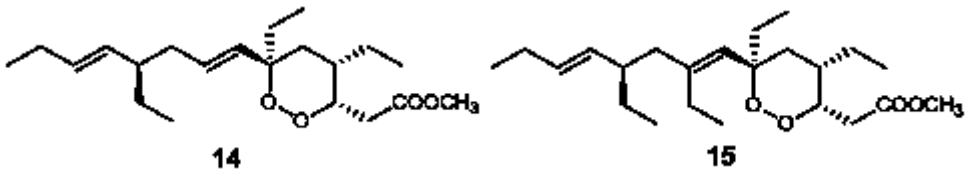

Figure 3.7. Chemical structures of plakortides O (**14**), and P (**15**)

It should be noted that all these plakortides have a close structural similarity with plakortin and, therefore, their lower level of antimalarial activity can be utilized to gain useful information about the structure-activity relationships within this class of simple cycloeproxide derivatives. One of the main differences among these compounds are ascribable to the stereochemistry. Indeed, while in the structure of plakortin the most hindered chains attached to the 1,2-dioxane ring are in *cis* orientation, in the other analogues a *trans* orientation is present. Most likely, these latter molecules experience a more problematic approach of the endoperoxide group to its target. However, the chemical structure of the side chains must be also important, as indicated by the marked difference of activity between plakortides K (**12**) and L (**13**) and between plakortides O (**14**) and P (**15**).

Further information on the structure-activity relationships come from data on synthetic and natural 3-alkoxy-1,2-dioxene and 3-alkoxy-1,2-dioxane (both peroxyketals) derivatives, which were shown to possess a very good antimalarial activity. In this class of molecules, the alkoxy substituent at position 3 could partly mime the non-peroxidic oxygen atom of the 1,2,4-trioxane ring of artemisinin.

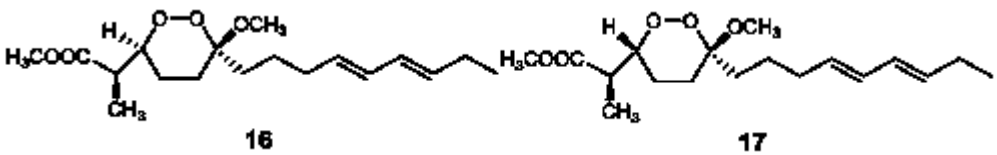

Figure 3.8. Chemical structures of peroxyplakoric acids A_3 (**16**) and B_3 (**17**) methyl esters

The methyl esters of peroxyplakoric acids A_3 (**16**) and B_3 (**17**) (Fig. 3.8), isolated from *Plakortis* sp., showed a very good antimalarial activity against *P. falciparum* with IC_{50} = 50

ng/mL and a good selective toxicity index (about 200).[16] Through the syntheses of some analogues of these active compounds, some conclusions about the structural requirements within these classes of antimalarials were drawn. For example, compound (**18**) (Fig. 3.9) proved to be almost completely inactive, whereas compound (**19**) (Fig. 3.9) retained the in vitro activity of peroxyplakoric acid B_3 methyl ester, indicating the importance of the side chain for the antimalarial activity.[17]

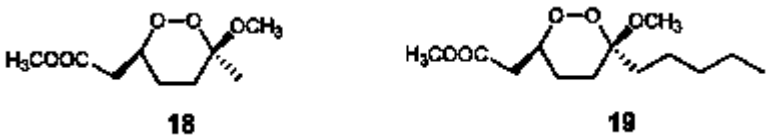

18 19

Figure 3.9. Two synthetic analogues of peroxyplakoric acids methyl esters

When compound **19** was examined through an in vivo system against *P. berghei* infection, it showed little antimalarial potency because of lability in mouse serum. This undesired finding was demonstrated to be due to the hydrolysis of the ester function to the inactive carboxylic acid. Indeed, the monoethyl amide analogue of **19**, that is stable to hydrolysis in the serum, showed a good in vivo activity.[18]

Finally, the low antimalarial activity observed for two additional marine endoperoxides strictly related to peroxyplakoric acid B_3 methyl ester, namely chondrillin, (**20**) (Fig. 3.10)[19] and muqubilone,[20] (**21**) (Fig. 3.10) provides other interesting suggestions. The insertion of a double bond within the 1,2-dioxane ring appears to be detrimental for the activity, while the presence of the methoxy group at C-3 exerts a pivotal role in the determination of the antimalarial activity for this group of molecules. Most likely, simple 1,2-dioxane molecules,

that, like plakortin, are consistently active, possess other features that are able to compensate the lack of the methoxy group.

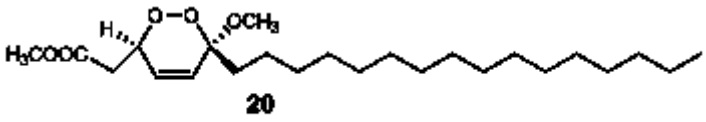

20

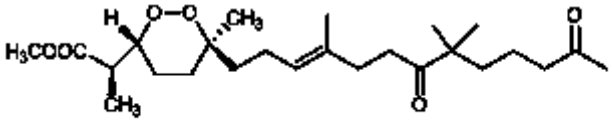

21

Figure 3.10. Chemical structures of chondrillin (**20**) and muqubilone (**21**)

3.3. Investigation of the plakortin mechanism of action[21]

The knowledge of further details on the mechanism of action constituted an issue of key importance to continue the investigation on the antimalarial activity of plakortin derivatives. Indeed, a more detailed comprehension of the mechanism of action of plakortins is essential for the development of totally synthetic simplified derivatives containing only the essential pharmacophoric portion of the plakortin scaffold.

Despite the large use of artemisinin, the exact molecular mechanism underlying its biological activity, and that of related antimalarial endoperoxides, is still a matter of debate.[22] Nevertheless, the ability of these molecules to interact with Fe(II)-heme and to produce oxidative stress hallmarks in the plasmodium and in the infected host cells has been proved.[22,23]

The reaction of endoperoxides with Fe(II) involves a one electron reduction leading to the cleavage of the oxygen-oxygen linkage with the consequent formation of an oxygen anion [bound to Fe(III)] and of an oxygen free radical. Two possible evolutions of the generated oxygen radical have been postulated for artemisinin (Figure 11). In pathway 1, the oxygen

O1 free radical evolves through an intramolecular 1,5-H shift leading to a secondary free radical at C4. Alternatively, in pathway 2, the oxygen O2 free radical evolves through a homolytic cleavage of the C3-C4 bond resulting in the formation of a primary C4 free radical, the driving force being the acquisition of thermodynamic stability by formation of the acetate group. [22]

Experimental data[24] and theoretical studies[25] show controversial results on the more relevant pathway for antimalarial activity. Anyway, reported structure-activity relationship (SAR) studies on artemisinin[26] (Fig. 3.11), as well as on other endoperoxide derivatives,[27] failed to relate *in vitro* antimalarial activity with a mechanism of action principally based on reaction pathway 2. In addition, the lack of antimalarial activity of artemisinin analogues with α-oriented substituents at C-4 can be related to their inability to undergo the intramolecular 1,5 H-shift (pathway 1)[26].

The crucial role of the endoperoxide function and of 1,2-dioxane ring conformation that we have demonstrated for (**8**), together with the lack of stereoselectivity in its antimalarial mechanism of action (3-epiplakortin showed the same activity as (**8**), strongly indicated that plakortin, similarly to artemisinin, should not interact with a specific protein target but rather with a Fe(II) ion, most likely the heme iron deriving from hemoglobin digestion[27].

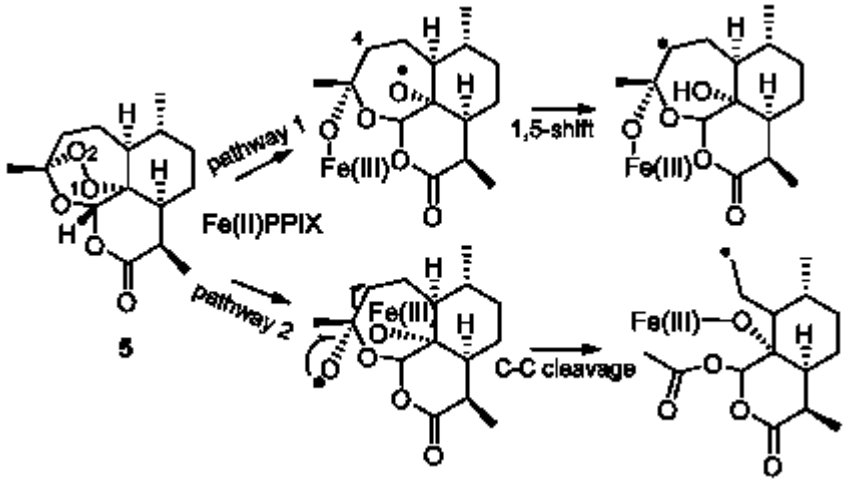

Figure 3.11. Schematic representation of the artemisinin postulated mechanism of action

Our previous conclusion that the antimalarial activity of plakortin and analogues is strongly affected by conformational parameters prompted us to speculate on a through-space reaction pathway for the formation of reactive species responsible for plasmodium death. Starting from this assumption, we carried out our investigation on plakortin and dihydroplakortin, two related compounds which showed comparable antimalarial activity (Table 3.1). The aim was to enlighten, for both these compounds, the steps following the reductive activation of the oxygen-oxygen bond by Fe(II) species and yielding to the death of the parasite.

Table 3.1. *In vitro* antimalarial activity of some *Plakortis* endoperoxide derivatives against D10 (CQ-S) and W2 (CQ-R) strains of *Plasmodium falciparum*.

	D10	**W2**
	IC_{50} µM	**IC_{50} µM**
Plakortin	0.87 ± 0.35	0.39 ± 0.13
Dihydroplakortin	0.90 ± 0.56	0.43 ± 0.16
Plakortide K	Not Available	> 2
Artemisinin	0.013 ± 0.004	0.009 ± 0.005

Our approach followed two independent methods based on computational analysis and chemical evidences and represents the first investigation on the mechanism of action of non-peroxyketal simple dioxane antimalarials. In this thesis, I will report details about the experimental studies, while for the computational investigation (carried out in collaboration with the group of prof. C. Fattorusso) only significant results will be provided.

3.3.1 Computational Studies

Semi-empirical (PM6) quantum-mechanical (QM) calculations indicated that Chair A is by far the most representative 1,2-dioxane ring conformational family for both plakortin and dihydroplakortin (Figure 3.12).

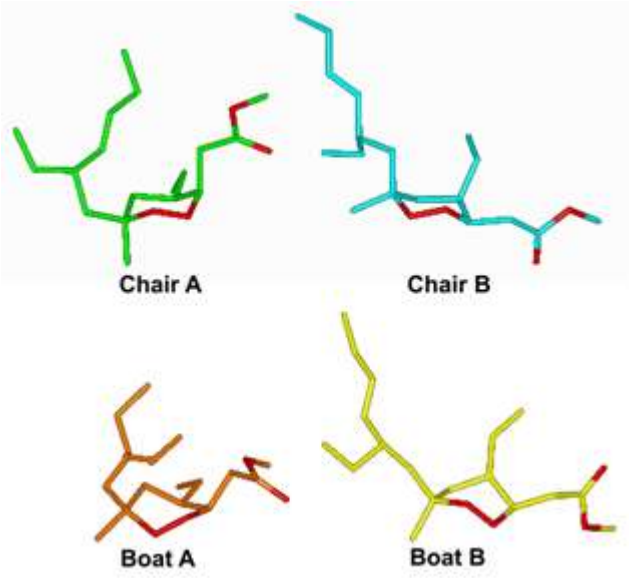

Figure 3.12 Family of conformations for plakortin and dihydroplakortin

Subsequent calculations were performed on the basis of the hypothesized reaction pathway responsible for antimalarial activity. The first reaction step, activation step,

involves a one-electron reduction by heme Fe(II), thus leading to the cleavage of the endoperoxide bond, through a dissociative electron transfer (DET) mechanism.[28,29] Within this step, an oxygen anion [bound to Fe(III)] and an oxygen free radical are produced. Since the endoperoxide linkage has two oxygen atoms exposed to heme iron (named O1 and O2), *ab initio* calculations were performed in order to investigate the alternative formation of O1 and O2 radicals. Results indicated unambiguously a higher stability for O1 radical. Since the energies of transition states for the two alternative homolytic cleavage reactions are likely in proportion to those of the corresponding products (oxygen radicals), we can assume that the formation of the O1 radical is kinetically preferred both for **8** and **9** (Fig. 3.6).

Accordingly, we continued our investigation with the assumption that the radical is preferentially formed on O1. An evaluation of the distances between the endoperoxide oxygen O1 and the possible partners for an intramolecular radical shift through an analysis of conformational search results suggested the double bond of plakortin and the methylene hydrogens at C13 of dihydroplakortin as the most likely partners for interaction with the O1-oxygen radical. Indeed, our calculations suggested that, as a consequence of the conformational rearrangement following the cleavage of the endoperoxide bond, in both compounds, the O1-centered radical approached to the "western" alkyl side chain [i.e., double bond in **8** and C(13)H in **9**, respectively] shrinking from the ester side chain [i.e., C(2)H]. This conformational shift is in agreement with the previously explored SARs on 1,2-dioxane derivatives that indicated a negligible role for the "eastern" ester side chain. On the other hand, the role of the "western" alkyl side chain for the antimalarial activity of 1,2-dioxanes is well highlighted by plakortide K (**12**) (Fig. 3.6). This compound, obtained from *Plakortis* sp.,[30] proved to be completely inactive as antimalarial agent

(Table 3.1), in spite of its similarity to plakortin, including an identical ester side chain. In agreement with our results, the lack of activity should be ascribed to the presence of the $\Delta^{7,8}$ *trans* double bond, whose geometry prevents the location of a reaction partner on the western side chain at a distance suitable for the intramolecular shift.

Taken together, all the computational outcomes indicated the structures reported in Figure 3.13 as putative plakortin and dihydroplakortin bioactive conformations, being able to undergo: 1) a one electron reduction reaction of the endoperoxide bond by heme Fe(II) through a DET mechanism, leading to the formation of an oxygen radical at O1; 2) a subsequent through-space one electron reaction between O1 radical and the double bond (C9), in the case of plakortin, and between O1 radical and an ethyl chain (C13) hydrogen, in the case of dihydroplakortin. The generated carbon radicals could represent, according to the hypothesized mechanism of action, toxic intermediates responsible for subsequent reactions leading to plasmodium death.

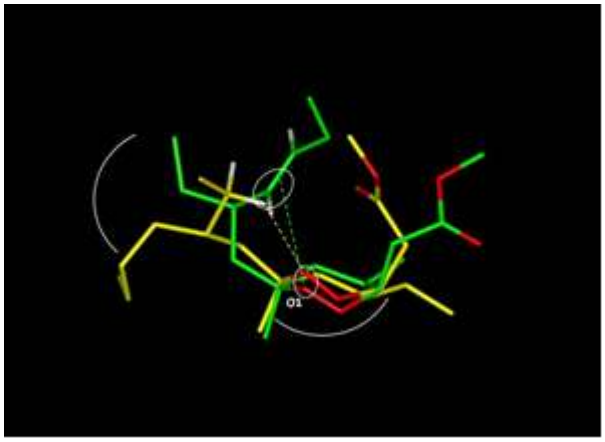

Figure 3.13. The bioactive conformation for plakortin (green) and dihydroplakortin /yellow)

3.3.2 Reaction with Fe(II) chloride

To check experimentally the results of computational calculations, we decided to utilize the model Fe(II)-induced reduction of the endoperoxide bond[31] and to analyze the behavior of both **9** and **8** by detailed characterization of their degradation products. Among the possible experimental models, we preferred the use of (inorganic) salts of Fe(II) in aqueous solution due to the efficiency and reproducibility of the reaction.[32] Data available in the literature for artemisinin and other endoperoxide antimalarials are almost exclusively based on the use of Fe(II) chloride, sulphate, or gluconate.[33] A recently appeared investigation has established that Fe(II) chloride is very efficient in triggering artemisinin endoperoxide bond cleavage and subsequent intramolecular rearrangement.[31] Thus, dihydroplakortin was allowed to react with $FeCl_2$ in CH_3CN/H_2O 4:1 at r.t. for 2 hours. Chromatographic purification of the reaction mixture afforded two major products (**9a** and **9b**), whose stereostructure has been identified by detailed spectroscopic investigation (Fig. 3.14).

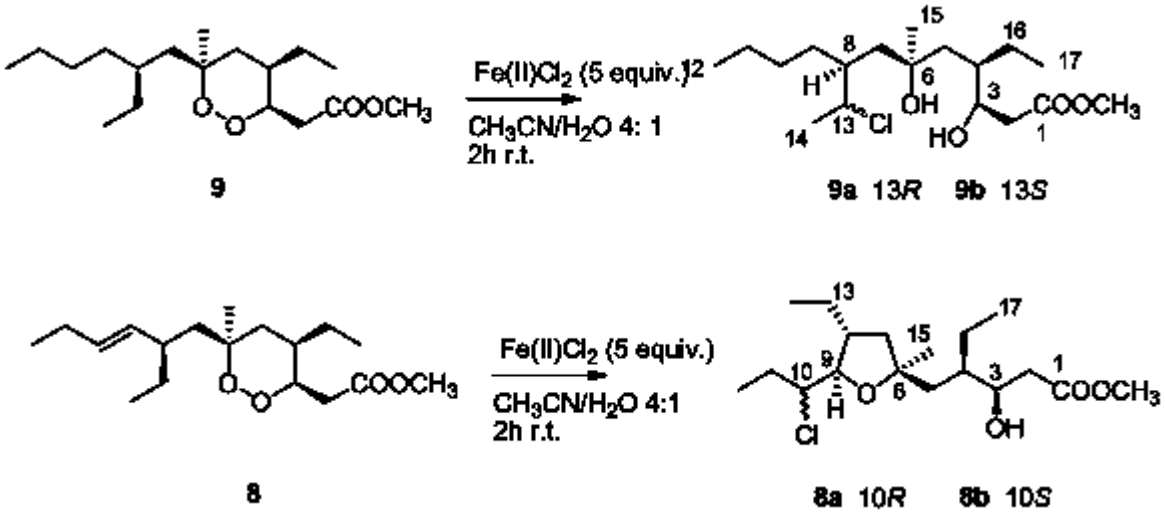

Figure 3.14. Products obtained upon reaction of bot plakortin (**8**) and dihydroplakortin (**9**) with iron(II)chloride

Compound **9a** showed ESIMS molecular ions at *m/z* 373 and 375 $[M+Na]^+$ (relative intensity approx. 3:1), an isotopic pattern suggesting the presence of a chlorine atom. This was confirmed by HR-EIMS, which indicated the molecular formula $C_{18}H_{35}ClO_4$, with one unsaturation degree. Since the methyl ester group is still present in compound **9a** (δ_C 174.6; δ_C 51.0, δ_H 3.72), the molecule must be acyclic. Analysis of the 2D COSY and HSQC spectrum of **9a** allowed us to disclose two distinct spin systems [highlighted in Fig. 3.15], which strictly mirrored the spin systems of dihydroplakortin, with more significant differences restricted to the "western" moiety. Within this moiety, the attachment of the chlorine atom at C13 (δ_H 4.53, δ_C 64.2) resulted from the COSY coupling of H13 with the relatively deshielded methyl protons at δ_H 1.45 (H_3-14) and with the methine H8 (δ_H 1.83), this latter proton belonging to a 6-carbon linear chain (from C7 to C12). The HMBC spectrum of **9a** confirmed this assignment and allowed the complete elucidation of the planar structure of compound **9a**. Most significant HMBC cross-peaks are reported in (Fig. 3.15). Elucidation of absolute configuration at the single newly created chiral center C13 was not trivial. To solve this issue, the *J-based configuration analysis* proposed by Murata for relative configurations in acyclic system was applied.[34]

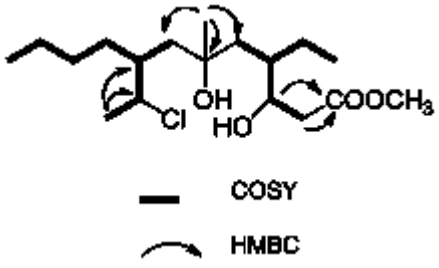

Figure 3.15. COSY and key HMBC cross-peaks detected for compound (**9a**)

This method is based on the combined analysis of the coupling constants $^{2}J_{C,H}$ (in systems ^{1}H-C-^{13}C-X, related to the dihedral angle between the proton and the heteroatom), $^{3}J_{H,H}$ and $^{3}J_{C,H}$ (both related to conformational parameters through the Karplus rule). The original method was proposed for X = OR but it was successively extended also to X = Cl and other different electron withdrawing groups.[35,36] Since C13 was adjacent to the chiral carbon atom C8, and the small value of $^{3}J_{H\text{-}8/H\text{-}13}$ (1.5 Hz) indicated that a dominant rotamer (with the two protons in a *gauche* orientation) existed around the C8/C13 axis, our molecule appeared to possess all the requirements essential for application of the Murata's method.[34] We qualitatively determined the four required heteronuclear coupling constants through an analysis of the phase-sensitive PS-HMBC spectrum and the obtained *J* data indicated a *threo* stereochemical relationship between C8 and C13 in compound **9a** (Fig. 3.16).

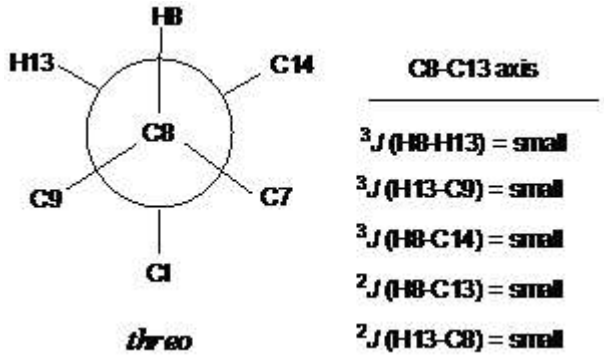

Figure 3.16. Application of the Murata method to the C8-C13 axis of compound (**9a**)

Consequently, on the basis of the known *S* configuration assigned at C8 for **9**, we deduced *R* configuration at C13 of **9a**.

Small amounts of the epimer at position 13, **9b** ($C_{18}H_{35}ClO_4$ by HR-EIMS), were also obtained. This molecule was easily identified on the basis of the broad similarities among its ^{1}H and ^{13}C NMR spectra and corresponding spectra of **9a**. The planar structure and

signal assignment were then unambiguously deduced on the basis of 2D NMR spectral (COSY, HSQC, HMBC) data. Since the small differences between the two series of NMR data are restricted to C/H resonances bordering with position 13, we confidently assigned the stereostructure of **9b** as the epimer of **9a** at the newly created chiral center C13. The reaction affording **9a** and **9b** is not stereospecific, however it produces **9a** in consistently higher amounts (about 6:1).

Reaction with $FeCl_2$ was then repeated for **8** in the same conditions (solv. CH_3CN/H_2O 4:1; r.t.; 2 hours) previously employed for **9** yielding only two major products, **8a** and **8b**, in ab. 2:1 relative yields. Determination of the complete stereostructures of these products proved to be quite simple, indeed, the structure of compound **8a**, $C_{18}H_{33}ClO_4$ by HR-EIMS, was assigned on the basis of the absolute identity of its spectroscopic data ($[\alpha]_D$, ^1H NMR, ^{13}C NMR) with those of plakortether C, a natural analogue of plakortin that we isolated some years ago from *Plakortis simplex* and whose complete absolute stereostructure was established.[37]

Compound **8b** showed the same molecular formula and very similar ^1H and ^{13}C NMR spectra compared to **8a**. Investigation of 2D NMR spectra (COSY, HSQC, HMBC) of **8b** indicated that this molecule must possess the same planar structure of **8a**; thus, as for **9**, the reaction produced a mixture of diastereomers. Inspection of the ROESY spectrum of **8b** disclosed a *cis* relationship between H-9 and H_3-15, identical to that of compound **8a**. Therefore, the difference between compounds **8a** and **8b** must reside on the configuration at C-10 and consequently, compound **8b** was identified as the epimer at C-10 of **8a**.

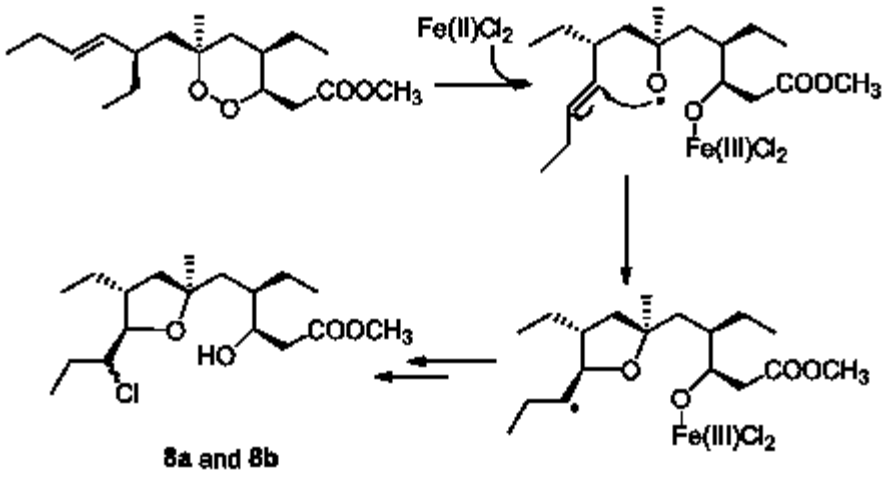

Figure 3.17. Mechanism hypothesized for the formation of compounds **8a** and **8b** upon reaction of plakortin (**8**) with $FeCl_2$

The above described computational and experimental investigations completely agree in suggesting the possible steps connecting the interaction Fe(II)heme/plakortin [or Fe(II)heme/dihydroplakortin] with the death of the parasite. In addition, obtained results stimulate some interesting considerations about the mechanism of antimalarial action of plakortins and related simple 1,2-dioxanes. The formation of the products **8a**/**8b** obtained upon reaction of **8** with $FeCl_2$, can be interpreted only by assuming the preferential formation of the oxygen radical at O1 (Fig. 3.17) in agreement with anticipation of computational calculations. In addition, the formation of O1-C9 linkage indicates that the O1 radical tends to react with the "western" side chain double bond, giving the consequent formation of the carbon radical at C10. Interestingly, the obtainment of a single configuration at C9 suggests that the reaction proceeds through a concerted mechanism, where the following events occur in a single step: 1) electron uptake from iron, 2) O1-O2 bond breaking with consequent O1 radical formation, 3) O1-C9 bonding with consequent C-10 radical formation.

This latter species represents the key toxic intermediate responsible for plakortin antimalarial activity and it is involved in a subsequent intermolecular reaction. These are valuable insights for the design of new derivatives since this reaction mechanism implies that the structure must simultaneously orientate all intramolecular reaction partners in order to trigger production of the toxic carbon radical. These results are in agreement with our previous conclusions that the lower activity of plakortins compared to artemisinin could be also attributed to the marked difference in the conformational behavior exhibited by these molecules .

In the experimental model, C10 carbon radical reacts to give the chlorine-linking mixture **8a/8b** (Fig. 3.17). The formation of this diastereomeric mixture evidenced that the chlorination was not concerted with the electron transfer reaction leading to formation of C10 radical. Also in the case of dihydroplakortin (Fig. 3.18), the obtained products suggest that the endoperoxide bond cleavage produced preferentially an oxygen radical at O1. In addition, products **9a/9b** indicate a selective involvement of C13 hydrogen atoms in the subsequent rearrangement which, most likely, takes place through a 1,5-H shift with formation of a carbon radical at that position. Then, the diastereoisomeric mixture of products **9a**/**9b** was formed upon chlorination at C13. As a consequence, in the case of **9**, the C13 carbon radical should be the toxic intermediate responsible for the antimalarial activity.

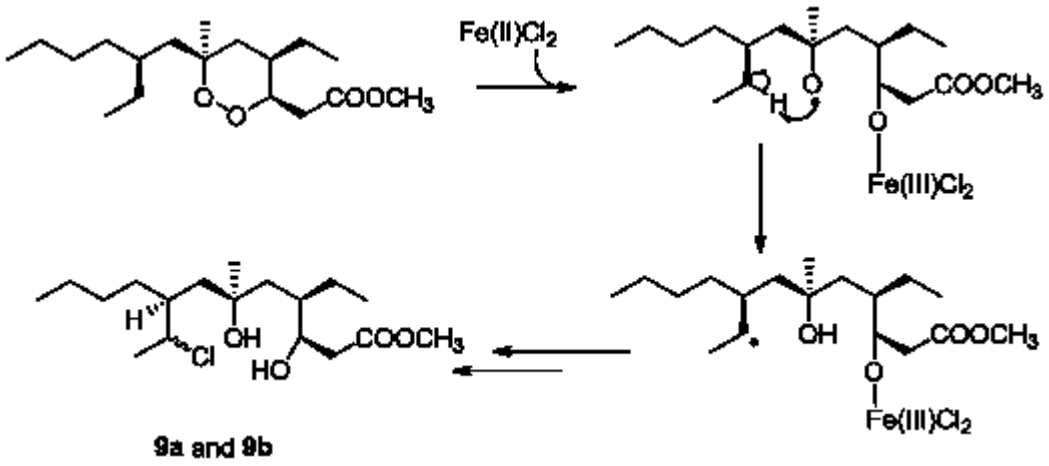

Figure 3.18. Mechanism hypothesized for the formation of compounds **9a** and **9b** upon reaction of dihydroplakortin (**9**) with $FeCl_2$.

Data about the exact mechanism going from carbon radicals of both plakortin (at C-10) and dihydroplakortin (at C13) to the corresponding chlorinated species are not available. A plausible hypothesis is a "chloro-Fenton" reaction involving direct abstraction of a chlorine atom linked at the Fe(III) center, recently proposed in a similar case.[38]

The observation of a diastereomeric mixture of chlorinated products, both for **8** and **9**, supports the availability of the formed carbon radicals (i.e., C10 and C13, respectively) for intermolecular reactions. These carbon radicals may exert their toxicity through direct reaction with plasmodium biomolecules (e.g., FV membrane lipids, heme, protein residues, glutathione), not requiring molecular oxygen to induce the oxidative stress in the parasite. The key role of carbon radicals, available for intermolecular reactions, is also supported by the behavior of artemisinin and derivatives, where steric hindrance significantly affecting carbon radical reactivity has a negative impact on antimalarial potency. [22,26]

Another remarkable outcome of our experiments is the complete absence (or undetectable presence) of cleavage products, upon reaction of **9** and **8** with $FeCl_2$. Indeed,

following the mechanism of oxygen radical evolution described for artemisinin derivatives (Fig. 3.10)[28,34] the formation of the carbon-carbon cleavage products, could be hypothesized. Thus, the absence of the postulated ketone derivatives as well as of products which could derive from the rearrangement/reaction of the postulated primary carbon radicals indicated that, at least in our experimental conditions, the cleavage mechanism does not operate for **8** and **9**. In this regard, it is interesting to notice that peroxyketal derivatives, structurally related to plakortin [e.g. compound **22**,[39] (Fig. 3.19), have been reported to produce, upon reaction in similar experimental conditions ($FeSO_4$ in aqueous solution), mostly cleavage products (Fig. 3.19).[40] Given the wide similarity between the two carbon scaffolds, the marked difference between the products obtained, upon reaction with ferrous ion, is a clear evidence that minor differences in the functionality pattern of a 1,2-dioxane [e.g. the presence of a peroxyketal in **22**] can result into dramatic differences in the evolution of the oxygen radicals.

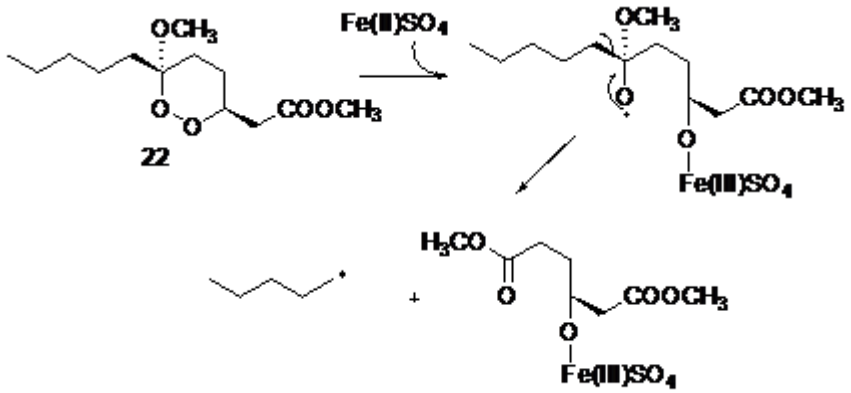

Figure 3.19. $FeSO_4$ induced cleavage of compound **22**

The results of our combined studies on plakortin and dihydroplakortin evidenced that plakortin alkyl chain double bond reactivity likely support carbon radical formation, on the

other hand, the weaker side chain reactivity of dihydroplakortin is balanced by favorable conformational parameters. This accounts for the comparable antimalarial activity of the two compounds (Table 1), despite the structural differences in their alkyl chains.

The results of this investigation, in agreement with previously reported SAR, also evidenced that the ester side chain is not directly involved in the formation of carbon radical intermediates, nevertheless, our docking results demonstrated that the presence of ester group may play a role in the interaction with iron, affecting endoperoxide approach to heme. Thus, the presence of iron-coordinating groups, other than the endoperoxide functionality, must be taken into consideration for the design of new plakortin-like antimalarials.

In summary, the mechanism of action of plakortin-based antimalarials involves the formation of an oxygen radical and its "through space" rearrangement to give a carbon radical centered on the “western” alkyl side chain, which is the toxic intermediate able to directly react with parasite biomolecules. Moreover, the following minimal structural requirements, necessary for the activity of this class of antimalarial agents, were identifie: 1) a 1,2 dioxane ring able to react with Fe(II) species through its endoperoxide group and to form an oxygen radical; 2) a side chain bearing possible partners for a “through space” intramolecular radical shift from the oxygen to a carbon atom, 3) a conformational preference for the conformer which allows the correct orientation of all the intramolecular reaction partners, and iv) the formation of a carbon radical amenable of intermolecular reactions. On these bases, a 1,2-dioxane ring side chain combining good reactivity (such as in plakortin) with favorable conformational preference (such as in dihydroplakoritn) should improve antimalarial activity.

3.4. Isolation of new endoperoxide derivatives from an Indonesian *Plakortis* sp.

In the course of an ongoing screening for bioactive secondary metabolites from Indonesian marine invertebrates,[41, 42] a specimen of *Plakortis* sp. collected in the Bunaken Marine Park of Manado (North Sulawesi, Indonesia) was analyzed. From the organic extract of this sponge we four new peroxyketal polyketides, named manadoperoxides A-D (**23**-**26**) (Fig. 3.20), have been obtained.

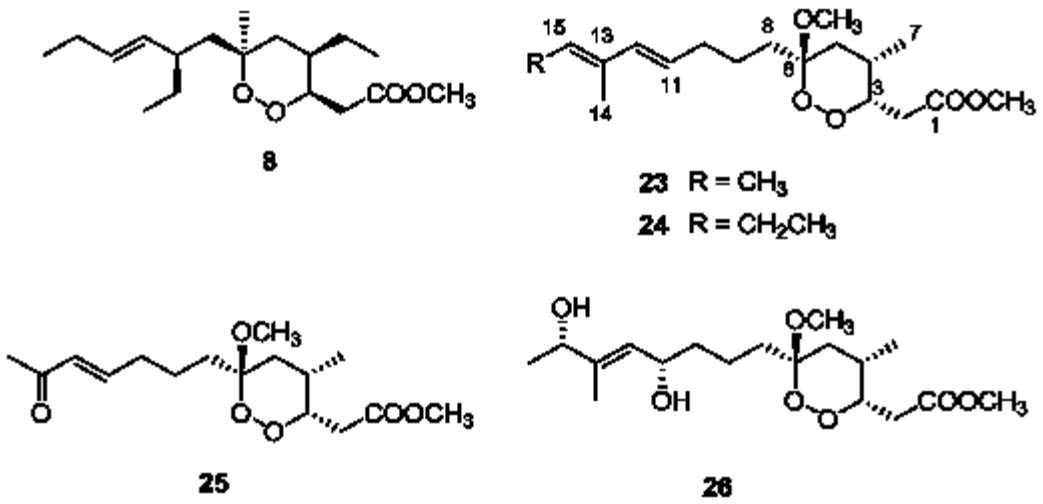

Figure 3.20. Chemical structures of manadopreoxides A (**23**), B (**24**), C (**25**) and D (**26**).

The isolation of these endoperoxide derivatives represented an attracting opportunity to extend the structure-antimalarial activity relationships previously established for the plakortin family. Thus, evaluation of their in vitro antimalarial activity was also carried out.

The sponge *Plakortis* sp. (order Homosclerophorida, family Plakinidae) was collected in January 2008 along the coasts of the Bunaken island in the Bunaken Marine Park of Manado. After homogenization, the organism was exhaustively extracted, in sequence, with methanol and chloroform. The combined extracts were subjected to chromatography over silica column followed by repeated column and HPLC chromatographies (*n*-

hexane/EtOAc mixtures) to afford manadoperoxides A-D (**23**-**26**) in the pure state. A small piece of the *Plakortis* sp. was also extracted with EtOH and, following the same chromatographic procedure, small amounts of manadoperoxides A-D were also obtained. This results rules out a possible role of the extraction solvent on the formation of the methoxylated manadoperoxides (see below).

Manadoperoxide A (**23**) showed pseudomolecular ion peaks at *m/z* 327 $[M + H]^+$ and 349 $[M + Na]^+$ in the positive ESI mass spectrum, while HR measurements assigned to **23** the molecular formula $C_{18}H_{30}O_5$, implying four unsaturation degrees. Analysis of ^1H and ^{13}C NMR spectra of **23** ($CDCl_3$, see Tables in Suporting Data), guided by inspection of the 2D HSQC experiment, revealed the presence of two sp^3 methines (one of which is oxygenated: δ_H 4.43, δ_C 80.1), five sp^3 methylenes, two double bonds [one trisubstituted (δ_H 5.44, δ_C 124.8; δ_C 133.3) and one disubstituted (δ_H 6.03, δ_C 135.8; δ_H 5.47, δ_C 126.0)], and five methyls (two of which are methoxy groups: δ_H 3.72, δ_C 52.2; δ_H 3.25, δ_C 48.8). The two remaining unprotonated carbon atoms (δ_C 171.9 and 103.4) were attributable to an ester and to a ketal group, respectively.

The COSY spectrum of **23** disclosed the sequential arrangement of proton resonances indicating the presence of three spin systems [A-C, depicted in bold in (Fig. 3.21)]. The first one (A) encompasses a methyl-branched C_4 chain (from C-2 to C-5); the second spin system (B) builds up a C_5 unbranched chain starting from the disubstituted double bond, while the third spin system (C) includes only an sp^2 methine coupled to a methyl group. These moieties were connected through interpretation of the 2D HMBC spectrum [key $^{2,3}J_{CH}$ correlations are depicted in (Fig. 3.21)].

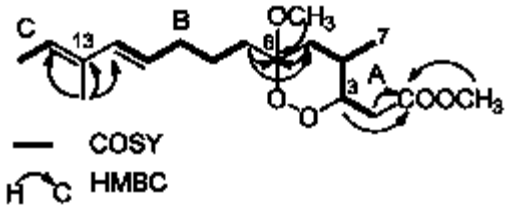

Figure 3.21. COSY and key HMBC cross-peaks detected for manadoperoxide A (**23**)

In particular, cross-peaks of H_3-14 with C-12, C-13 and C-14 allowed the joining of moieties B and C through C-13; analogously, the cross-peaks of H_2-5, of H_2-8 and of the oxymethyl group resonating at δ_H 3.25 with the ketal carbon resonating at δ_C 103.4 established C-6 as the connection point for moieties A and B. Furthermore, the ester carbonyl (δ_C 171.9) was placed at C-1 on the basis of its HMBC correlations with H_2-2 and H-3. Finally, the presence of an endoperoxidic bond connecting C-3 and C-6, accounting for the remaining unsaturation degree of the molecular formula, was supported by ^{13}C NMR resonances at δ_C 80.1 (C-3) and 103.4 (C-6), typical values for oxygenated carbons belonging to endoperoxyketal rings. [43]

The *E* geometry of the double bond Δ^{11} was deduced from the large vicinal coupling constant $J_{H\text{-}11/H\text{-}12}$ = 15.9 Hz. On the other hand, the spatial proximity (evidenced through a ROESY spectrum) between H-12 and H-15 indicated the *E* geometry of the double bond $\Delta^{13(15)}$. The ROESY spectrum (Fig. 3.22) allowed us also to define the relative orientation of the three stereogenic carbons belonging to the six-membered ring.

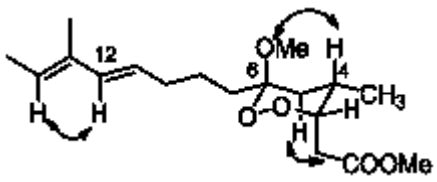

Figure 3.22. Key ROESY cross-peaks detected for manadoperoxide A (**23**)

Particularly informative were the ROESY cross-peaks of H-4 with OMe-6 and of H-5ax with H-2a. The *trans* equatorial-axial orientation of H-3/H-4 was also supported by the low value of the vicinal coupling constant $J_{H\text{-}3/H\text{-}4}$ = 3.0 Hz.

The determination of absolute configuration at the three stereogenic centers of manadoperoxide A was accomplished through application of the modified Mosher's method[44] on a semisynthetic derivative (Fig. 3.23).

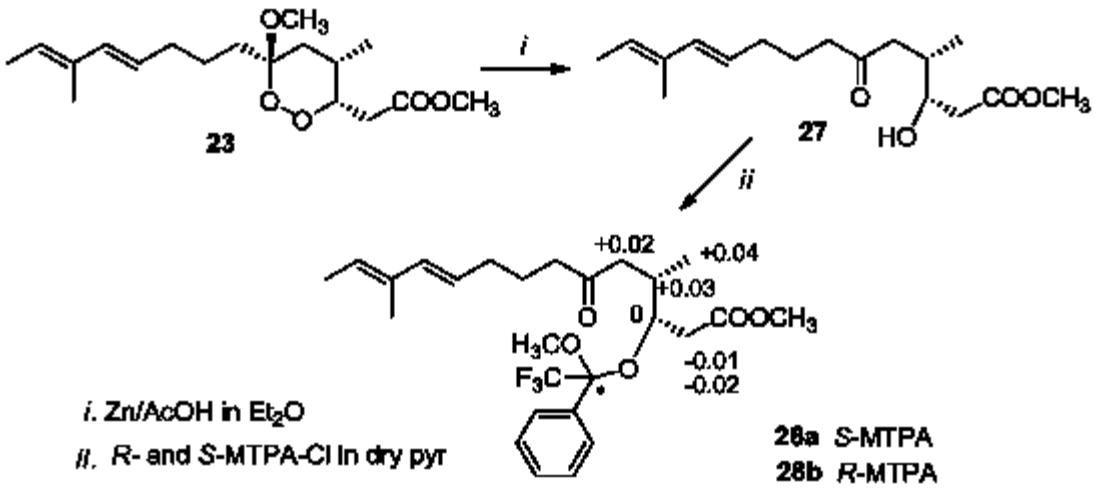

Figure 3.23. Application of the modified Mosher's method for determination of absolute configuration at C-3 of manadoperoxide A

Thus, reductive cleavage (Zn/AcOH) of the endoperoxide bond of **23** yielded the hydroxyketone derivative **27** (present in equilibrium with the cyclic hemiketal forms), which was allowed to react with *R*- and *S*-MTPA chloride to obtain the corresponding *S*- and *R*-MTPA esters (**28a** and **28b**), respectively. Analysis of the Δδ(S – R) values of the MTPA esters according to the Mosher's model indicated the *S* configuration at C-3. On the basis of the previously determined relative configuration, a 3*S*,4*S*,6*R* configuration was assigned to manadoperoxide A.

Interestingly, Scheuer and coworkers reported from a *Plakortis* sp. collected near Manado, in the same area of our specimen, the isolation of manadic acid A,[45] a diastereomer of manadoperoxide A differing only for the configuration at C-6. It should be noted that manadic acid or its esters were completely undetectable in the organic extract of our *Plakortis* sp., and, thus, apparently, the two different *Plakortis* sp. specimens elaborate the same secondary metabolite but with opposite configuration at a single carbon atom. A similar case, involving a different class of marine metabolites, has been recently reported by Crews and coworkers, [46] who discovered distinct *Theonella swinhoei* populations producing either 2*S*-motuporin or 2*R*-motuporin. In our opinion, these intriguing observations would be worthy of further investigations.

Three additional manadoperoxides (B-D, **24**-**26**) were isolated from the organic extract of *Plakortis* sp. and their stereostructural elucidation followed the same spectroscopic approach above detailed for **23**, including analysis of 1D and 2D NMR (COSY, HSQC, HMBC, ROESY) spectra. The complete assignment of proton and carbon resonances is reported in the Experimental Section. For brevity, in the following discussion, I will highlight only the significant differences between each of these molecules and manadoperoxide A. These differences are restricted to the length and/or functionalization of the "western" alkyl chain, and, accordingly, their H/C resonances from positions 1 to 9 resulted to be almost coincident to those of **23**. Furthermore, ROESY cross-peaks obtained for **24**-**26** confirmed that also the relative configuration around the six-membered ring is identical to that of compound **23**. Due to the limited amount available for manadoperoxides B-D, partly employed also for biological tests, the absolute configurations at C-3/C-4/C-6 of **24**-**26** have not been determined; their structures have been drawn extending those above deduced for manadoperoxide A. In the case of manadoperoxide D (**26**), we preferred to

employ an aliquot of the sample to determine the absolute configuration of side chain stereocenters (see below).

Manadoperoxide B (**24**), $C_{19}H_{32}O_5$ by HRMS, contained only an additional methylene group compared to compound **23**. This group was easily located at C-16 (δ_H 2.09; δ_C 21.9) on the basis of the vicinal couplings of H_2-16 with both H-15 (δ_H 5.40, t) and the methyl H_3-17 (δ_H 1.00, t). Also in this case, the ROESY cross-peak H-12/H-15 indicated the *E* geometry of the double bond $\Delta^{13(15)}$.

Manadoperoxide C (**25**), $C_{16}H_{26}O_6$ by HRMS, showed a shortened side chain compared to compound **23**. Inspection of ^{1}H, ^{13}C NMR and 2D NMR COSY spectrum of **25** indicated the presence of a single double bond, located at the terminus of the five-carbons spin system starting with H_2-8. The relatively low field resonances of H-11 (δ_H 6.78) and H-12 (δ_H 6.18) and the presence of a carbonyl resonance at δ_C 198.7, in the ^{13}C NMR spectrum of **25**, suggested the presence of a conjugated ketone group. This was supported by the $^{2,3}J$ HMBC cross-peaks of the relatively downfield shifted methyl singlet at δ_H 2.25 both with the ketone carbonyl (C-13) and with C-12. The coupling constant $J_{H\text{-}11,H\text{-}12}$ = 16.4 Hz was indicative of the *trans* geometry of $\Delta^{11,12}$.

The molecular formula of manadoperoxide D (**26**), $C_{18}H_{32}O_7$ by HRMS, indicated the presence of two additional oxygen atoms compared to compound **23**. 1D NMR spectra of **26**, analyzed with the help of 2D NMR COSY and HSQC spectra, disclosed the arrangement of the proton multiplets of the “western” side chain within two spin systems (Fig. 3.24), comprising two oxygenated methines.

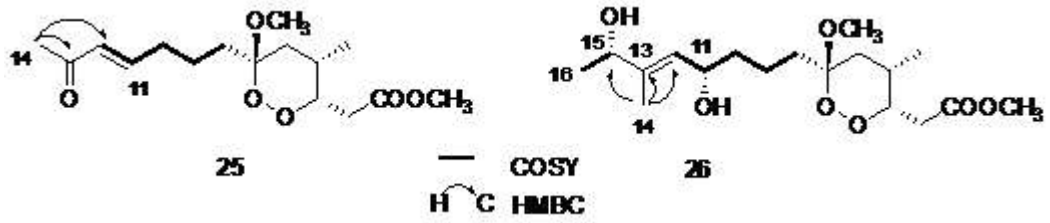

Figure 3.24. COSY and HMBC correlations detected for manadoperoxides C (**25**) and D (**26**)

The first spin systems spans from H_2-8 to the single sp^2 methine H-12 (δ_H 5.45, δ_C 127.1), and includes an oxymethine at position 11 (δ_H 4.40, δ_C 70.1); the second spin system includes only the second oxymethine (δ_H 4.22, δ_C 72.8) coupled with a methyl group (δ_H 1.27, δ_C 17.9). The HMBC cross-peaks of H_3-14 with C-12, C-13 and C-15 determined the connection for the above moieties, thus defining the gross structure of the "western" side chain for manadoperoxide D. The spatial proximity of H_3-14 with H-11 (ROESY cross-peak) indicated the *E* geometry of the side chain double bond.

The absolute configurations at the two stereogenic carbons C-11 and C-15 of **26** were determined through application of the Riguera method for 1,*n*-diols.[47] To this aim, two aliquots of **26** were allowed to react with *R*- and *S*-MTPA chloride, obtaining the diesters **29a** and **29b**, respectively (Fig. 3.25). Positive Δδ (S – R) values for protons going from H-10 to H-16 indicated, according to the Riguera model[47] the 11*S*, 15*S* configuration.

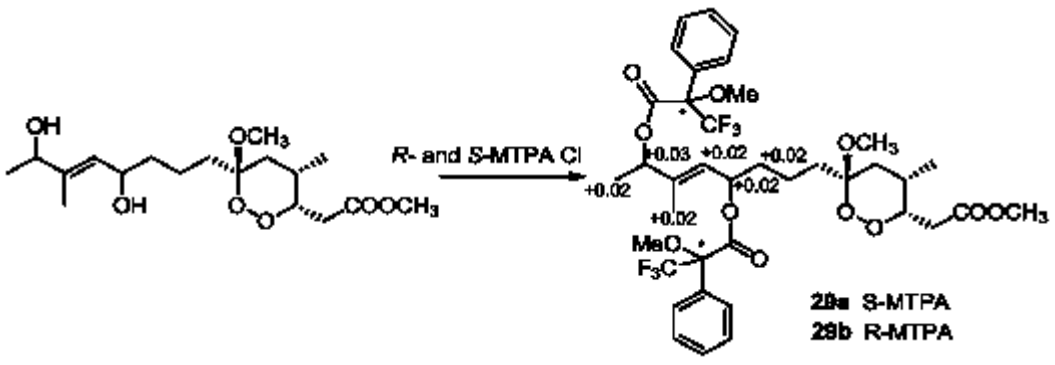

Figure 3.25. Application of the Riguera's model for determination of side chain absolute configuration in mandaoperoxide D (**26**)

The endoperoxide derivatives **23**-**26** were assayed in vitro against D10 (chloroquine sensitive, CQ-S) and W2 (chloroquine resistant, CQ-R) strains of *Plasmodium falciparum* using the pLDH assay. Obtained results (compiled in Table 2) evidenced a moderate antimalarial activity (low μM range) against both CQ-R and CQ-S *P. falciparum* clones for the four manadoperoxides **23**-**26**. The variations in the side chains cause slight, but significant, differences in the antimalarial activity, with manadoperoxide C (**25**) being the most active compound of the series. Furthermore, the IC_{50} values of **23-26** against the CQ-R strain were almost the half (higher efficacy) of those against the CQ-S strain, as already found for artemisinin and plakortin analogues. [11,1]

Table 3.2. In vitro antimalarial activity of manadoperoxides A-D (**23**-**26**), against D10 (CQ-S) and W2 (CQ-R) strains of *P. falciparum*.

	D10	W2
	IC_{50} μM	IC_{50} μM
23	6.88 ± 0.37	3.74 ± 0.92
24	6.76 ± 0.32	3.69 ± 0.88
25	4.54 ± 0.66	2.33 ± 0.48
26	10.38 ± 0.76	7.93 ± 0.68
Chloroquine	0.043 ± 0.006	0.65 ± 0.09

Data are means ± SD of four different experiments in triplicate

The modest antimalarial activity of manadoperoxides is particularly surprising for example upon comparison of manadoperoxide B (**24**) with peroxyplakoric B_3 ester (**30**), (Fig. 3.25)[43].

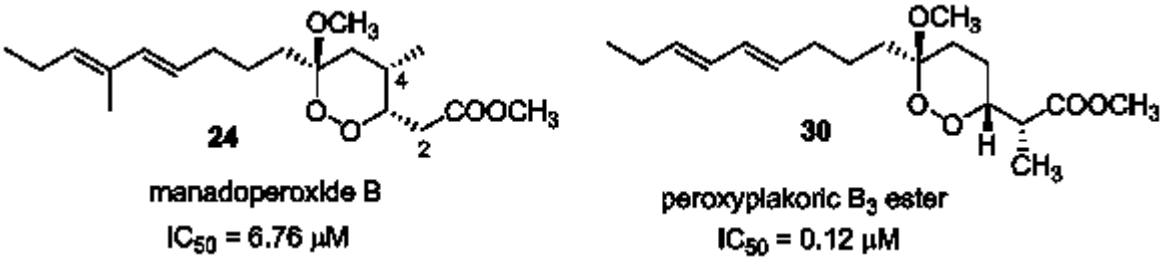

Figure 3.26. Comparison of structures and activities of manadoperoxide B (**24**) and peroxyplakoric B_3 (**30**) ester

In spite of the very small structural differences (a methyl group linked at C-2, in **30**, in place of C-4, in **24**), compound **30** exhibited a 56-times higher in vitro antimalarial activity compared to **24**.[48] However, this unexpected difference can be rationalized on the basis of our recently published model for the antimalarial activity of 1,2-dioxanes.[1]

Briefly, the presence of a methyl at C-4 on the dioxane ring of manadoperoxides induces a preferential chair B conformations were two groups are in axial positions. This implies that the approach of manadoperoxides to heme iron is complicated (if not prevented) by the orientation of groups on the dioxane ring. Of course, this problem is not present for compound **30**, thus highlighting the impact on antimalarial activity also of subtle structural changes.

3.5. Synthesis of simplified antimalarial endoperoxides

As reported in the previous paragraphs, the isolation of plakortin analogues from *Plakortis simplex*[2] and related sources and the preparation of a series of semi-synthetic plakortin derivatives[1] provided information about the structural requirements of these simple 1,2-dioxanes for exhibiting antimalarial activity. These results confirmed the crucial role of the endoperoxide functionality (the plakortin diol is completely inactive), suggested the importance of the "western" alkyl side chain and revealed conformation-dependent features critical for antimalarial activity.[1]

In a preceding paragraph,[21] using a combined chemical and computational approach, I have described our results on the possible mechanism of antimalarial action for molecules belonging to the plakortin family. This investigation resulted in the proposal that, upon interaction with the Fe(II) (likely heme) center, and consequent formation of an oxygen-

centered radical (preferentially O1), a simultaneous "through space" 1,4 or 1,5 intramolecular radical shift to a western side chain carbon takes place. This yields to the formation of carbon radicals at the "western" side chain which should be the toxic species responsible for the antimalarial activity through intermolecular reactions with unidentified plasmodium macromolecular targets. Thus, accessibility of endoperoxide oxygens to the reactive iron species and correct orientation of O1 with respect to reaction partners for an intramolecular radical shift, are essential requirements of the bioactive conformation.

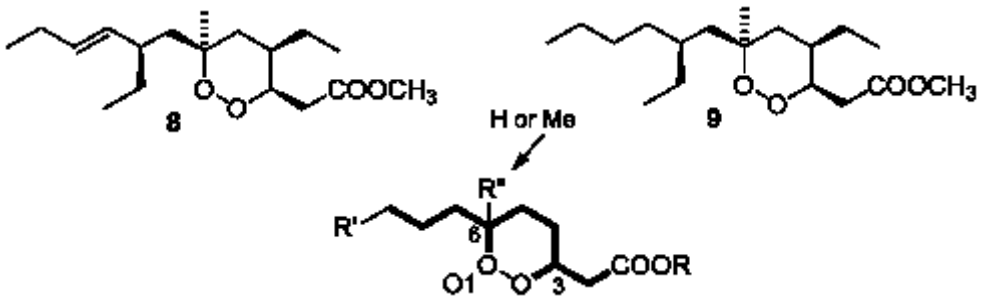

Figure 3.27. The simplified plakortin scaffold

Basing on these results, I have designed and accomplished the synthesis of simplified plakortin analogues, which have been evaluated for their antimalarial activity. A simplified plakortin molecular scaffold, including only the essential pharmacophoric portions, should include (Fig. 3.27): 1) a dioxane ring; 2) a monosubstitution at position 3; 3) a mono- or disubstitution at position 6, which should guarantee the presence of an alkyl chain long enough to provide a partner for the above described intramolecular shift.

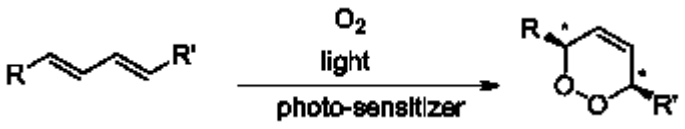

Figure 3.28. Schematic photo-oxygenation of 1,3-butadiene derivatives

The need for an easy and cheap synthesis directed our interest toward the singlet oxygen addition to 1,3-butadiene derivatives for the construction of the endoperoxide ring, the critical step of the synthetic procedure. This reaction, depicted in figure 3.29, yields 3,6-disubstituted 1,2-diox-4-ene derivatives and occurs readily for acyclic conjugated dienes.[49] The mechanism of this reaction has been investigated in detail[50,51] and some aspects are worthy of being noted: 1) As shown in figure 3.28, the relative configuration of the product is directly dependent from the geometry of the reagent as a consequence of a pseudo-concerted mechanism of reaction.[50] 2) For reactions with butadienes, the dienophilic reactivity of $^1O_2$ surpasses the other two possible modes of reaction, which would afford hydroperoxides (even if allylic hydrogen atoms are present) and 1,2-dioxetanes. 3) This reaction requires a *cisoid* conformation of the butadiene derivative and the *E,E* isomer reacts faster than the *E,Z* and *Z,Z* isomers. This is likely the result of differences in the planar *cisoid/transoid* conformational equilibrium. The planar transoid conformation is predominant for all the butadiene derivatives, but the energy differences between the cisoid and transoid conformations are significantly different due to steric constraints associated with each isomer. 4) Substituents R and R' (Fig. 3.28) should not be electron-withdrawing groups. In this regard, it has been already reported that the ethyl ester of *E,E*-2,4-hexadienoic acid is practically inert to sensitized photooxygenation.[52] In the design of the present synthetic project we have experimentally verified that the same is true for *E,E*-2,4-alkadienal derivatives (e.g. *E,E*-2,4-nonadienal) and for *E,E*-alka-3,5-dien-2-one derivatives.

On the basis of this available information, I planned to utilize the photo-oxygenation of *E,E*-alka-3,5-dienoic acid esters, where the double bond system is not conjugated with the carbonyl group. A literature search revealed that the Ragoussis' modified Knoevenagel

condensation could be fruitfully exploited for our needs.[53,54] The most important features of this reaction are: 1) the non-basic solvent (DMSO), 2) the addition of catalytic amounts of piperidinium acetate. The combined effect of both these changes is a minimization of the decarboxylative elimination of water, which occurs in the normal Knoevenagel mechanism, while the dehydration of the hydroxylated intermediate to a non-conjugated β,γ-unsaturated dicarboxylic derivative is favored. The final decarboxylation of this intermediate yields an ester of alk-3-enoic acid (Fig 3.29).

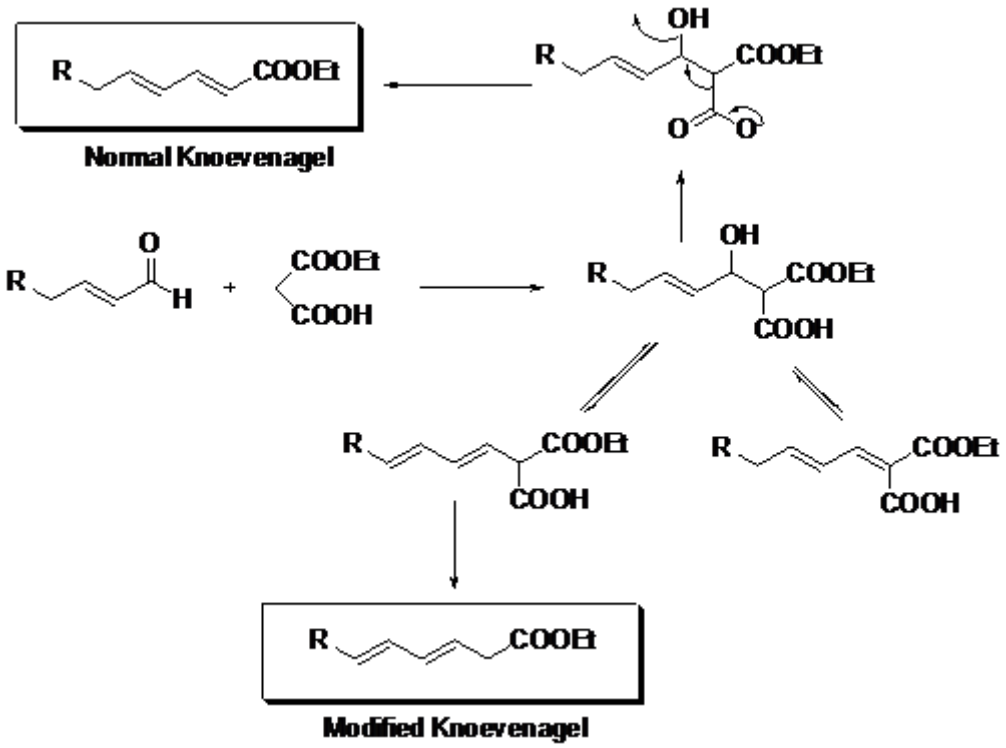

Figure 3.29. Schematic description of the Ragoussis' modified Knoevenagel reaction

Thus, the commercially available *trans*-2-nonenale (**31**) was allowed to react with ethyl hydrogen malonate in DMSO at 85 °C for 4 hrs in the presence of catalytic amounts of piperidinium acetate (Fig. 3.30). After work up, the mixture of obtained dienyl esters was further purified through repeated HPLC and argentation chromatography, to obtain ethyl

undeca-3*E*,5*Z*-dienoate (**33**), ethyl undeca-3*E*,5*E*-dienoate (**34**), and trace amounts of the conjugated derivative **32**, in the pure state.

Compound **34** was then subjected to photo-oxygenation reaction using methylene blue as photo-sensitizer. A solution of **34** and methylene blue in chloroform was irradiated under an oxygen atmosphere with a halogen lamp (500W) for 8 hrs at -20 °C to afford in high yields the endoperoxide derivative **35**. Given the laborious chromatographic procedure necessary to obtain the diene derivative **34** in the pure state, we attempted the photo-oxygenation reaction on the crude dienyl esters fraction obtained from the above modified Knoevenagel procedure. When the mixture was allowed to react in the same conditions, we obtained a product which contained a mixture of the unreacted dienes **32** and **33** and the endoperoxide **35** as a single diastereomer, whose purification proved to be particularly simple. This outcome is in perfect agreement with the above reported order of reactivity for dienyl esters: *E,E* (non-conjugated) > *Z,E* (non-conjugated) >> *E,E* (conjugated). Of course, in the search of an economically affordable procedure for the synthesis of simple antimalarial dioxanes, the elimination of a complex and low-yielding chromatographic step, is a particularly appreciated result.

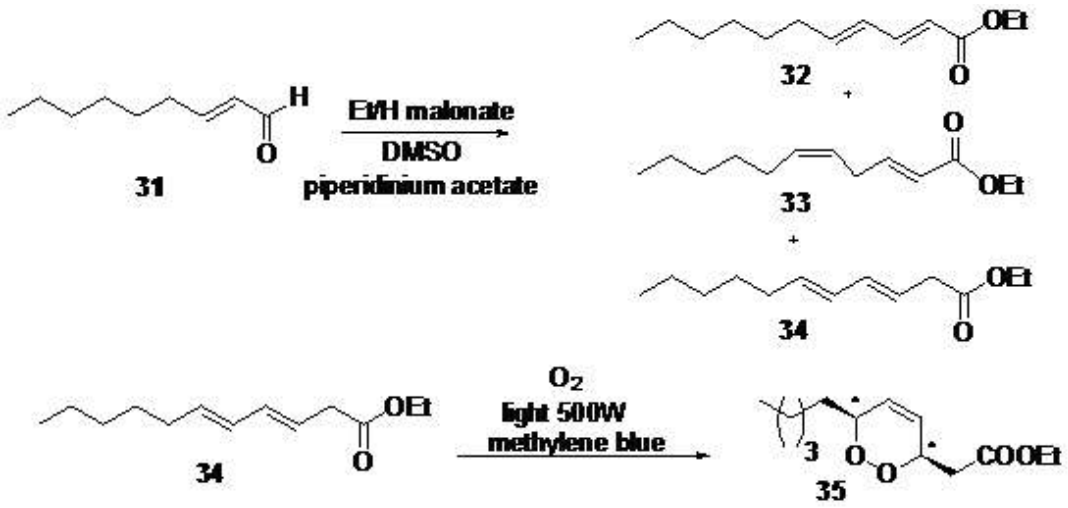

Figure 3.30. Synthesis of the endoperoxide **35**

Then, taking advantage of the reactivity of both the ester and the endocyclic double bond groups, a series of derivatives of the endoperoxide **35** were prepared. Starting from modifications at the ester group (Fig. 3.31), following parallel reaction conducted for plakortin,[2] selective ester reduction to the corresponding alcohol **36** was accomplished with the use of $LiBH_4$. Standard acetylation of **36** gave the corresponding ester **37**, while LiOH-mediated hydrolysis of the ester group afforded the carboxylic acid derivative **38** in good yield. Interestingly, attempts of obtaining reaction of the ester group with an organometallic reagent (butyl magnesium bromide) afforded, exclusively, attachment of the butyl group at one of the endoperoxide oxygen atoms, with consequent cleavage of the endoperoxide bond and formation of the ether derivative **39**.

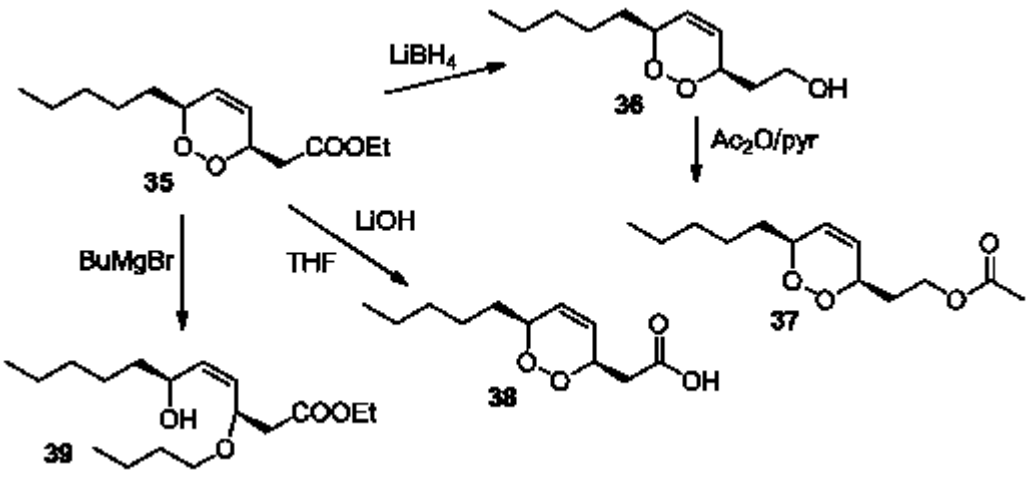

Figure 3.30. Compounds prepared upon reaction of endoperoxide **35** at the ester center

Subsequently, reactions at the double bond of **35** afforded derivatives shown in Figure 3.31. Compound **35** was initially subjected to a K_2OsO_4-mediated dihydroxylation reaction, following a recently reported procedure aimed at asymmetric sugar synthesis.[13] This

reaction produced, almost exclusively (> 99%), the single diastereomer **40** (structure and stereochemistry assigned through 2D NMR spectroscopy), as a racemic mixture. This compound is formed by *anti* addition of the 1,2-diol unit with respect to the substituents α to the peroxide linkage, as a result of the tendency of the hydroxylation reagent to add from the least hindered face. Compound **40** proved to be relatively unstable at room temperature and was kept at 0 °C.

Treatment of **35** with m-CPBA in CH_2Cl_2 afforded, in high yields, a mixture of two compounds, which were purified through normal-phase HPLC. Extensive use of 1D and 2D NMR spectroscopy (particularly of ROESY experiment for the stereochemical assignment) allowed the identification of the diastereomeric epoxide derivatives **41** and **42**, corresponding to the products of the two possible approaches of the epoxidizing reagent to the double bond. Of course, both compounds were obtained as racemic mixtures. Analogously, bromination at the double bond afforded the two diastereomeric racemic mixtures **43** and **44**.

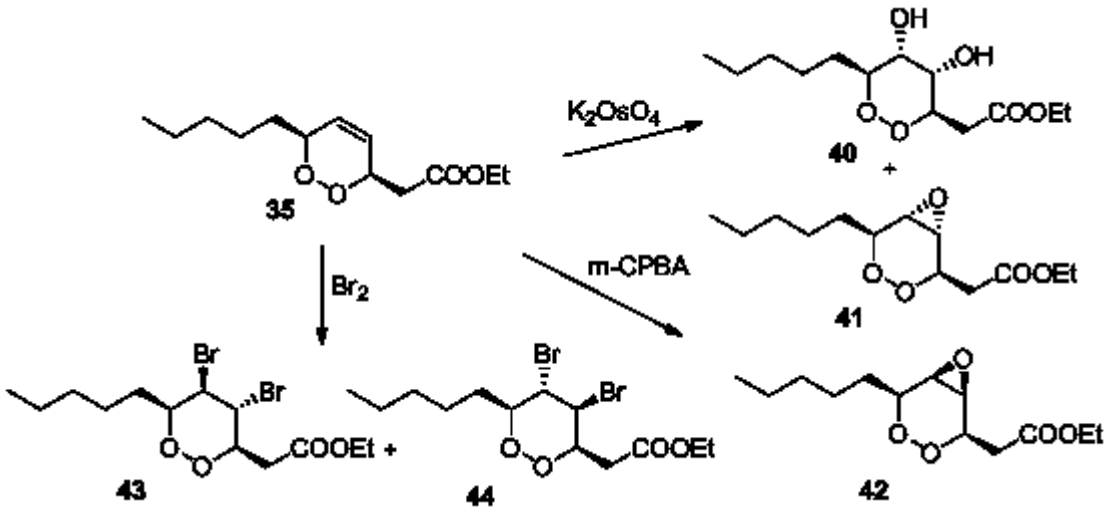

Figure 3.31 Compounds prepared upon reaction of endoperoxide **35** at the endocyclic double bond

Finally, we attempted chemoselective reduction of the double bond. Diimide-mediated reduction appeared to be the best candidate reaction to accomplish this transformation. Unfortunately, all our attempts, including *in situ* generation of diimide in different conditions, proved to be unfruitful. While diimide reduction has been reported for dioxene derivatives embedded in bicyclic systems,[14,15] as those deriving from singlet oxygenation of 1,3-cycloalkadienes, the same reaction is practically ineffective for simple monocyclic dioxene derivatives.

All the synthetic derivatives prepared in the course of this study have been evaluated for in vitro antimalarial activity against D10 (chloroquine-sensitive) and W2 (chloroquine-resistant strains). Obtained results, reported in (Table 3.3), deserve interesting comments.

Table 3.3. In vitro antimalarial activity of compounds **35-44** against D10 (CQ-S) and W2 (CQ-R) strains of *Plasmodium falciparum*.

	D10	**W2**
	IC_{50} μM	**IC_{50} μM**
35	1.20 ± 0.21	1.49 ± 0.22
36	Inactive	Inactive
37	21.90 ± 1.33	12.50 ± 2.51
38	3.33 ± 0.68	3.42 ± 0.56
39	Inactive	Inactive
40	Inactive	Inactive
41	22.10 ± 6.55	10.30 ± 3.21
42	Inactive	Inactive
43	8.15 ± 1.34	5.11 ± 0.98
44	9.12 ± 0.88	5.65 ± 1.22
Chloroquine	0.11 ± 0.01	1.39 ± 0.25

Data are means ± SD of four different experiments in triplicate
Inactive means IC_{50} > 30 μM

The most active compound of the series is compound **35**, which showed a quite good antimalarial activity (low μM range, about one half of the plakortin potency) on both

strains of *P. falciparum*. On the contrary, all the synthetic derivatives prepared from **35** proved to be less active than their parent compound, but in different extent. While the inactivity of **39** was expected on the basis of its lack of the endoperoxide bond, it is interesting to notice the marked decrease of activity caused by reduction of the ester group, dihydroxylation and epoxidation of the double bond. On the other hand, although still causing a decrease in the pharmacological activity, bromination and hydrolysis of the ester group appeared to be better tolerated.

In conclusion, basing on the plakortin pharmacophore, I have prepared a good antimalarial compound starting from commercially available material and using a sequence of two easy and cheap reactions. All the attempted modifications on the molecular scaffold of **35** caused a decrease in the pharmacological activity. However, a number of different "long" alkyl chains could be prepared by starting from a different α,β-unsaturated aldehyde.

CHAPTER 4- FURTHER SECONDARY METABOLITES FROM MARINE ORGANISMS

4.1. *Theonella swinhoei*[3]

Taking advantage of the official agreement established between the University Federico II of Naples and the University of Sam Ratulangi of Manado (Indonesia), we have the opportunity of participating to an annual expedition along the coasts of Bunaken Islands, Manado (Indonesia). During this expeditions, a number of marine invertebrates are collected to be annalyzed for their chemical composition and biological activity of the secondary metablites. In the frame of this project,[58] I had the opportunity to examine a specimen of *Theonella swinhoei* collected along the coasts of Manado (North Sulawesi, Indonesia).

Marine sponges belonging to the genus *Theonella* (Lithistida, Theonellidae) are remarkably prolific sources of structurally intriguing and diverse secondary metabolites, which have been calculated to represent more than nine biosynthetic classes.[59] These include non-ribosomal peptides with promising biological activities (as the antifungal theonellamides,[60] the cytotoxic polytheonamides,[61] and the antiviral papuamides[62]), complex polyketides as swinholide A,[63] and tetramic acid glycosides as aurantosides.[64] There is a continuing speculation that symbiotic microorganisms could be the true producers of many of these compounds. This hypothesis has been convincingly supported in the cases of swinholide A and onnamides: the former has been isolated from two field collections of marine

cyanobacteria,[65] while the involvement of symbiotic microorganisms in the production of the latter has been demonstrated through the isolation of the biosynthetic gene cluster from the complex metagenome of the sponge.[66]

A specimen of the sponge *Theonella swinhoei* was collected by hand in the area of the Bunaken Marine Park of Manado and kept frozen until sequentially extracted with methanol and dichloromethane by soaking the diced sponge tissue (560 g wet wt.). The extracts were concentrated, combined, and then partitioned between ethyl acetate and water. The EtOAc-soluble material was chromatographed on silica gel, using a gradient solvent system of *n*-hexane/EtOAc/MeOH. Fractions eluted with *n*-hexane/EtOAc (3:7) were combined and further purified by reverse-phase HPLC to obtain a new chlorinated polyene as yellow amorphous solid, which we named aurantoic acid (**45**) (Fig. 4.1). From the less polar fractions of the organic extract, we obtained also and a 4-methylene sterol, named dehydroconicasterol (**46**), together with the known molecules aurantoside G (**47**), conicasterol (**48**), and theonellasterol (**49**).

The electrospray mass spectrum of **45** showed pairs of ions at *m*/*z* 225/227 $[M + H]^+$ and at *m*/*z* 247/249 $[M + Na]^+$, both in ab. 3:1 ratio, suggesting the presence of a chlorine atom. The low resolution ESIMS data, along with ^1H and ^{13}C NMR data, pointed to a molecular formula of $C_{12}H_{13}ClO_2$, indicating six unsaturation degrees, which was confirmed by HR-MS. The UV-visible spectrum (MeOH) showed absorptions characteristic of a polyene system (λ_{max} 346 and 363 cm^{-1}). The ^1H NMR spectrum of **45** (500 MHz, $CDCl_3$) showed the signals of a vinylic methyl (δ 2.19, bs) and of nine multiplets in the downfield region (δ 5.8-7.4). Four of these resonances appeared as well resolved and isolated signals (δ 7.31, 6.54, 6.26, and 5.86), while two clusters centred around δ 6.62 (two overlapping signals) and 6.40 (three overlapping signals) were deconvoluted with the aid of 2D NMR experiments.

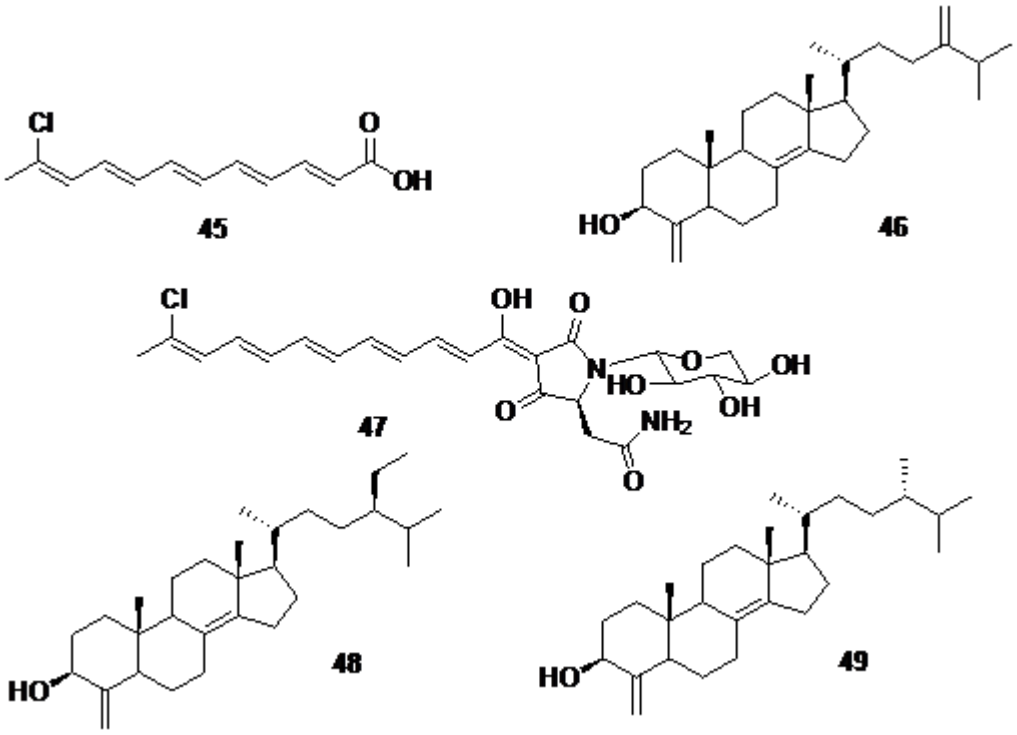

Figure 4.1 Chemical structures of aurantoic acid (**45**), dehydroconicasterol (**46**), aurantoside G (**47**), conicasterol (**48**), and theonellasterol (**49**)

Careful analysis of the COSY and TOCSY spectra allowed us to build up a single spin system going from H-2 to H-10, while the HSQC experiment guaranteed the association of the resonances of all these sp^2 methines with those of the relevant carbon atoms. In addition to the resonance of the methyl at δ_C 25.3, the ^{13}C NMR spectrum of **45** showed also the signals of two sp^2 unprotonated carbons at δ_C 132.6 and 169.1, respectively. The latter resonance could be assigned to a carboxylic group, located at C-1 on the basis of its HMBC cross-peaks with both H-2 and H-3. Analogously, the resonance at δ_C 132.6 should necessarily be assigned to the chlorine-linking carbon atom, which was placed at C-11 on the basis of its HMBC cross-peaks with Me-12, H-10 and H-9. The *trans* geometry of the four disubstituted double bonds was easily inferred from the coupling constant values ($J_{H-2/H-3}$, $J_{H-4/H-5}$, $J_{H-6/H-7}$, $J_{H-8/H-9}$), ranging from 14.9 to 15.4 Hz. The *Z* geometry of the Δ^{10} double bond was deduced from the NOE correlation of H-10 with CH_3-12.

The extensively conjugated system of aurantoic acid **45**, consisting of a sequence of five double bonds and one carboxylic acid, make this compound a particularly labile molecule. Indeed, we observed that both the storage in moderately acidic solvents, as chloroform, and the exposure to light triggered the slow formation of a mixture of products. Although the structures of these molecules have not been characterized in detail, partial available data suggest the occurrence of extensive *trans/cis* isomerizations. Indeed, the ESI mass spectrum of the mixture showed unchanged molecular ions at *m/z* 225/227 $[M + H]^+$ and at *m/z* 247/249 $[M + Na]^+$, while its ^1H NMR spectrum exhibited a series of new resonances in the vinylic region, overlapping to those of the original molecule.

Aurantoic acid **45** can be viewed as a unique member in the class of naturally occurring conjugated polyene derivatives. Interestingly, also the non-chlorinated analogue of aurantoic acid (2,4,6,8,10-dodecapentenoic acid) has never been found in nature, while, the isomeric 3,5,7,9,11-dodecapentenoic acid was obtained from the insect *Llaveia axin*.[67]

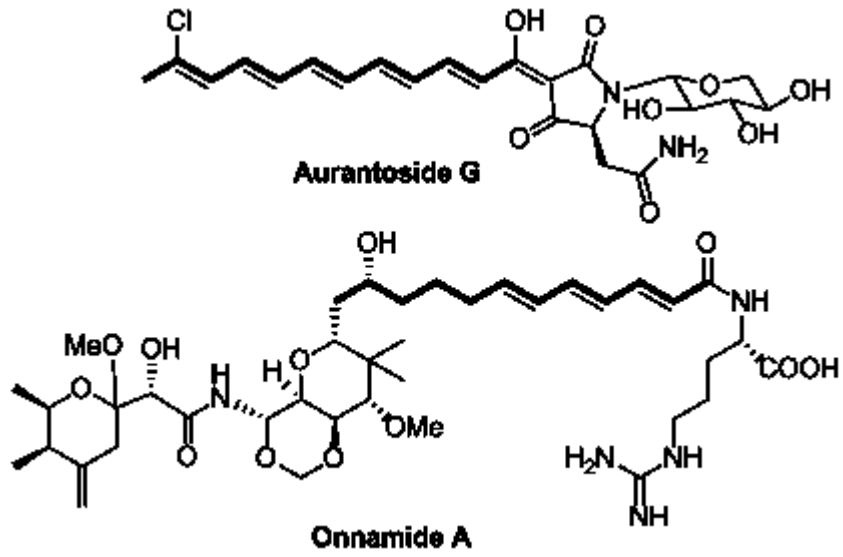

Figure 4.2 The aurantoic acid moiety (highlighted in bold) in the structure of aurantoside G and a related dodecenoic acid moiety (highlighted in bold) in the structure of onnamide A

Figure 4.2 highlights that a non-chlorinated aurantoic-like subunit is detectable in the structure of onnamide A[68] and that a chlorinated polyene moiety, clearly reminiscent of aurantoic acid, is evident in the structures of aurantosides, particularly of aurantosides G-H.[64] These tetramic acid glycosides have been proposed to derive from a condensation reaction between an aminoacid (*L*-aspartic acid) and a polyene acid, followed by *N*-glycosilation.[64] Thus, it is interesting to notice that the carbon chain of aurantoic acid (C_{12}) lacks one acetate unit compared to the postulated polyene precursor of aurantosides G-H (C_{14}) and two acetate units compared to the corresponding precursor of aurantosides A-E (C_{16}).[69]

Interestingly, we isolated aurantoside G (**47**) as a reddish solid from the polar fractions (Si-fractions eluted with EtOAc/MeOH 9:1) of the organic extract of *T. swinhoei*, and assigned its structure basing on the comparison with literature data.[64] Our isolation of aurantoside G is in perfect agreement with the Crews proposal for the classification of *T. swinhoei* phenotypes.[59] Indeed, sponges belonging to phenotype III, characterized by red-orange ectosomes and endosomes (as our specimen), should contain good amounts of aurantosides, while non-ribosomial polypeptides and complex polyketides should be very scarce or absent.

After, I turned ur attention to the sterol composition of *T. swinhoei*. Fractions of the Si-column eluted with *n*-hexane/EtOAc (7:3) were combined and subjected to further HPLC purification. This procedure allowed us to obtain pure samples of the 4-methylene sterols conicasterol (**48**)[70] and theonellasterol (**49**),[70] which represent the major components of the sterol fraction of several *Theonella* species. Careful inspection of the ^{1}H NMR spectra of tail fractions resulting from the above purification led us to suspect the presence of an

additional sterol showing a different pattern of sp^2 methylene proton signals (see Fig. 4.3), which was later supported by GC-MS.

Thus, the peracetylated crude sterol fraction, obtained upon reaction with an excess of Ac_2O in dry pyridine, was subjected to GC-MS analysis in standard conditions for peracetyl sterols. The GC separation evidenced the presence of three peaks, which, on the basis of the corresponding mass spectra, were assigned to conicasterol acetate, theonellasterol acetate and to a third molecule, whose molecular ion (*m/z* 452) was two mass units lower than that of conicasterol acetate (*m/z* 454). Unfortunately, all our attempts to completely separate the crude fraction, through repeated HPLC on normal and reversed stationary phases, also employing different solvent mixtures, proved to be unfruitful.

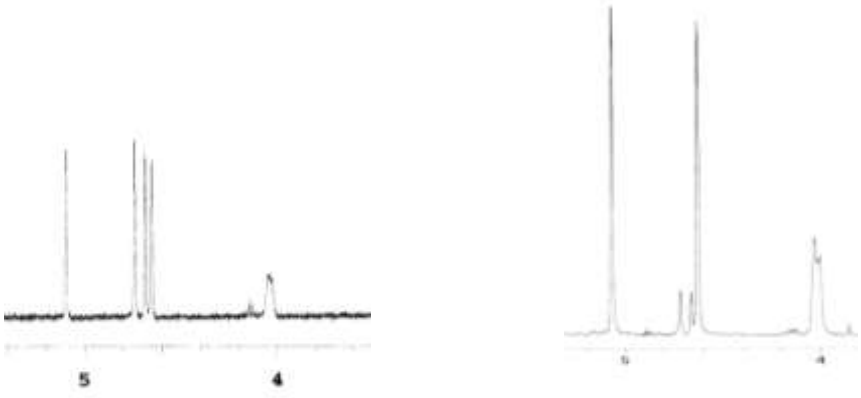

Figure 4.3. The middle-field region in the ^1H NMR spectrum (in $CDCl_3$) of dehydroconicasterol (ledt) and of the sterol crude fraction (right)

At this stage, we reasoned that the efficiency of this separation could be significantly improved through the use of the so-called argentation silica gel chromatography, a technique involving the impregnation of the stationary phase with a silver ion (from $AgNO_3$).[71] Since Ag^+ ion and alkenes form a strong complex by two-electron/three-center bonding, the retention times of molecules differing in the number of double bonds, as the yet unidentified sterol and conicasterol likely were, should be sufficiently different.

Thus, the sterol crude fraction was chromatographed through a Ag^+-impregnated silica gel column, eluting with *n*-hexane/EtOAc mixtures of increasing polarities. As expected, the new sterol **46** was eluted after conicasterol and theonellasterol, in pure form. Dehydroconicasterol **46** was obtained as an optically active colorless amorphous solid. The molecular formula $C_{29}H_{46}O$, requiring seven degrees of unsaturation, was established through NMR data (see Experimental Section) and HRMS. The ^{13}C NMR spectrum of **46** (in $CDCl_3$), interpreted with the help of the 2D HSQC experiment, showed the presence of 29 carbon atoms, including one oxygen-bearing methine carbon (δ_C 73.4) and six sp^2 carbons, four of which were unprotonated (δ_C 125.7, 142.9, 153.1, 156.8), while the remaining two carbons were identified as sp^2 methylenes (δ_C 105.8, δ_H 4.71 and 4.65; δ_C 102.8, δ_H 5.07 and 4.63). The ^1H NMR spectrum of **46** (in $CDCl_3$), in addition to the four broad singlets assigned to the sp^2 methylene protons, showed two methyl singlets (δ_H 0.83 and 0.58), three methyl doublets (δ_H 0.96, 1.01 and 1.03), a series of multiplets between δ_H 1.00 and 2.50, and a carbinol methine resonance at δ_H 4.04.

The COSY experiment allowed the building of the four spin systems indicated in bold in Fig. 4.4, while a series of HMBC correlations (Fig. 4.4) allowed the connection of these fragments and the assembling of dehydroconicasterol (**46**) structure.

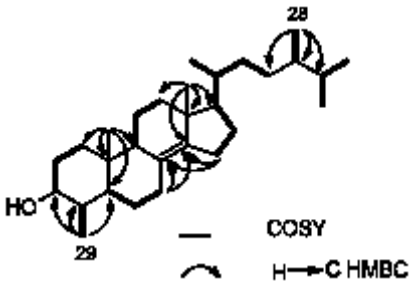

Figure 4.4. COSY and key HMBC correlations detected for dehydroconicasterol (**46**)

Particularly informative were the cross-peaks exhibited by the two methyl singlets Me-18 and Me-19; moreover, the correlations of H_2-29 with C-3, C-4, and C-5 indicated the attachment of an sp^2 methylene at C-4, while the other sp^2 methylene was attached at C-24 on the basis of the correlations of H_2-28 with C-23, C-24 and C-25. Finally, the tetrasubstituted double bond was placed at $\Delta^{8(14)}$ on the basis of the HMBC cross-peaks of both H_2-7 and H_2-15 with C-8 (δ_C 125.7) and C-14 (δ_C 142.9). These data indicated that **46** was a C_{29} sterol differing from conicasterol in the presence of an additional double bond between C-24 and C-28. Comparison of the ^{1}H and ^{13}C NMR data of **46** (Table 5) with those of conicasterol (**48**)[70] provided further support to this assignment and also indicated that the two compounds share the same configuration at the common stereogenic carbons.

Steroids bearing a 4-methylene group are relatively rare metabolites; to date, only five papers have been published on 4-methylene steroids from marine organisms.[72] This unusual group has been proposed to biogenetically arise from a shunt in the oxidative demethylation of the 4α-methyl series, through the dehydration of the primary alcohol formed in the first oxidation of the methyl group.[70] The isolation of dehydroconicasterol **46** adds an interesting piece to this hypothesis, indeed this compound is the likely biogenetic precursor of both conicasterol **48** and theonellasterol **49**, which could derive from compound **46** through reduction or transmethylation with *S*-adenosylmethionine, respectively.

In conclusion, the chemical analysis of an Indonesian specimen of the widely studied sponge *Theonella swinhoei*[73] yielded two new compounds, aurantoic acid **45** and dehydroconicasterol **46**, both having a likely biogenetic relationship with well-known *Theonella* metabolites (aurantosides and conicasterol/theonellasterol, respectively).

Compounds **45**-**49** were tested for in vitro cytotoxic activity against three cell lines (C6, glioma; HeLa, epithelial carcinoma; H9c2, cardiac myoblast) and they exhibited no significant inhibition of the cell growth (IC_{50} > 70 μM).

4.2. *Plakortis simplex*[74]

As part of an ongoing search for biologically active compounds from marine invertebrates, the research group of prof. Taglialatela-Scafati has been devoting considerable efforts to the chemical investigation of the Caribbean sponge *Plakortis simplex*. This research project, started about ten years ago, has been strongly fostered by the discovery of a large array of structurally unique and biologically active metabolites. This richness of secondary metabolite production has been discussed in a review paper[75] and has been recently correlated to the wide presence of bacterial and fungal symbionts associated to the sponge host cells.[76] For example, *P. simplex* provided a series of promising lead compounds for drug development, including the immunosuppressive glycolipids plakosides[77] and simplexides[78] and a series of endoperoxide-containing derivatives related to plakortin (**8**) (see previous chapter),[79,2] for which a potent antimalarial activity (in the nM range) has been discovered.[80] Structurally unique metabolites were also disclosed as components of the most polar fractions obtained from the organic extracts of *P. simplex*. Indeed, these fractions showed to contain the first natural betaine derivatives to be characterized by a iodinated indole ring,[81,82] e.g. plakohypaphorine E (**50**) (Fig. 4.5), and the unique 4-alkylpyridinium alkaloid simplakidine (**51**) (Fig. 4.5).[83]

Careful examination of the polar fractions of *P. simplex* carried out during my PhD course yielded to the isolation of a new 4-alkylpyridinium alkaloid that we have named simplexidine (**52**), (Fig. 4.5).

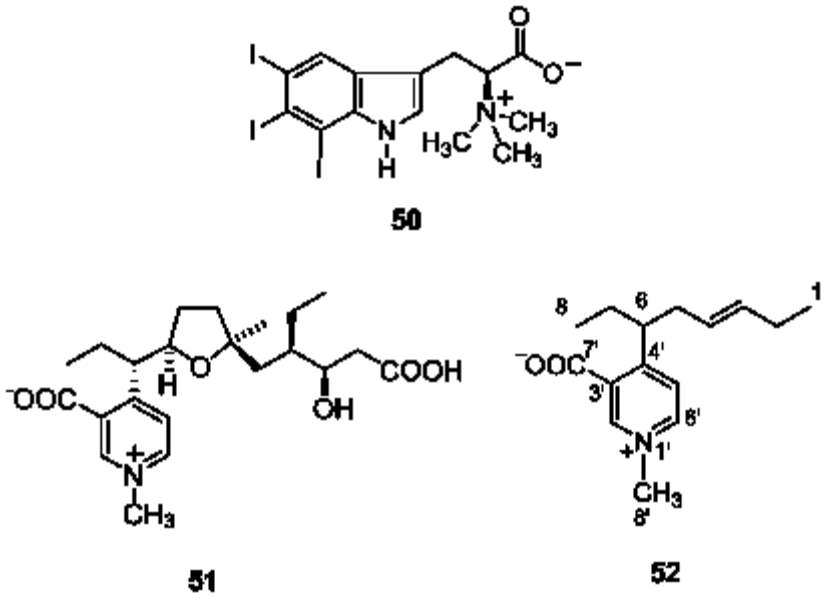

Figure 4.5. Compounds from *Plakortis simplex*, including the new simplexidine (**52**).

A specimen of the sponge *Plakortis simplex* (Demospongiae, order Homosclerophorida, family Plakinidae) was collected during the summer of 2002 along the coasts of The Bahamas and immediately frozen. After homogenization, the organism was exhaustively extracted, in sequence, with methanol and chloroform. The methanol layer was partitioned between *n*-BuOH and water, and, subsequently, the organic phase, combined with the $CHCl_3$ extract, was subjected to chromatography over a reversed phase (RP_{18}) silica column eluted with a solvent gradient from H_2O/MeOH 9:1 to MeOH and then to MeOH/$CHCl_3$ 9:1. The most polar fractions were preliminarily separated over silica gel (gradient from EtOAc to MeOH) and then re-chromatographed by reverse-phase HPLC (eluent MeOH/H_2O 4:6) to finally yield 2.0 mg of pure simplexidine (**52**).

The molecular formula C15H21NO2 was assigned to simplexidine ([α]D = –5.8) based on mass spectrometry evidence [ESI-MS (negative ions): *m/z* 246 $(M-H)^-$; ESI-MS (positive ions): *m/z* 248 $(M+H)^+$, 270 $(M+Na)^+$; HR-FABMS: *m/z* 248.1647 $(M+H)^+$, calcd. for $C_{15}H_{22}NO_2$ *m/z* 248.1651].

The ^{1}H-NMR spectrum of simplexidine (see Experimental Section) showed three signals (a singlet at δ_H 8.81 and two doublets at δ_H 8.63 and 7.91) in the aromatic region, three methine multiplets (δ_H 5.48, 5.35, and 3.81) and a methyl singlet (δ_H 4.34) in the midfield region, and a series of well resolved signals confined in the spectral region ranging from δ_H 2.50 to 0.80, including two methyl triplets at δ_H 0.93 and 0.89. The presence of an aromatic chromophore in the structure of simplexidine (**52**) was further suggested by the UV absorption at ν_{max} 268 nm and by the presence of five signals between δ_C 127 and 164 in the ^{13}C-NMR spectrum.

The 15 carbon signals present in the ^{13}C-NMR spectrum were assigned, with the aid of DEPT experiments, to three methyls, three methylenes, six methines and three unprotonated sp^2 type carbons.

Among these latter resonances, the signal at δ_C 168.6 could be ascribed to a carboxylate group, as suggested also by the IR absorption at ν_{max} 1642 cm^{-1}. Association of the resonances of the 12 proton-bearing carbons with those of the relevant protons was accomplished through the analysis of a 2D NMR gradient-HSQC spectrum. Inspection of the ^{1}H-^{1}H COSY NMR spectrum of simplexidine (**52**) allowed us to arrange all the proton multiplets within the two spin systems showed in red in Figure 4.6.

The first fragment includes only the two mutually coupled aromatic doublets at δ_H 8.63 and 7.91, while the second moiety is an eight-carbon fragment connecting the two methyl triplets (from H_3-1 to H_3-8) and comprising two coupled sp_2 methines (H-3 and H-4) and a single branching at the sp^3 methine C-6 (δ_H 3.81).

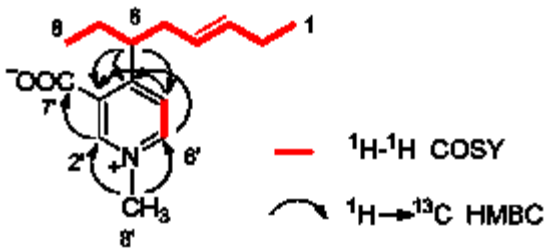

Figure 4.6. ^{1}H-^{1}H COSY and key $^{2,3}J_{C\text{-}H}$ HMBC correlations of simplexidine (**52**)

With these data in our hands and taking into account the molecular formula, the assembly of the carbon framework of simplexidine (**52**) required the elucidation of an aromatic $C_7H_6NO_2$ subunit, probably linked at C-6 and comprising a carboxylate group. Interpretation of diagnostic gradient-HMBC cross-peaks (Fig. 4.6) was of pivotal importance to resolve this issue and suggested the presence of a disubstituted *N*-methyl pyridinium ring. This assignment was corroborated by perfect agreement of ^{1}H-and ^{13}C-NMR resonances of this subunit with literature values.[83,84]

In particular, the *N*-methyl singlet at δ 4.34 (H_3-8') showed g-HMBC cross-peaks with two almost overlapped protonated carbons at δ_C 143.1 (C-2', H-2' = δ_H 8.81, s) and 143.4 (C-6', H-6' = δ_H 8.63, d, J = 6.9 Hz). Substitution at C-2' and C-6' of the pyridinium ring was consequently excluded, and, since considering the doublet nature of H-6', C-5' must be protonated as well, this leaves only a 3,4 disubstitution as possible. The intense g-HMBC cross-peak H-2'/C-7' suggested the placement of the carboxylate group at C-3', while the cross peaks H-6/C-3', H-6/C-4', H-6/C-5' and H-5'/C-6 confirmed the linkage of the alkyl chain at C-4', thus completely defining the planar structure of simplexidine (**52**). The coupling constant $J_{H\text{-}3/H\text{-}4}$ = 15.4 Hz was indicative of the *trans* geometry of the $\Delta^{3,4}$ double bond, while, also considering the limited amounts of sample available (2.0 mg), strategies

aimed at the definition of the absolute configuration at the single stereogenic carbon C-6 were not undertaken.

Pyridinium alkaloids are frequently isolated from the polar extracts of marine invertebrates, mostly sponges; however, in spite of the wide diffusion, the chemical diversity within this class of compounds is somewhat limited and only two structural groups can be identified. The most common group of pyridinium derivatives includes oligomeric structures with alkyl linear chains linked at positions C-3 and N-1 of the pyridinium ring, e.g. the recently reported pachychaline C (**53**) (Fig. 4.7).[85] These molecules are known to exhibit a range of bioactivities including cytotoxic[86] and anti-cholinesterase[87] properties. The second structural group includes the carboxyl-containing homarine (**54**) (Fig. 4.7) or trigonelline (**55**) (Fig. 4.7) substituted at C-3 or C-2, respectively, with short alkyl chains.

The isolation of simplexidine (**52**) is particularly remarkable since it confirms the existence, within the *Plakortis simplex* biosynthetic machinery, of enzymes deputed to the attachment of polyketidederived carbon chains at the 4 position of pyridinium rings. In the case of simplakidine (**51**), this unique reaction led to the linkage between the trigonelline nucleus and a C_{17} moiety that clearly shared the plakortin (**8**) carbon backbone. On the other hand, the biosynthetic origin of the C_8 group present in the structure of simplexidine (**52**) cannot be unambiguously predicted, although similarly to that postulated for plakortin derivatives,[88] a polyketide origin can be hypothesized also in this case.

Simplexidine (**52**) exhibited very weak cytotoxicity toward murine macrophages (RAW 264-7) with 30% of growth inhibition at 80 μg/mL.

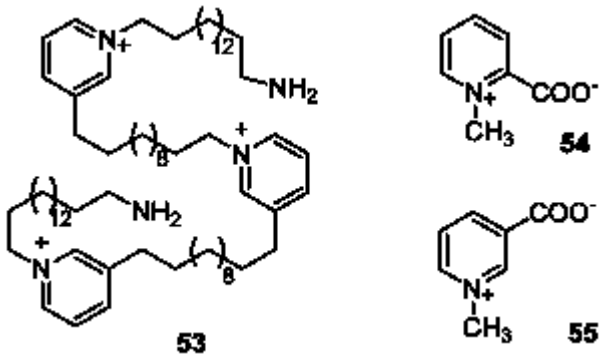

Figure 4.7. Chemical structures of pachychaline C (**53**), homarine (**54**) and trigonelline (**55**)

CHAPTER 5 - EXPERIMENTAL SECTION

5.1. General Experimental Procedures

Optical rotations ($CHCl_3$ or MeOH) were measured at 589 nm on a Perkin-Elmer 192 polarimeter. ^1H (500 and 700 MHz) and ^{13}C (125 and 175 MHz) NMR spectra were measured on Varian INOVA spectrometers. Chemical shifts were referenced to the residual solvent signal ($CDCl_3$: δ_H 7.26, δ_C 77.0; CD_3OD: δ_H 3.30, δ_C 49.0;). Homonuclear ^1H connectivities were determined by the COSY experiment; one-bond heteronuclear ^1H-^{13}C connectivities by the HSQC experiment; two- and three-bond ^1H-^{13}C connectivities by gradient-HMBC experiments optimized for a $^{2,3}J$ of 8 Hz . ESI-MS spectra were performed on a LCQ Finnigan MAT mass spectrometer. GC/MS analysis was performed on a Focus GC-Polaris Q (Thermo) with EI (70eV) ionization. A 5% diphenyl 30m x 0.25mm x 0.25 µm (Trace TR-5, Thermo) was used, with He as carrier gas. Medium pressure liquid chromatography was performed on a Büchi apparatus using a silica gel (230-400 mesh) column. In the argentation silica gel chromatography, the silica gel stationary phase was impregnated with a solution of $AgNO_3$ in EtOH/H_2O, then the liquid was evaporated and the silica dried in the oven at 100 °C overnight. HPLC were achieved on a Knauer apparatus equipped with a refractive index detector and analytical LUNA (Phenomenex) SI60 or RP18 (250 × 4 mm) columns.

5.2. Investigation of the plakortin mechanism of action

5.2.1 Reaction of dihydroplakortin (9) with $FeCl_2$. Dihydroplakortin (**9**, 25.0 mg, 0.080 mmol) was dissolved in CH_3CN/H_2O 4:1 (5 mL) and freshly purchased $FeCl_2 \cdot 4H_2O$ (78 mg, 0.40 mmol) were added. The reaction mixture was left under stirring at room temperature for 2 hours. Light was excluded from the reaction. Then the obtained mixture was

partitioned between water and EtOAc. The organic phase, dried over Na_2SO_4, was purified by HPLC (SI60 *n*-hexane/EtOAc 85:15) affording compounds **9a** (15.0 mg, 0.040 mmol, 50%) and **9b** (2.5 mg, 0.0067 mmol, 8%) in the pure state.

5.2.2. Compound 9a. Colorless oil. $[\alpha]_D^{25}$ + 35 (*c* 0.10 in $CHCl_3$). ^{1}H NMR ($CDCl_3$, 500 MHz): δ 4.53 (H-13, dq, *J* 6.90, 1.5); 4.19 (H-3, m); 3.72 (OMe, s); 2.56 (H-2a, dd, *J* 16.4, 10.5); 2.37 (H-2b, dd, *J* 16.4, 10.5); 1.97 (H-4, m); 1.83 (H-8, m); 1.77 (H-7a, dd, *J* 14.2, 5.6); 1.67 (H-5a, dd, *J* 14.4, 9.0); 1.45 (H_3-14, d, *J* 6.90); 1.39-1.31 (H_2-9, H_2-10, H_2-11, m) 1.31 (H-7b, overlapped); 1.29 (H-5b, overlapped); 1.27 (H-16a, overlapped); 1.17 (H_3-15, s); 1.16 (H-16b, overlapped); 0.90 (H_3-12, t, *J* 7.2). ^{13}C NMR ($CDCl_3$, 125 MHz): δ 174.6 (C-1); 71.9 (C-6); 70.8 (C-3); 64.2 (C-13); 51.0 (OMe); 45.1 (C-7); 42.8 (C-5); 41.3 (C-8); 40.1 (C-4); 37.0 (C-2); 31.2 (C-9); 30.3 (C-10); 26.9 (C-17); 26.4 (C-15); 23.4 (C-11); 23.0 (C-14); 13.4 (C-12); 12.9 (C-18). ESIMS: *m/z* 373 and 375 (3: 1) $[M + Na]^+$. EIMS: *m/z* 350 and 352 (M). HREIMS: *m/z* 350.2229, calcd. for $C_{18}H_{35}{}^{35}ClO_4$ *m/z* 350.2224.

52.3.Compound 9b. Colorless oil. $[\alpha]_D^{25}$ + 22 (*c* 0.10 in $CHCl_3$). ^{1}H NMR ($CDCl_3$, 500 MHz): δ 4.58 (H-13, m); 4.19 (H-3, m); 3.72 (OMe, s); 2.56 (H-2a, dd, *J* 16.4, 10.5); 2.37 (H-2b, dd, *J* 16.4, 10.5); 1.97 (H-4, m); 1.83 (H-8, m); 1.77 (H-7, dd, *J* 14.2, 5.6); 1.67 (H-5a, dd, *J* 14.4, 9.0); 1.37 (H_3-14, d, *J* 7.2); 1.39-1.31 (H_2-9, H_2-10, H_2-11) 1.31 (H-7b, overlapped); 1.29 (H-5b, overlapped); 1.27 (H-16a, overlapped); 1.17 (H_3-15, s); 1.16 (H-16b, overlapped); 0.90 (H_3-12, t, *J* 7.2). ESIMS: *m/z* 373 and 375 (3: 1) $[M + Na]^+$. EIMS: *m/z* 350 and 352 (M). HREIMS: *m/z* 350.2217, calcd. for $C_{18}H_{35}{}^{35}ClO_4$ *m/z* 350.2224.

5.2.4. Reaction of plakortin (8) with $FeCl_2$. Plakortin (**8**, 50.2 mg, 0.16 mmol) was dissolved in CH_3CN/H_2O 4:1 (8 mL) and $FeCl_2{\cdot}4H_2O$ (155 mg, 0.80 mmol) were added. The reaction mixture was left under stirring at room temperature for 2 hours. Light was excluded from the reaction. Then the obtained mixture was partitioned between water and EtOAc. The

organic phase, dried over Na_2SO_4, was purified by HPLC (SI60 *n*-hexane/EtOAc 9:1) affording compounds **8a** (27.0 mg, 0.077 mmol, 48%) and **8b** (13 mg, 0.037 mmol, 23%) in the pure state.

5.2.5.Compound 8a. Colorless oil. $[\alpha]_D^{25}$ - 6 (*c* 0.10 in $CHCl_3$). ESIMS: *m/z* 371 and 373 (3: 1) $[M + Na]^+$. HREIMS: *m/z* 348.2059, calcd. for $C_{18}H_{33}{}^{35}ClO_4$ *m/*z 348.2067. ^1H and ^{13}C NMR: see data reported in ref. 37.

5.2.6.Compound 8b. $[\alpha]_D^{25}$ - 13 (*c* 0.10 in $CHCl_3$). ^1H NMR ($CDCl_3$, 500 MHz): δ 4.32 (H-3, m); 3.91 (H-10, m); 3.81 (H-9, m); 3.70 (OMe, s); 2.66 (H-2a, dd, *J* 16.4, 10.5); 2.36 (H-2b, dd, *J* 16.4, 10.5); 2.22 (H-8, m); 2.06 (H-7a, m); 1.87 (H_2-11, m); 1.78 (H-4, m); 1.69 (H-5a, dd, *J* 14.0, 9.0); 1.55 (H-7b, overlapped); 1.51 (H-5b, overlapped); 1.39 (H-16a, m); 1.28 (H_3-15, s); 1.25 (H_2-13, m); 1.20 (H-16b, m); 1.06 (H_3-12, t, *J* 7.2); 0.94 (H_3-14, t, *J* 7.2); 0.92 (H_3-17, d, *J* 6.90). ESIMS: *m/z* 371 and 373 (3: 1) $[M + Na]^+$. HREIMS: *m/z* 348.2070, calcd. for $C_{18}H_{33}{}^{35}ClO_4$ *m/*z 348.2067.

5.3. Isolation of manadoperoxides

5.3.1. ***Animal material, extraction, isolation*****:** A specimen of *Plakortis* sp. (order Homosclerophorida, family Plakinidae) was collected in January 2008 along the coasts of the Bunaken island in the Bunaken Marine Park of Manado. A voucher sample has been deposited at the Dipartimento di Chimica delle Sostanze Naturali, Università di Napoli Federico II. After homogenization, the organism was exhaustively extracted, in sequence, with methanol and chloroform (dry weight after extraction 199.3 g). The combined extracts (8.6 g) were subjected to chromatography over silica column (230-400 mesh) eluting with a solvent gradient of increasing polarity from hexane to MeOH. Fractions eluted with *n*-hexane/EtOAc 9:1 were subjected to repeated column and HPLC chromatographies (*n*-hexane/EtOAc 95:5) affording manadoperoxides A (**23**, 8.5 mg) and B

(**24**, 6.2 mg) in the pure state. Fractions eluted with *n*-hexane/EtOAc 8:2 were re-chromatogrpahed by HPLC (*n*-hexane/EtOAc 85:15) to give manadoperoxide C (**25**, 2.0 mg). Fractions eluted with *n*-hexane/EtOAc 3:7 were re-chromatographed by HPLC (*n*-hexane/EtOAc 4:6) affording pure manadoperoxide D (**26**, 3.1 mg).

5.3.2. Manadoperoxide A: Colorless amorphous solid; $[\alpha]_D$ -5.2 (*c* 0.3, $CHCl_3$); ^1H NMR ($CDCl_3$, 500 MHz) see Table; ^{13}C NMR ($CDCl_3$, 125 MHz) see Table; (+) ESI-MS *m/z* 327 $[M + H]^+$, 349 $[M + Na]^+$. HR-ESIMS found 327.2177; $C_{18}H_{31}O_5$ requires 327.2171.

^1H (500 MHz) NMR data of manadoperoxides A (**23**), C (**25**) and D (**26**) in $CDCl_3$

Pos.	23	25	26
	δ_H (mult., *J* in Hz)	δ_H (mult., *J* in Hz)	δ_H (mult., *J* in Hz)
2a	2.97 (dd, 15.5, 9.5)	2.93 (dd, 15.7, 9.6)	2.94 (dd, 15.5, 9.5)
2b	2.44 (dd, 15.5, 4.5)	2.46 (dd, 15.7, 4.1)	2.46 (dd, 15.5, 4.3)
3	4.43 (ddd, 9.5, 4.5, 3.0)	4.46 (ddd, 9.6, 4.1, 3.0)	4.44 (ddd, 9.5, 4.3, 3.0)
4	2.57 (m)	2.56 (m)	2.58 (m)
5a	1.68[a]	1.73[a]	1.68[a]
5b	1.28[a]	1.29[a]	1.33
7	0.84 (d, 7.1)	0.85 (d, 7.1)	0.86 (d, 7.1)
8a	1.66[a]	1.69[a]	1.63[a]
8b	1.32[a]	1.30[a]	1.34[a]
9a	1.40[a]	1.53 (m)	1.42[a]
9b	1.40[a]	1.53 (m)	1.35[a]
10a	2.07 (m)	2.25[a]	1.64[a]
10b	2.07 (m)	2.25[a]	1.55 (m)
11	5.47 (dt, 15.9, 6.0)	6.78 (dt, 16.4, 6.6)	4.40 (m)
12	6.03 (d, 15.9)	6.18 (d, 16.4)	5.45 (d, 8.7)
14	1.70 (bs)	2.25 (s)	1.71 (bs)
15	5.44 (bq, 6.9)		4.22 (q, 7.1)
16	1.69[a]		1.27 (d, 7.1)
1-OMe	3.72 (s)	3.72 (s)	3.73 (s)
6-OMe	3.25 (s)	3.27 (s)	3.27 (s)

[a] Overlapped with other signals

5.3.3. Reductive cleavage of manadoperoxide A (23) and reaction with R- and S-MTPA chlorides: Compound **23** (5.0 mg, 15.3 µmol) in 100 ⍰L of dry ether was treated with 50 ⍰L of acetic acid and an excess (20 mg) of Zn dust and then stirred vigorously for 24 h at room temperature. After confirmation of disappearance of the starting material by TLC, solution was neutralized with Na_2CO_3 and the solid removed by filtration. The solvent was then

evaporated and the obtained product was partitioned between H_2O and $CHCl_3$. The organic phase contained ketoalcohol **27** (3.5 mg, 77% yield. An aliquot of **27** (1.0 mg, 3.4 μmol) was treated with *R*-MTPA chloride (30 μL) in 400 μL of dry pyridine with a catalytic amount of DMAP overnight at rt. Then, the solvent was removed and the product was purified by HPLC (*n*-hexane/EtOAc 97:3) to obtain the *S*-MTPA ester **28a** (1.3 mg, 80% yield). When compound **27** (1.0 mg, 3.4 μmol) was treated with *S*-MTPA chloride, following the same procedure, 1.3 mg (80% yield) of *R*-MTPA ester **28b** were obtained.

5.3.4 (S)-MTPA ester (28a): Amorphous solid. ESIMS (positive ions): *m/z* 485 $[M + H]^+$. ^1H NMR ($CDCl_3$): d 7.35 and 7.45 (MTPA phenyl protons), 6.03 (1H, d, *J* = 15.9 Hz, H-12), 5.65 (H-3, m); 5.45 (1H, q, *J* = 6.9 Hz, H-15), 5.42 (1H, dt, *J* = 15.9, 6.0 Hz, H-11), 3.72 (3H, s, 1-OMe), 3.55 (3H, s, OMe), 2.77 (1H, dd, *J* = 15.5, 9.5 Hz, H-2a), 2.54 (1H, m, H-4), 2.44 (1H, dd, *J* = 15.5, 4.5 Hz, H-2b), 2.42 (1H, m, H-5a), 2.41 (2H, t, *J* = 7.4 Hz, H-8), 2.17 (1H, m, H-5b), 2.09 (2H, m, H-10), 1.70 (3H, overlapped, H-16), 1.68 (3H, s, H-14), 1.68 (2H, overlapped, H-9), 0.89 (3H, d, *J* = 7.1 Hz, H-7).

5.3.5. (R)-MTPA ester (28b): Amorphous solid. ESIMS (positive ions): *m/z* 485 $[M + H]^+$. ^1H NMR ($CDCl_3$): d 7.32 and 7.55 (MTPA phenyl protons), 6.03 (1H, d, *J* = 15.9 Hz, H-12), 5.65 (H-3, m); 5.45 (1H, q, *J* = 6.9 Hz, H-15), 5.42 (1H, dt, *J* = 15.9, 6.0 Hz, H-11), 3.72 (3H, s, 1-OMe), 3.55 (3H, s, OMe), 2.78 (1H, dd, *J* = 15.5, 9.5 Hz, H-2a), 2.51 (1H, m, H-4), 2.46 (1H, dd, *J* = 15.5, 4.5 Hz, H-2b), 2.40 (1H, m, H-5a), 2.41 (2H, t, *J* = 7.4 Hz, H-8), 2.15 (1H, m, H-5b), 2.08 (2H, m, H-10), 1.70 (3H, overlapped, H-16), 1.68 (3H, s, H-14), 1.67 (2H, overlapped, H-9), 0.85 (3H, d, *J* = 7.1 Hz, H-7).

5.3.6. Manadoperoxide B (24): Colorless amorphous solid; $[\alpha]_D$ -5.5 (*c* 0.2, $CHCl_3$); ^1H NMR ($CDCl_3$, 500 MHz) δ_H 6.03 (1H, d, *J* = 15.9 Hz, H-12), 5.47 (1H, dt, *J* = 15.9, 6.0 Hz, H-11), 5.40 (1H, t, *J* = 6.1 Hz, H-15), 4.43 (1H, m, H-3), 3.72 (3H, s, 1-OMe), 3.26 (3H, s, 6-OMe),

2.97 (1H, dd, *J* = 15.5, 9.5 Hz, H-2a), 2.57 (1H, m, H-4), 2.44 (1H, dd, *J* = 15.5, 4.5 Hz, H-2b), 2.09 (2H, overlapped, H-16), 2.07 (2H, overlapped, H-10), 1.70 (3H, s, H-14), 1.69 (1H, overlapped, H-5a), 1.66 (1H, overlapped, H-8a), 1.40 (2H, overlapped, H-9), 1.36 (1H, overlapped, H-8b), 1.28 (1H, m, H-5b), 1.00 (3H, t, *J* = 7.1 Hz, H-17), 0.84 (3H, d, *J* = 7.1 Hz, H-7); ^{13}C NMR ($CDCl_3$, 125 MHz) δ_C 172.5 (s, C-1), 136.0 (d, C-12), 133.8 (d, C-15), 133.3 (s, C-13), 125.8 (d, C-11), 103.4 (s, C-6), 80.2 (d, C-3), 52.2 (q, 1-OMe), 48.8 (q, 6-OMe), 34.6 (t, C-5), 33.6 (t, C-10), 32.1 (t, C-8), 31.4 (t, C-2), 27.6 (d, C-4), 23.5 (t, C-9), 21.9 (t, C-16), 17.0 (q, C-7), 15.0 (q, C-17), 13.0 (q, C-14); (+) ESI-MS *m/z* 341 $[M + H]^+$, 363 $[M + Na]^+$. HR-ESIMS found 341.2333; $C_{19}H_{33}O_5$ requires 341.2328.

^{13}C (125 MHz) NMR data of of manadoperoxides A (**23**), C (**25**)

aPos.	**23**	**25**	**26**
	δ_C (mult.)	δ_C (mult.)	δ_C (mult.)
1	171.9 (C)	172.3 (C)	172.2 (C)
2	31.8 (CH_2)	31.4 (CH_2)	31.7 (CH_2)
3	80.1 (CH)	79.8 (CH)	79.7 (CH)
4	27.6 (CH)	27.1 (CH)	27.2 (CH)
5	34.6 (CH_2)	34.4 (CH_2)	34.5(CH_2)
6	103.4 (C)	103.0 (C)	103.0 (C)
7	17.0 (CH)	17.2 (CH_3)	17.1 (CH)
8	32.4 (CH_2)	34.3 (CH_2)	31.4 (CH_2)
9	23.6 (CH_2)	21.8 (CH_2)	22.0 (CH_2)
10	33.7 (CH_2)	32.6 (CH_2)	38.4 (CH_2)
11	126.0 (CH)	147.0 (CH)	70.1 (CH)
12	135.8 (CH)	132.1 (CH)	127.1 (CH)
13	133.3 (C)	198.7 (C)	142.0 (C)
14	13.0 (CH_3)	27.3 (CH_3)	13.7 (CH_3)
15	124.8 (CH)		72.8 (CH)
16	12.2 (CH_3)		17.9 (CH_3)
1-OMe	52.2 (CH_3)	52.2 (CH_3)	52.2 (CH_3)
6-OMe	48.8 (CH_3)	48.8 (CH_3)	48.7 (CH_3)

5.3.7. Manadoperoxide C (25): Colorless amorphous solid; $[\alpha]_D$ -3.3 (*c* 0.1, $CHCl_3$); ^{1}H NMR ($CDCl_3$, 500 MHz) see Table; ^{13}C NMR ($CDCl_3$, 125 MHz) see Table; (+) ESI-MS *m/z* 315 $[M + H]^+$, 337 $[M + Na]^+$. HR-ESIMS found 315.1801; $C_{16}H_{27}O_6$ requires 315.1808.

5.3.8. Manadoperoxide D (26): Colorless amorphous solid; $[\alpha]_D$ -4.2 (*c* 0.2, $CHCl_3$); ^1H NMR ($CDCl_3$, 500 MHz) see Table; ^{13}C NMR ($CDCl_3$, 125 MHz) see Table; (+) ESI-MS *m/z* 361 $[M + H]^+$, 383 $[M + Na]^+$. HR-ESIMS found 361.2222; $C_{18}H_{33}O_7$ requires 361.2226.

5.3.9. Reaction of 26 with R- and S-MTPA chlorides: Compound **26** (1.0 mg, 2.8 µmol) was treated with *R*-MTPA chloride (30 µL) in 400 µL of dry pyridine with a catalytic amount of DMAP overnight at rt. Then, the solvent was removed and the product was purified by HPLC (*n*-hexane/EtOAc 97:3) to obtain the *S*-MTPA diester **29a** (1.8 mg, 81% yield). When compound **26** (1.0 mg, 2.8 µmol) was treated with *S*-MTPA chloride, following the same procedure, 1.7 mg (76% yield) of *R*-MTPA ester **29b** were obtained.

5.3.10. (S)-MTPA ester (29a): Amorphous solid. ESIMS (positive ions): *m/z* 793 $[M + H]^+$. ^1H NMR ($CDCl_3$): d 7.35 and 7.45 (MTPA phenyl protons), 5.61 (1H, m, H-11), 5.45 (1H, d, *J* = 8.7 Hz, H-12), 5.41 (1H, q, *J* = 7.1 Hz, H-15), 4.37 (1H, m, H-3), 3.70 (3H, s, 1-OMe), 3.55 (6H, s, MTPA-OMe), 3.17 (3H, s, 6-OMe), 2.83 (1H, dd, *J* = 15.5, 9.5 Hz, H-2a), 2.47 (1H, m, H-4), 2.37 (1H, dd, *J* = 15.5, 4.5 Hz, H-2b), 1.77 (3H, s, H-14), 1.65 (1H, overlapped, H-5a), 1.60 (1H, m, H-10a), 1.55 (2H, m, H-8), 1.40 (1H, m, H-10b), 1.35 (2H, overlapped, H-9), 1.35 (1H, overlapped, H-5b), 1.31 (3H, d, *J* = 7.1 Hz, H-16), 0.78 (3H, d, *J* = 7.1 Hz, H-7).

5.3.11. (R)-MTPA ester (29b): Amorphous solid. ESIMS (positive ions): *m/z* 793 $[M + H]^+$. ^1H NMR ($CDCl_3$): d 7.32 and 7.55 (MTPA phenyl protons), 5.59 (1H, m, H-11), 5.43 (1H, d, *J* = 8.7 Hz, H-12), 5.38 (1H, q, *J* = 7.1 Hz, H-15), 4.37 (1H, m, H-3), 3.70 (3H, s, 1-OMe), 3.55 (6H, s, MTPA-OMe), 3.22 (3H, s, 6-OMe), 2.83 (1H, dd, *J* = 15.5, 9.5 Hz, H-2a), 2.45 (1H, m, H-4), 2.37 (1H, dd, *J* = 15.5, 4.5 Hz, H-2b), 1.75 (3H, s, H-14), 1.65 (1H, overlapped, H-5a), 1.60 (1H, m, H-10a), 1.55 (2H, m, H-8), 1.37 (1H, m, H-10b), 1.37 (1H, overlapped, H-5b), 1.34 (2H, overlapped, H-9), 1.29 (3H, d, *J* = 7.1 Hz, H-16), 0.78 (3H, d, *J* = 7.1 Hz, H-7).

5.4. Synthesis of simplified endoperoxides

5.4.1. Modified Knoevenagel condensation: A solution of ethyl hydrogen malonate (5.0 g, 0.040 mol) and piperidinium acetate (36.8 mg, 0.26 mmol) in DMSO (20 mL) was strirred in a round-bottom flask for 15 min and then (*E*)-2-nonenal was (3.4 mL, 0.026 mol) was added at once. Stirring was continued for 30 min and then the reaction mixture was heated slightly until 85 °C for 4h, following the production of carbon dioxide. After cooling at room temperature, the reaction mixture was poured into cold water (40 mL) and extracted with diethyl ether (30 mL). The combined extracts were washed with water (3 x 40 mL) and dried over anhydrous Na_2SO_4 and the solvent removed under vacuum. The crude product was separated over silica column (eluent *n*-hexane/EtOAc 9: 1) to give a mixture of Ethyl undeca-3*Z*,5*E*-dienoate (**3**), Ethyl undeca-3*E*,5*E*-dienoate (**4**), Ethyl undeca-2*E*,4*E*-dienoate (**2**). All the attempts to further purify this crude mixture over silica columns failed and also HPLC purifications gave no pure products. A portion of the obtained mixture was separated into its constituents through Ag^+-impregnated silica gel column, eluting with *n*-hexane/EtOAc mixtures from 95:5 to 8:2 and obtaining ethyl undeca-3*Z*,5*E*-dienoate (**3**), ethyl undeca-3*E*,5*E*-dienoate (**4**), and ethyl undeca-2*E*,4*E*-dienoate (**2**).

5.4.2. Ethyl undeca-3E,5Z-dienoate (3)*:* Colorless oil. EIMS: *m/z* 210 $[M]^+$, HREIMS: *m/z* 210.1613, calcd. for $C_{13}H_{22}O_2$ *m/z* 210.1620. ^{1}H NMR ($CDCl_3$): d 6.42 (H-4, dd); 5.98 (H-5, dd); 5.73 (H-6, dt); 5.42 (H-3, dt); 4.10 (OCH_2, q); 3.13 (H-2, d); 2.16 (H-7, m); 1.30-1.20 (H_2-8, H_2-9, H_2-10, m); 1.15 (OCH_2CH_3, t); 0.88 (H_3-11, t, *J* = 7.3 Hz).

5.4.3. Ethyl undeca-3E,5E-dienoate (4)*:* Colorless oil. EIMS: *m/z* 210 $[M]^+$, HREIMS: *m/z* 210.1627, calcd. for $C_{13}H_{22}O_2$ *m/z* 210.1620. ^{1}H NMR ($CDCl_3$): d 6.08 (H-4, dd, *J* =15.1, 10.3 Hz); 5.99 (H-5, dd, 15.1, 10.3 Hz); 5.64 (H-6, m); 5.56 (H-3, dt, *J* = 15.1, 7.0 Hz); 4.10 (OCH_2, q, *J* = 7.2 Hz); 3.06 (H-2, d, *J* = 7.0 Hz); 2.05 (H-7, m); 1.30-1.20 (H_2-8, H_2-9, H_2-10, m); 1.15

(OCH_2CH_3, t, *J* = 7.2 Hz); 0.88 (H_3-11, t, *J* = 7.0 Hz). ^{13}C NMR ($CDCl_3$): d 172.0 (C-1); 135.3 (C-6); 134.2 (C-4); 129.5 (C-5); 122.5 (C-3); 61.0 ($O\underline{C}H_2CH_3$); 38.0 (C-2); 29.7-29.5 (C-8; C-9; C-10); 25.7 (C-7); 14.6 ($OCH_2\underline{C}H_3$); 14.1 (C-11).

5.4.4. Ethyl undeca-2E,4E-dienoate (2)*:* Colorless oil. EIMS: *m/z* 210 $[M]^+$, HREIMS: *m/z* 210.1615, calcd. for $C_{13}H_{22}O_2$ *m/*z 210.1620. ^{1}H NMR ($CDCl_3$): d 7.30 (H-3, dd); 5.94 (H-2, d); 5.86 (H-4, dd); 5.68 (H-5, dt); 4.10 (OCH_2, q); 2.20 (H-6, m); 1.30-1.20 (H_2-7, H_2-8, H_2-9, H_2-10, m); 1.15 (OCH_2CH_3, t); 0.90 (H_3-11, t, *J* = 7.3 Hz).

5.4.5. Photo-oxygenation reaction: A solution of compound **4** in $CHCl_3$/MeOH 95:5 (120 mL) was photolysed with a 500 W halogen lamp in the presence of methylene blue (0.6 mg) as photosensitizer, through which was bubbled a constant stream of oxygen at a flow rate of 50 mL/min for 24 hrs. The reaction was performed in a Pyrex flask fitted with an external cooling jacket. The reaction mixture was then concentrated in vacuo and the resulting residue was purified by column choromatography (*n*-hexane/EtOAc mixtures from 99:1 to 9:1) to yield pure compound **5** in almost quantitative yields. When the same reaction was repeated in the same conditions for the mixture of dienes **2-4**, after chromatographic purification the single endoperoxide 5 was obtained.

5.4.6. Compound 5: Colorless oil. EIMS: *m/z* 242 $[M]^+$, HREIMS: *m/z* 242.1515, calcd. for $C_{13}H_{22}O_4$ *m/*z 242.1518. ^{1}H NMR ($CDCl_3$): d 5.93 (H-4, overlapped); 5.91 (H-5, overlapped); 4.83 (H-3, m); 4.60 (H-6, m); 4.08 (OCH_2, q, *J* = 7.2 Hz); 2.85 (H-2a, dd); 2.60 (H-2b, dd); 1.56 (H_2-7, m); 1.25-1.20 (H_2-8, H_2-9, H_2-10, m); 1.15 (OCH_2CH_3, overlapped); 0.88 (H_3-11, t, *J* = 7.0 Hz). ^{13}C NMR ($CDCl_3$): d 170.8 (C-1); 129.5 (C-5); 126.7 (C-4); 78.6 (C-6); 75.2 (C-3); 61.0 ($O\underline{C}H_2CH_3$); 38.8 (C-2); 32.7 (C-7); 32.0 (C-10); 22.8 (C-8; C-9); 14.6 ($OCH_2\underline{C}H_3$); 14.4 (C-11).

5.4.7. $LiBH_4$-mediated reduction of compound 5 and acetylation of the product: Compound **5** (12.0 mg, 0.050 mmol) was dissolved in 0.8 mL of dry THF under argon flow at 0 °C and

then 150 µL of a 2 M solution of $LiBH_4$ in THF (0.3 mmol) and 10 µL of dry MeOH were added dropwise to the solution. The reaction was kept under stirring for 2 h at 0 °C. Then, 10 µL of 1 M aqueous NaOH were added to the obtained mixture, which was partitioned between water and $CHCl_3$. The organic phase, dried with Na_2SO_4 and concentrated in vacuo was purified by HPLC (eluent *n*-hexane/EtOAc 75:25) affording pure compound **6** (9.0 mg, 0.045 mmol, 90 % yield). Compound **6** (3.0 mg, 0.015 mmol) was dissolved in dry pyridine (1 mL) and treated with Ac_2O (1 mL). After standing overnight, the reaction was worked up by addition of a few drops methanol to destroy the excess Ac_2O, water (*ca.* 3 mL) and EtOAc (*ca.* 10 mL). The organic phase was washed sequentially with 2N H_2SO_4, saturated $NaHCO_3$ and brine. After drying (Na_2SO_4) and removal of the solvent, 3.0 mg (0.012 mmol) of compound **7** were obtained.

5.4.8. Compound 6: Colorless solid. EIMS: *m/z* 200 $[M]^+$, HREIMS: *m/z* 200.1422, calcd. for $C_{11}H_{20}O_3$ *m/*z 200.1412. ^{1}H NMR ($CDCl_3$): d 5.90 (H-4, overlapped); 5.90 (H-5, overlapped); 4.63 (H-3, m); 4.55 (H-6, m); 3.80 (H_2-1, m); 1.88 (H_2-2, m); 1.62 (H_2-7, m); 1.31 (H_2-8, H_2-9, H_2-10, m); 0.88 (H_3-11, t, *J* = 7.0 Hz).

5.4.9. Compound 7: Colorless solid. EIMS: *m/z* 200 $[M]^+$, HREIMS: *m/z* 200.1527, calcd. for $C_{13}H_{22}O_4$ *m/*z 200.1518. ^{1}H NMR ($CDCl_3$): d 5.91 (H-4, overlapped); 5.91 (H-5, overlapped); 4.58 (H-3, overlapped); 4.58 (H-6, overlapped); 4.22 (H_2-1, m); 2.08 ($C\underline{H}_3CO$, s); 1.92 (H_2-2, m); 1.62 (H_2-7, m); 1.31 (H_2-8, H_2-9, H_2-10, m); 0.88 (H_3-11, t, *J* = 7.0 Hz).

5.4.10. Hydrolysis of compound 5: Compound **5** (9.0 mg, 0.037 mmol) was dissolved in a THF/H_2O 3:1 solution (3.0 mL) and 4 mg of LiOH were added. The solution was stirred at 0 °C overnight. Then, the reaction mixture was partitioned between EtOAc and water. The organic phase, evaporated to dryness, contained compound pure compound **8** (7.0 mg, 0.033 mmol).

5.4.11. Compound 8: Colorless oil. EIMS: *m/z* 214 $[M]^+$, HREIMS: *m/z* 214.1215, calcd. for

$C_{13}H_{22}O_4$ *m/z* 214.1205. ^{1}H NMR (CD_3OD): d 5.90 (H-4, d); 5.68 (H-5, d); 5.15 (H-3, m); 4.95 (H-6, m); 2.75 (H-2a, dd); 2.55 (H-2b, dd); 1.56 (H_2-7, m); 1.25-1.20 (H_2-8, H_2-9, H_2-10, m); 0.88 (H_3-11, t, *J* = 7.0 Hz).

5.4.12. Dihydroxylation of compound 5: To a stirred solution of compound **5** (10 mg, 0.042 mmol) in *t*-BuOH (2.5 mL) and water (2.5 mL) was added K_2OsO_4 (0.5 mol %) and citric acid, followed by NMO (5.1 mg). The mixture was stirred for 3 hours and followed by TLC. Then, the reaction mixture was extracted with CH_2Cl_2, dried over Na_2SO_4 concentrated in vacuo and the product purified by HPLC (normal phase *n*-hexane/EtOAc 1:1) to obtain compound **10** (8.1 mg, 0.029 mmol).

5.4.13. Compound 10: Colorless solid. EIMS: *m/z* 276 $[M]^+$, HREIMS: *m/z* 276.1579, calcd. for $C_{13}H_{24}O_6$ *m/z* 276.1573. ^{1}H NMR ($CDCl_3$): d 4.59 (H-3, m); 3.79 (H-6, m); 3.68 (H-4, overlapped); 3.61 (H-5, m); 4.08 (OCH_2, q, *J* = 7.2 Hz); 2.78 (H-2a, dd); 2.60 (H-2b, dd); 1.60 (H_2-7, m); 1.25-1.20 (H_2-8, H_2-9, H_2-10, m); 1.15 (OCH_2CH_3, overlapped); 0.88 (H_3-11, t, *J* = 7.0 Hz).

5.4.14. Epoxidation of compound 5. Compound **5** (18.0 mg, 0.074 mmol) was dissolved in 2.5 mL of dry CH_2Cl_2 and 130 mg of *meta*-chloroperbenzoic acid (0. 74 mmol) were added to the solution that was then stirred overnight at room temperature. Subsequently, the reaction mixture was partitioned between $CHCl_3$ and saturated aqueous $NaHCO_3$. The organic phase, dried and concentrated in vacuo, was then purified by reversed-phase HPLC (eluent MeOH/H_2O 9:1) yielding compounds **11** (9.6 mg) and **12** (2.5 mg) in the pure state.

5.4.15. Compound 11 Colorless solid. EIMS: *m/z* 258 $[M]^+$, HREIMS: *m/z* 258.1477, calcd. for $C_{13}H_{22}O_5$ *m/z* 258.1467. ^{1}H NMR (CD_3OD): d 4.76 (H-3, m); 4.30 (H-6, m); 3.60 (H-4, m); 3.32 (H-5, m); 4.18 (OCH_2, q, *J* = 7.2 Hz); 2.90 (H_2-2, m); 1.60 (H_2-7, m); 1.45 (H_2-8, m); 1.33-1.30 (H_2-9, H_2-10, m); 1.30 (OCH_2CH_3, overlapped); 0.90 (H_3-11, t, *J* = 7.0 Hz). ^{13}C NMR ($CDCl_3$): d

170.8 (C-1); 83.7 (C-6); 74.1 (C-3); 60.7 ($O\underline{C}H_2CH_3$); 51.5 (C-4); 48.9 (C-5); 37.5 (C-2); 32.0 (C-7); 32.8 (C-8; C-9); 23.5 (C-10); 14.1 (C-11); 13.4 ($OCH_2\underline{C}H_3$).

5.4.16. Compound 12 Colorless solid. EIMS: *m/z* 258 $[M]^+$, HREIMS: *m/z* 258.1473, calcd. for $C_{13}H_{22}O_5$ *m/z* 258.1467. ^{1}H NMR (CD_3OD): d 4.70 (H-3, m); 4.37 (H-6, m); 3.37 (H-4, m); 3.25 (H-5, m); 4.13 (OCH_2, q, *J* = 7.2 Hz); 2.92 (H-2a, dd); 2.78 (H-2b, dd); 1.62 (H_2-7, m); 1.45 (H_2-8, m); 1.33-1.30 (H_2-9, H_2-10, m); 1.29 (OCH_2CH_3, overlapped); 0.90 (H_3-11, t, *J* = 7.0 Hz). ^{13}C NMR ($CDCl_3$): d 170.4 (C-1); 78.8 (C-6); 74.7 (C-3); 61.2 ($O\underline{C}H_2CH_3$); 51.3 (C-4); 47.9 (C-5); 36.0 (C-2); 32.0 (C-7); 32.1 (C-8; C-9); 23.0 (C-10); 14.1 (C-11); 13.4 ($OCH_2\underline{C}H_3$).

5.4.17. Bromination of compound 5: Bromine (12.5 mg, 0.078 mmol) was added in the dark to a solution of compound **5** (15 mg, 0.062 mmol) in CH_2Cl_2 (2.0 mL) in a vial kept at 0 °C. After 15 minutes the solvent was removed under a stream of nitrogen and the residue was purified by HPLC (normal phase *n*-hexane/EtOAc 85:15) to yield compounds **13** (16.3 mg, 0.041 mmol) and **14** (7.1 mg, 0.018 mmol).

5.4.18. Compound 13: Colorless solid. EIMS: *m/z* 400 $[M]^+$, HREIMS: *m/z* 399.9888, calcd. for $C_{13}H_{22}{}^{79}Br_2O_4$ *m/z* 399.9885. ^{1}H NMR ($CDCl_3$): d 5.17 (H-3, m); 4.80 (H-4, m); 4.32 (H-5, m); 4.18 (H-6, m); 4.10 (OCH_2, q, *J* = 7.2 Hz); 2.82 (H-2a, dd); 2.72 (H-2b, dd); 1.45 (H_2-7, m); 1.33-1.30 (H_2-8, H_2-9, H_2-10, m); 1.20 (OCH_2CH_3, overlapped); 0.92 (H_3-11, t, *J* = 7.0 Hz).

5.4.19. Compound 14: Colorless solid. EIMS: *m/z* 400 $[M]^+$, HREIMS: *m/z* 399.9882, calcd. for $C_{13}H_{22}{}^{79}Br_2O_4$ *m/z* 399.9885. ^{1}H NMR ($CDCl_3$): d 4.84 (H-3, m); 4.25 (H-6, m); 4.20 (H-4, m); 3.80 (H-5, m); 4.10 (OCH_2, q, *J* = 7.2 Hz); 2.92 (H-2a, dd); 2.88 (H-2b, dd); 1.48 (H_2-7, m); 1.33-1.30 (H_2-8, H_2-9, H_2-10, m); 1.20 (OCH_2CH_3, overlapped); 0.90 (H_3-11, t, *J* = 7.0 Hz).

5.5. Theonella *swinhoei*

***5.5.1. Animal material, extraction, isolation*:** A specimen of *Theonella swinhoei* (order Lithistida, family Theonellidae) was collected in January 2008 along the coasts of the

Bunaken island in the Bunaken Marine Park Park (North Sulawesi, Indonesia). The species is very common in this area, from 20 to 50 m depth, on substrata subjected to strong currents. In vivo, the sponge is red-orange but specimens living in shadow habitats are pale pink to white. It is frequently exploited as food by fishes and turtles. A voucher sample has been deposited at the Dipartimento di Chimica delle Sostanze Naturali, Università di Napoli Federico II. After homogenization, the organism (wet weight 560.2 g) was exhaustively extracted, in sequence, with methanol and dichloromethane. The combined extracts were partitioned between water and EtOAc and the obtained organic extract (2.6 g) was subjected to chromatography over silica column (230-400 mesh) eluting with a solvent gradient of increasing polarity of *n*-hexane/EtOAc/MeOH. Fractions eluted with EtOAc/MeOH 9:1 were combined and further purified by reverse-phase HPLC (eluent MeOH/H_2O 65:35) to obtain aurantoside G (**47**, 12.4 mg). Fractions eluted with *n*-hexane/EtOAc 3:7 were combined and further purified by reverse-phase HPLC (eluent MeOH/H_2O 85:15) to obtain aurantoic acid (**45**, 2.5 mg). Fractions eluted with *n*-hexane/EtOAc 7:3 were combined and subjected to normal phase HPLC (*n*-hexane/EtOAc 75:25) to obtain conicasterol (**48,** 75.2 mg) and theonellasterol (**49**, 63.4 mg). The crude sterol fraction was also peracetylated with an excess of Ac_2O in dry pyridine and subjected to GC/MS analysis with the following gradient: initial 200°C (3.5 min), increment of 10°C/min to reach 330 °C, inlet 270 °C, transfer line 280°C, ion source 250 °C, blink window 3.5 min. Theonellasterol acetate (min. 13.18, *m/z* 468), conicasterol acetate (min. 12.49, *m/z* 454) and dehydroconicasterol acetate (min. 12.42, *m/z* 452) were detected. The crude sterol fraction was also chromatographed through a Ag^+-impregnated silica gel column, eluting with *n*-hexane/EtOAc mixtures from 95:5 to 55:45. Fractions eluted with *n*-hexane/EtOAc 65:35 afforded dehydroconicasterol (**46**, 4.8 mg) in the pure state.

5.5.2. Aurantoic Acid (45): Yellow amorphous solid*;* UV-vis (MeOH) λ_{max} 346 (ε 20100), 363 (ε 18500), ^{1}H NMR ($CDCl_3$, 500 MHz) δ_H 7.31 (1H, dd, *J* = 15.4, 11.5 Hz, H-3), 6.69 (1H, dd, *J* = 14.9, 11.2 Hz, H-5), 6.60 (1H, dd, *J* = 15.3, 10.6 Hz, H-9), 6.54 (1H, dd, *J* = 15.0, 11.3 Hz, H-7), 6.43 (1H, dd, *J* = 14.9, 11.0 Hz, H-4), 6.41 (1H, dd, *J* = 15.3, 11.3 Hz, H-8), 6.39 (1H, dd, *J* = 15.0, 11.2 Hz, H-6), 6.26 (1H, d, *J* = 10.6 Hz, H-10), 5.86 (1H, d, *J* = 15.4 Hz, H-2), 2.19 (3H, bs, H-12); ^{13}C NMR ($CDCl_3$, 125 MHz) δ_C 169.1 (s, C-1), 145.0 (d, C-3), 140.7 (d, C-5), 139.0 (d, C-6), 137.0 (d, C-7), 132.7 (d, C-8), 132.6 (s, C-11), 130.1 (d, C-4), 130.0 (d, C-9), 125.4 (d, C-10), 120.6 (d, C-2), 25.3 (q, C-12). (+) ESI-MS *m/z* 225 and 227 (3:1) $[M + H]^+$, *m/z* 247 and 249 (3:1) $[M + Na]^+$. HR-ESIMS found *m/z* 247.0505; $C_{12}H_{13}{}^{35}ClO_2Na$ req. *m/z* 247.0502.

^{13}C (125 MHz) and ^{1}H (500 MHz) NMR Data for Dehydroconicasterol (**46**) in $CDCl_3$

Posit.	δ_H (mult., *J* in Hz)	δ_C (mult.)	Posit.	δ_H (mult., *J* in Hz)	δ_C (mult.)
1a	1.76[a]	36.7 (CH_2)	16a	1.58[a]	24.6 (CH_2)
1b	1.32[a]		16b	1.37[a]	
	2.01 (ddt, 12.8, 7.3, 4.0)	33.1 (CH_2)	17	1.16[a]	57.0 (CH)
2a					
2b	1.37[a]	31.8 (CH_2)	18	0.83 (s)	18.2 (CH_3)
3	4.04 (dd, 11.0, 4.0)	73.4 (CH)	19	0.58 (s)	13.7 (CH_3)
4		153.1 (C)	20	1.50[a]	34.3 (CH)
5	1.82[a]	49.4 (CH)	21	0.96, (d, 7.3)	19.1 (CH_3)
6a	1.85[a]	27.0 (CH_2)	22a	1.59[a]	34.4 (CH_2)
6b	1.40[a]		22b	1.24[a]	
7	2.25 (m)	25.8 (CH_2)	23a	2.09[a]	25.8 (CH_2)
8		125.7 (C)	23b	1.90 (dt, 12.4, 3.0)	30.9 (CH_2)
9	1.79[a]	49.1 (CH)	24		156.8 (C)
10		40.1 (C)	25	2.22 (hep, 7.3)	33.9 (CH)
11a	1.64[a]	20.4 (CH_2)	26	1.03 (d, 7.3)	22.0 (CH_3)
11b	1.57[a]		27	1.01 (d, 7.3)	22.0 (CH_3)
12a	1.94[a]	37.5 (CH_2)	28a	4.71 (bs)	105.8 (CH_2)
12b	1.13[a]		28b	4.65 (bs)	
13		42.8 (C)	29a	5.07 (bs)	102.8 (CH_2)
14		142.9 (C)	29b	4.63 (bs)	
15a	2.47 (ddd, 14.5, 4.0, 2.0)	29.4 (CH_2)			
15b	1.74[a]				

[a] Overlapped with other signals

5.5.3. Dehydroconicasterol (46): Colorless amorphous solid; $[\alpha]_D$ + 82.1 (c 0.2, $CHCl_3$); *;* UV-vis (MeOH) λ_{max} 237 (ε 1450), ^{1}H NMR ($CDCl_3$, 500 MHz) see Table; ^{13}C NMR ($CDCl_3$, 125 MHz) see Table; (+) EI-MS *m/z* 410 $[M]^+$. HR-EIMS found *m/z* 341.2333; $C_{29}H_{46}O$ requires *m/z* 410.3549.

5.6. Plakortis simplex

5.6.1. Animal material, Extraction and Isolation Procedure.

A specimen of *Plakortis simplex* was collected in July 2002 along the coasts of The Bahamas. A voucher specimen is deposited at the Dipartimento di Chimica delle Sostanze Naturali, Italy with the ref. n° 02-10. The organism was immediately frozen after collection and kept frozen until extraction, when the sponge (43 g, dry weight after extraction) was homogenized and extracted with methanol (4 × 500 mL) and with chloroform (4 × 500 mL). The methanol extract was initially partitioned between H_2O and *n*-BuOH and then the organic phase was combined with the $CHCl_3$ extract and concentrated *in vacuo* to afford a brown oil (22.1 g). This was subjected to chromatography on a column packed with RP_{18} silica gel and eluted with 9:1 H_2O/MeOH (A_1), 7:3 H_2O/MeOH (A_2), 4:6 H_2O/MeOH (A_3), 2:8 H_2O/MeOH (A_4), MeOH (A_5), and 9:1 MeOH/$CHCl_3$ (A_6). Fraction A_3 (442 mg) was further chromatographed by MPLC (SiO_2 230-400 mesh; solvent gradient system of increasing polarity from EtOAc to MeOH). Fractions eluted with EtOAc/MeOH 2:8 were re-chromatographed by reverse-phase HPLC (eluent MeOH/H_2O 4:6) affording pure simplexidine (**52**, 2.0 mg).

5.6.3. Simplexidine (52) Colorless amorphous solid. $[\alpha]_{D\ 25}$ –5.8 (c = 2.0 mg/mL in MeOH); IR (KBr): λ_{max} 1642, 1078, 922 cm^{-1}; UV (MeOH): λ_{max} 268 (logε -3.41); ESI-MS (negative ions): *m/z* 246 $(M-H)^-$. ESI-MS (positive ions): *m/z* 248 $(M+H)^+$, 270 $(M+Na)^+$. HR-FABMS analysis: *m/z* 248.1647 $(M+H)^+$, calcd. For $C_{15}H_{22}NO_2$ *m/z* 248.1651. ^{1}H- and ^{13}C-NMR:

^{1}H (500 MHz) and ^{13}C (125 MHz) NMR Data of Simplexidine (**52**) in CD_3OD

Pos.	δH, mult., *J* in Hz	δC, mult.	Pos.	δH, mult., *J* in Hz	δC, mult.
1	0.93, t, 7.3	14.5,CH_3			
2	1.97, q, 7.3	25.8, CH_2	2’	8.81, s	143.1, CH
3	5.48, dt, 15.4, 7.3	136.2, CH	3’		141.9, C
4	5.35, dt, 15.4, 7.0	126.2, CH	4’		163.5, C
5	2.43, q, 7.0	38.1, CH_2	5’	7.91, d, 6.9	127.3, CH
6	3.81, m	43.4, CH	6’	8.63, d, 6.9	143.4, CH
7a	1.87, m	27.7, CH_2	7’		168.6, C
7b	1.73, m		8’	4.34, s	46.7, CH_3
8	0.89, t, 7.5	12.2, CH_3			

5.7 Evaluation of antimalarial activity

Plasmodium falciparum cultures were carried out according to Trager and Jensen’s[89] with slight modifications. The CQ-sensitive, moderately mefloquine-resistant clone D10, the CQ-resistant, mefloquine-susceptible clone W2 were maintained at 5% haematocrit (human type A-positive red blood cells) in complete culture medium at 37 °C. Complete medium contained RPMI 1640 medium (Gibco BRL, $NaHCO_3$ 24 mM) with the addition of 10% heat-inactivated A-positive human plasma, 20mM Hepes (Biological Industries, Kibbutz, Israel), 2mM Glutammine (Biological Industries, Kibbutz, Israel). All the cultures were maintained in a standard gas mixture consisting of 1% O_2, 5% CO_2, 94% N_2. When parasitemia exceeded 5%, subcultures were taken; the culture medium was changed every second day.

Compounds were dissolved in either water (chloroquine) or DMSO and then diluted with medium to achieve the required concentrations (in all cases the final concentration contained <1% DMSO, which was found to be non-toxic to the parasite). Drugs were

placed in 96 wells flat-bottom microplates (Costar # 3596) and serial dilution made. Asynchronous cultures with parasitemia of 1-1.5% and 1% final haematocrit were aliquoted into the plates and incubated for 72 hours at 37 °C. Parasite growth was determined spectrophotometrically (OD_{650}) by measuring the activity of the parasite lactate dehydrogenase (LDH), according to a modified version of the method of Makler[90,91] in control and drug-treated cultures. Antimalarial activity was expressed as the 50% inhibitory concentrations (IC_{50}, μM); each IC_{50} value presented in the Tables is the mean and standard deviation of four separate experiments performed in triplicate.

CHAPTER 6 - SUPPORTING DATA

^{1}H NMR spectrum (500 MHz) of compound **9a** in $CDCl_3$

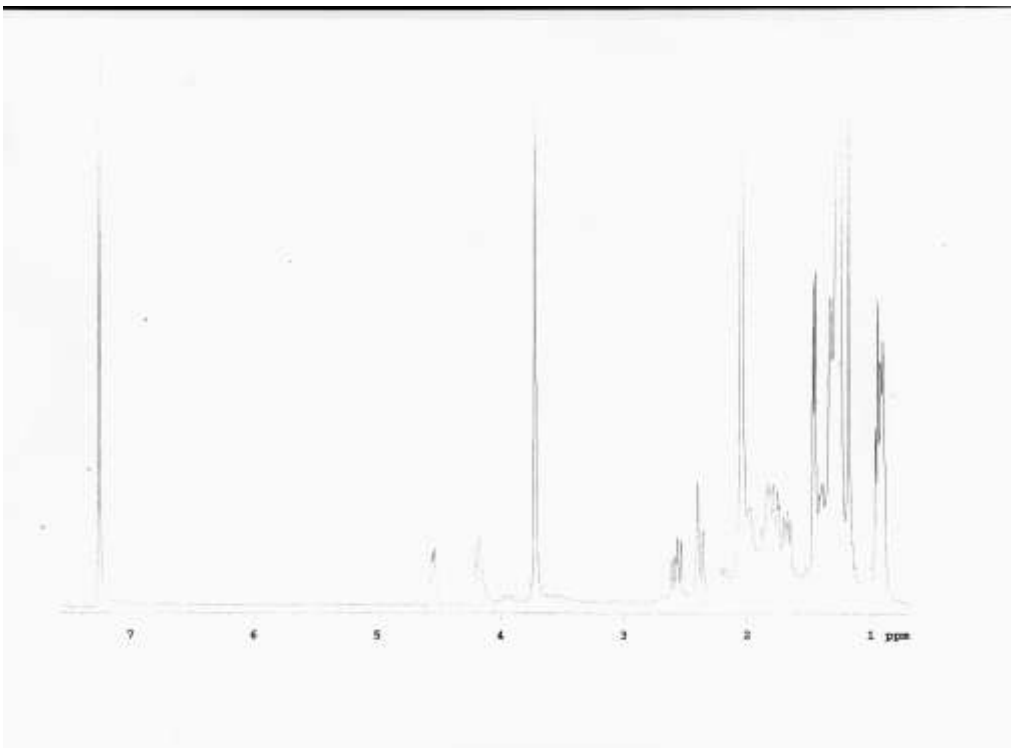

^{1}H NMR spectrum (500 MHz) of compound **8a** in $CDCl_3$

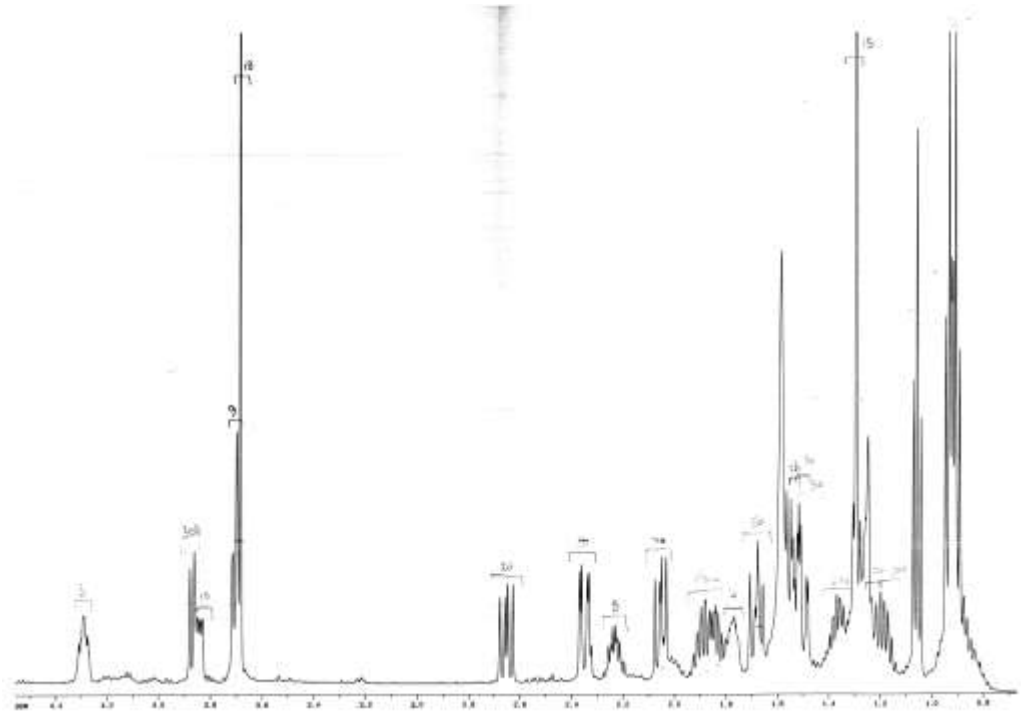

COSY spectrum (500MHz) of manadoperoxide A (**23**) in $CDCl_3$

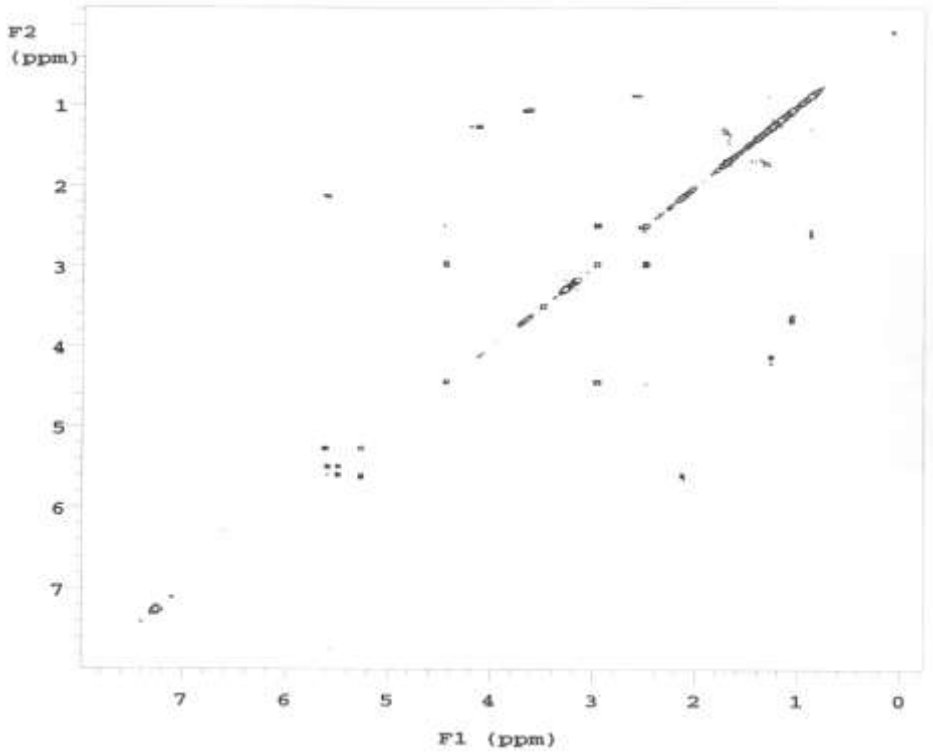

HMBC spectrum (500MHz) of manadoperoxide A (**23**) in $CDCl_3$

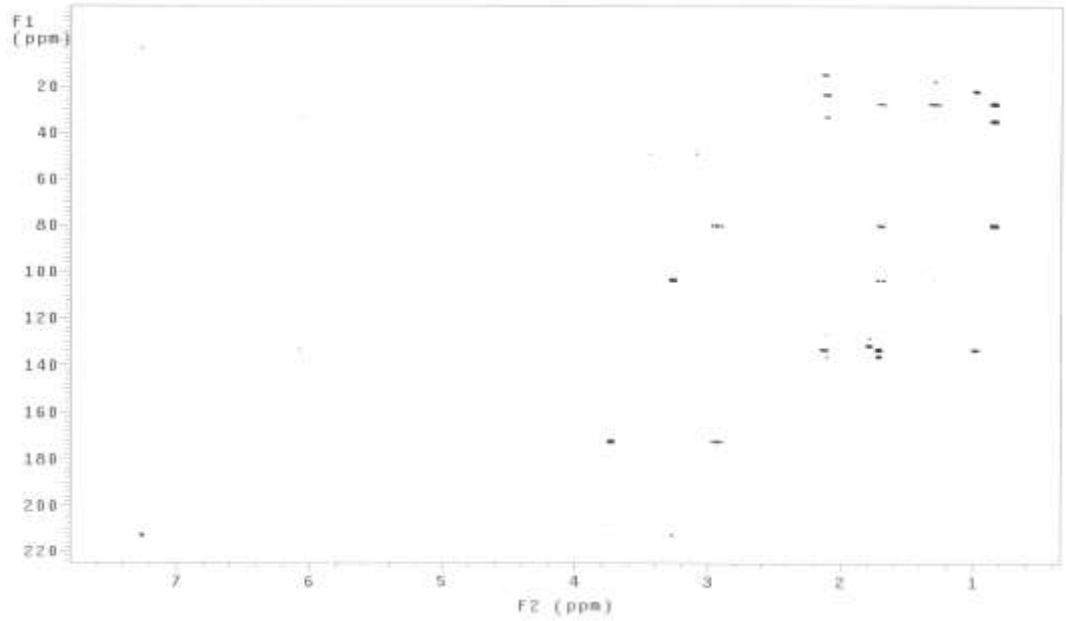

^{1}H NMR spectrum (500 MHz) of manadoperoxide B (**24**) in $CDCl_3$

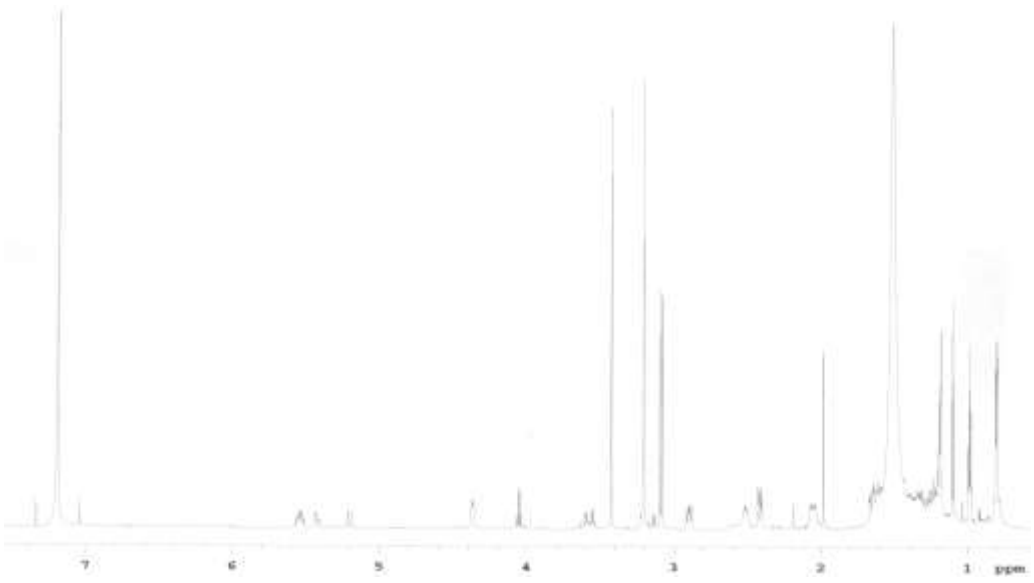

COSY spectrum (500MHz) of manadoperoxide B (**24**) in $CDCl_3$

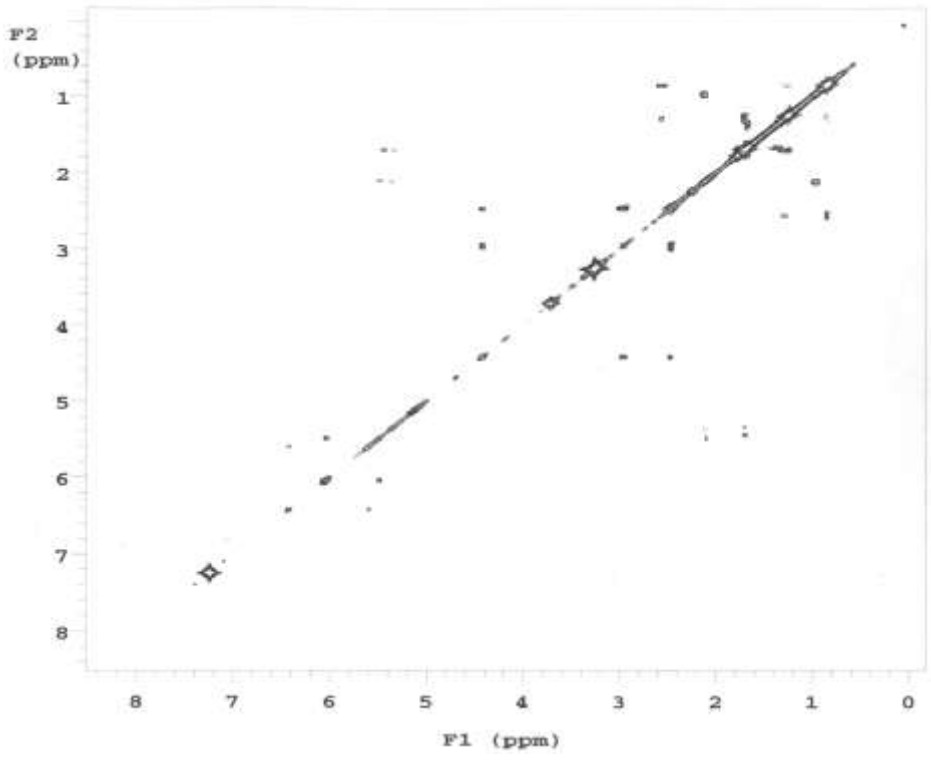

^{1}H NMR spectrum (500 MHz) of manadoperoxide C (**25**) in $CDCl_3$

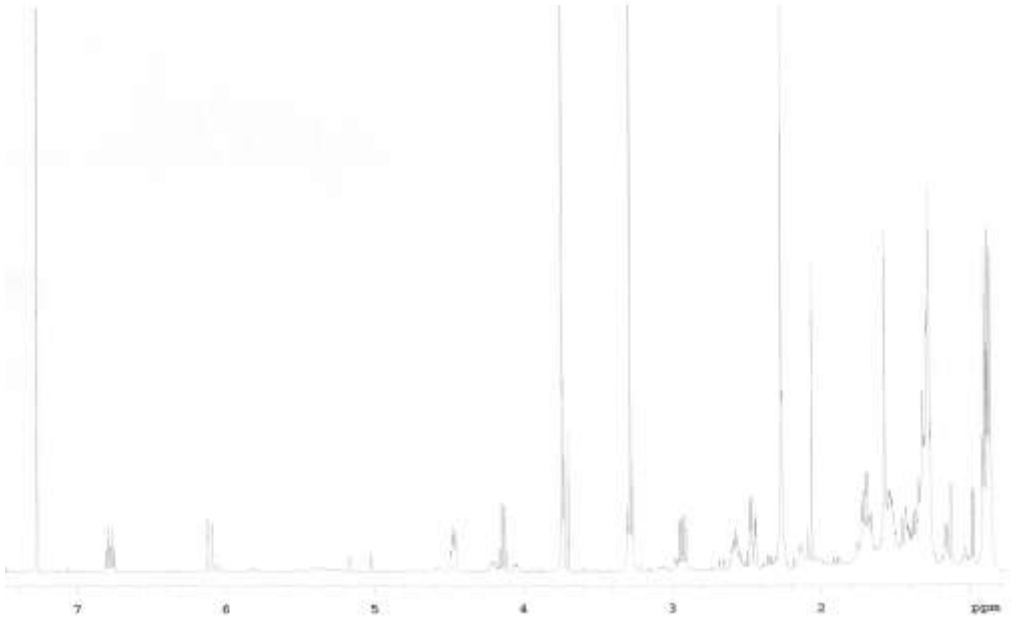

HMBC spectrum (500MHz) of manadoperoxide C (**25**) in $CDCl_3$

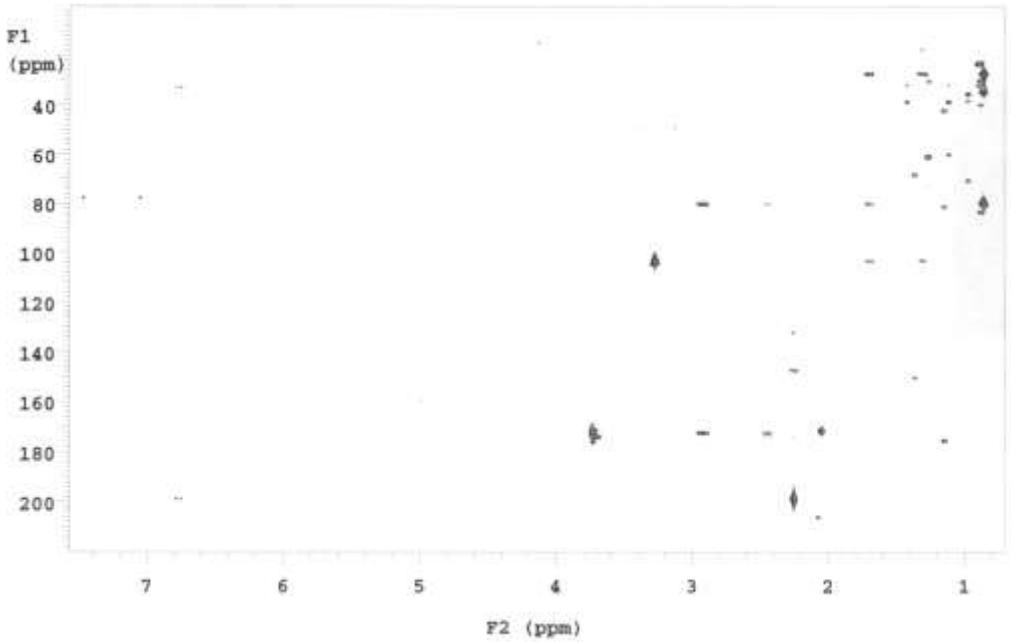

^{1}H NMR spectrum (500 MHz) of compound **35** in $CDCl_3$

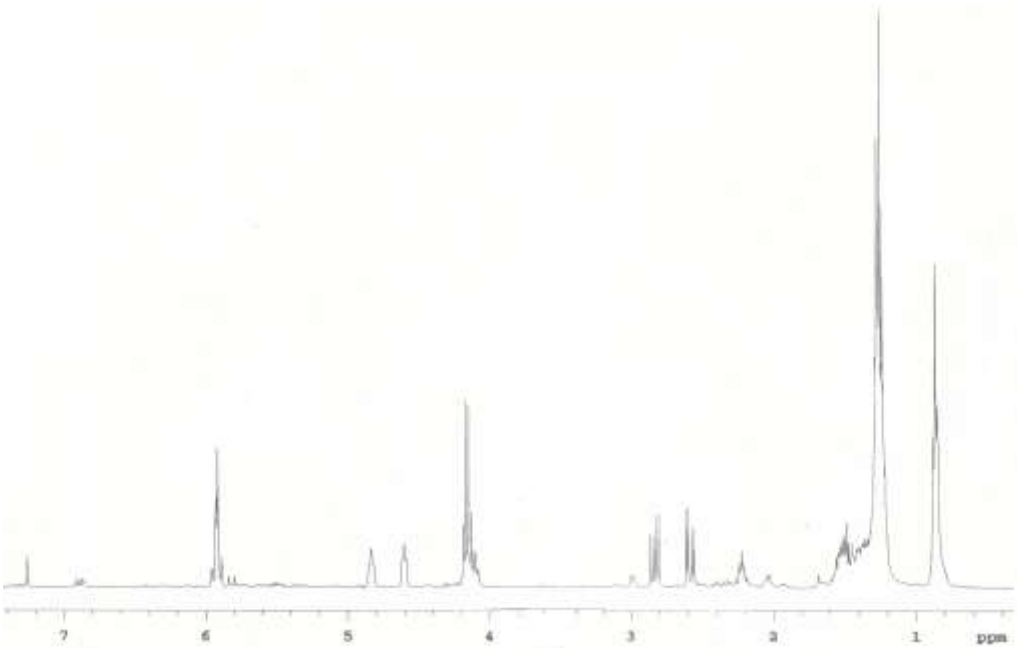

COSY spectrum (500 MHz) of compound (**35**) in $CDCl_3$

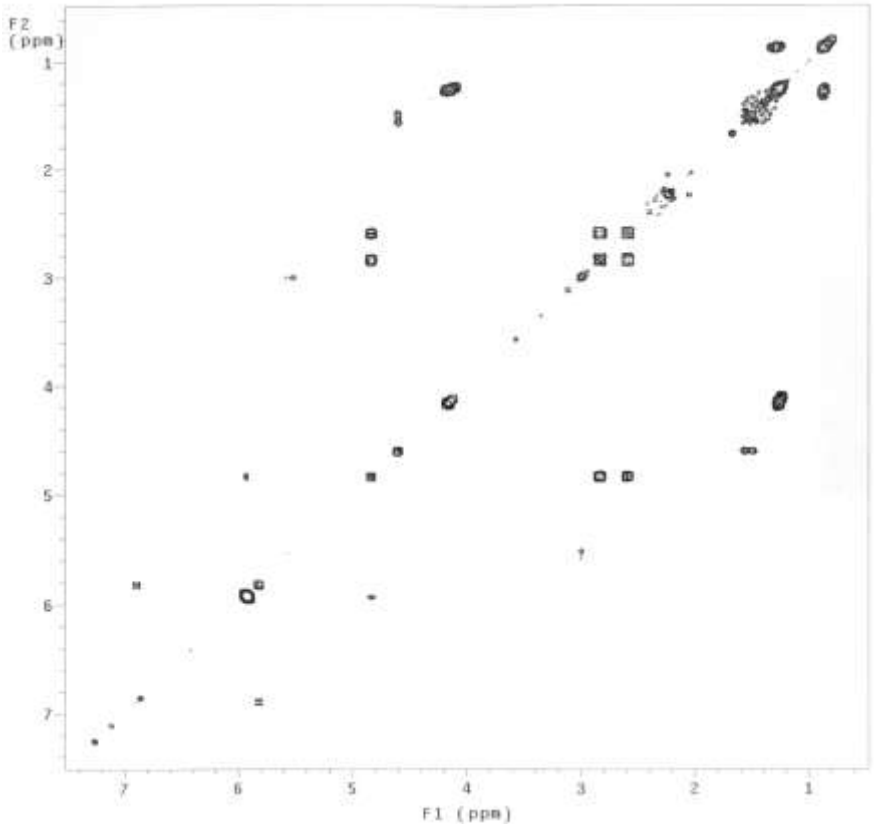

HMBC spectrum (500MHz) of compound **35** in $CDCl_3$

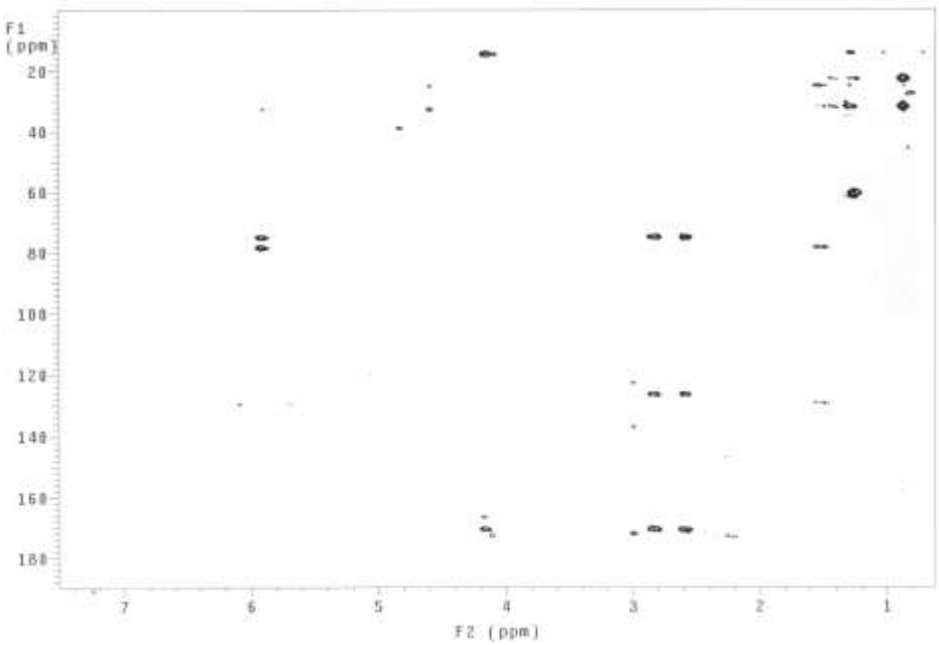

COSY spectrum (500MHz) of compound **42** in $CDCl_3$

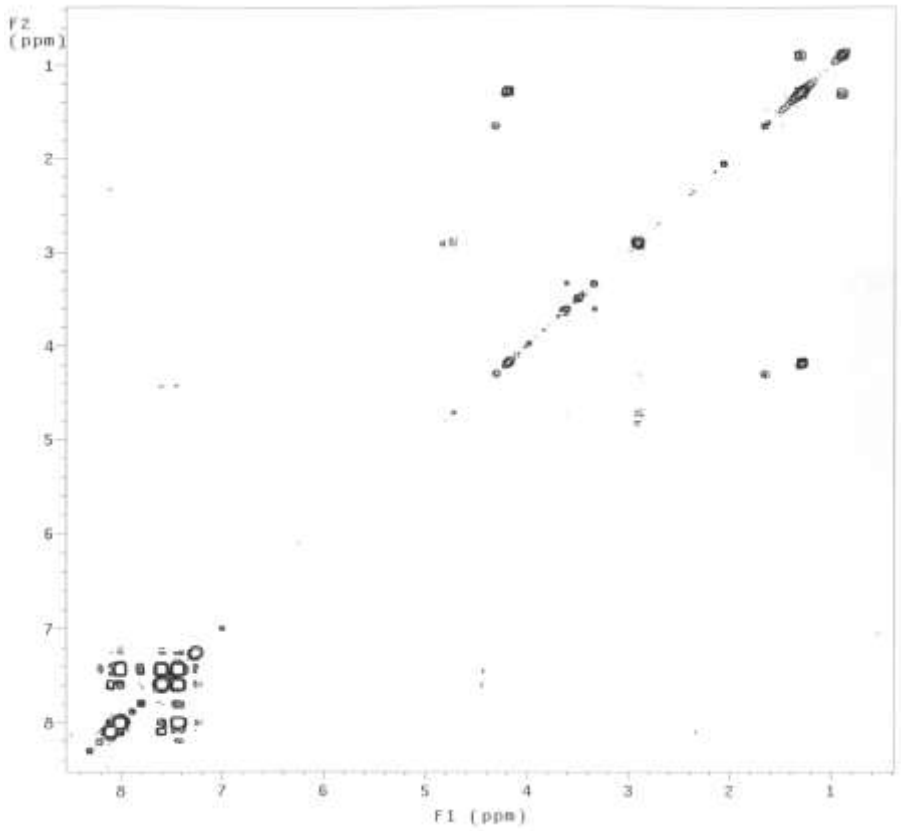

HMBC spectrum (500MHz) of compound **42** in $CDCl_3$

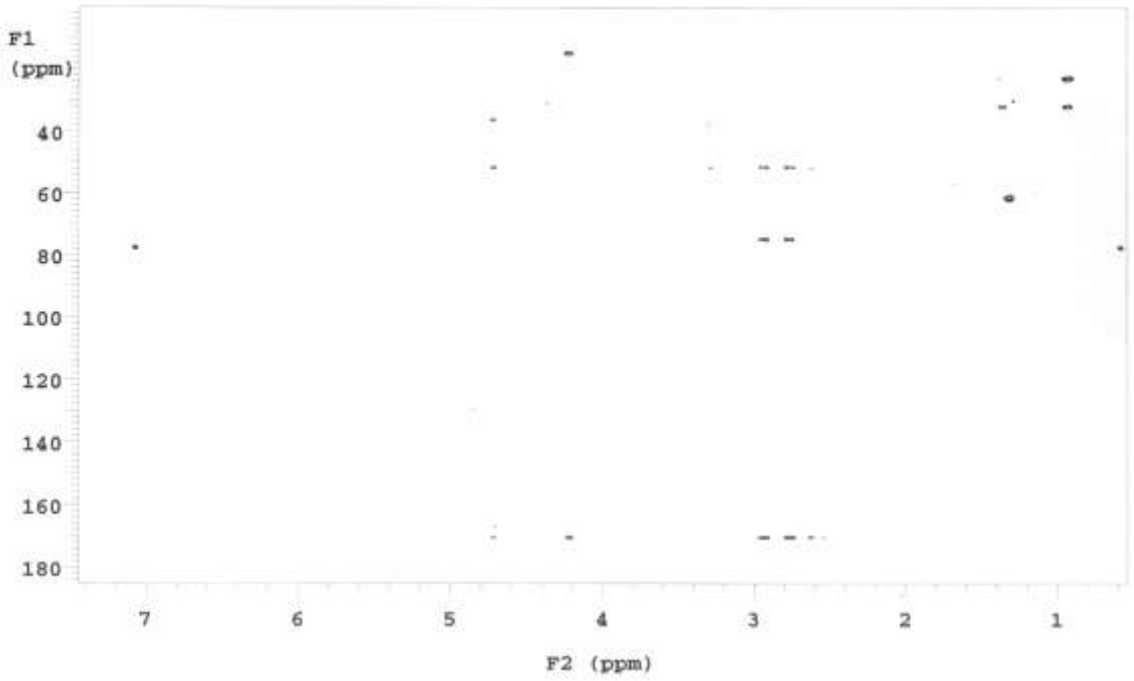

^{1}H NMR spectrum (500 MHz) of compound **44** in $CDCl_3$

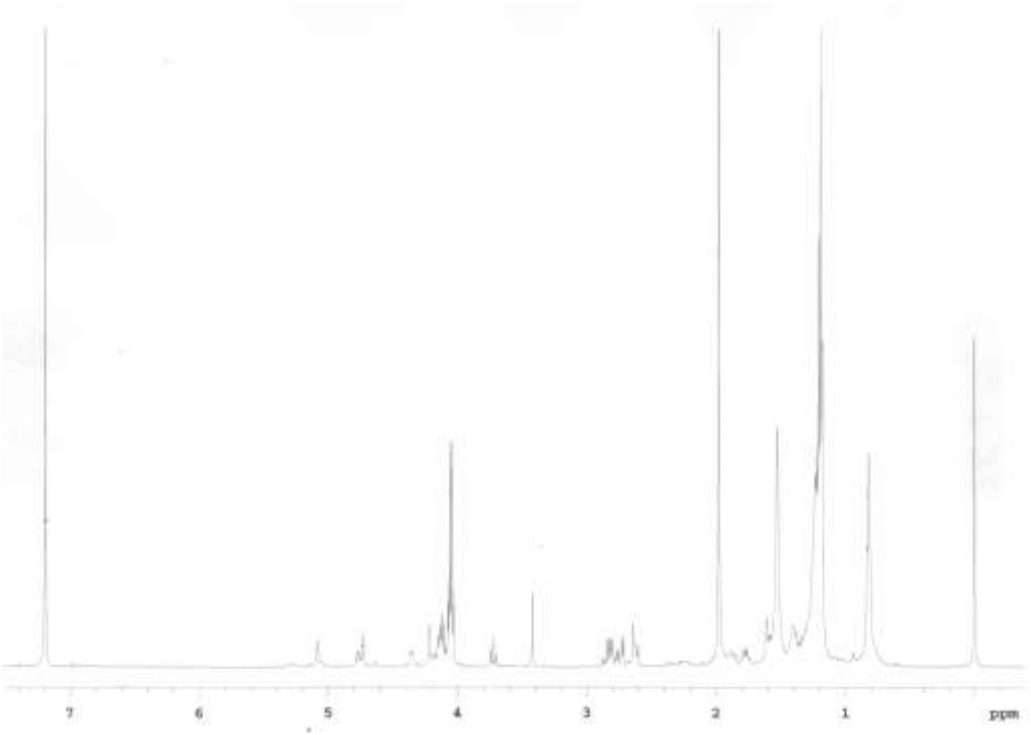

COSY spectrum (500MHz) of compound **44** in $CDCl_3$

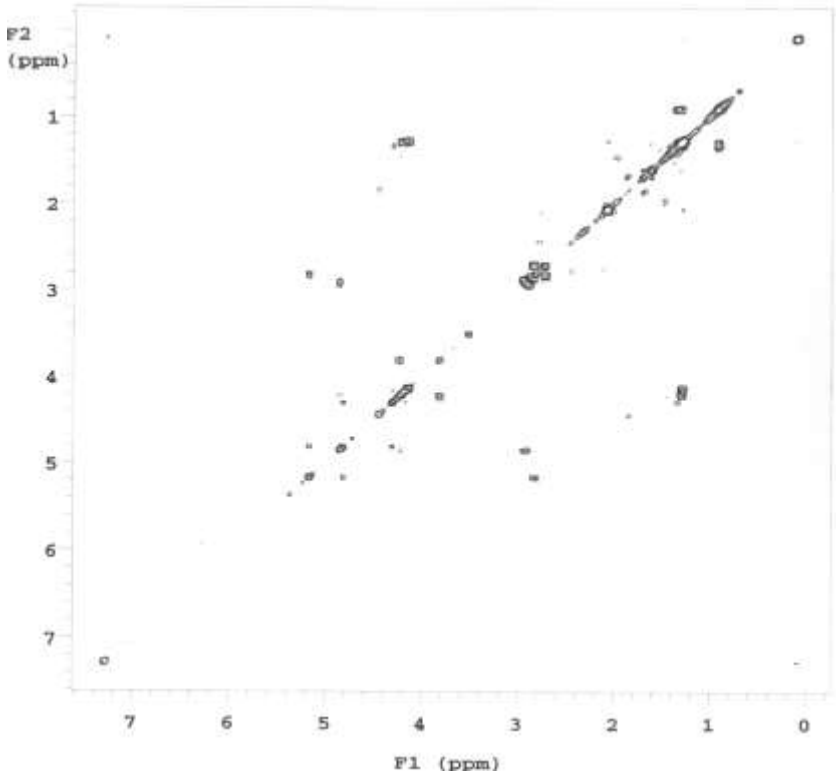

HMBC spectrum (500MHz) of compound **44** in $CDCl_3$

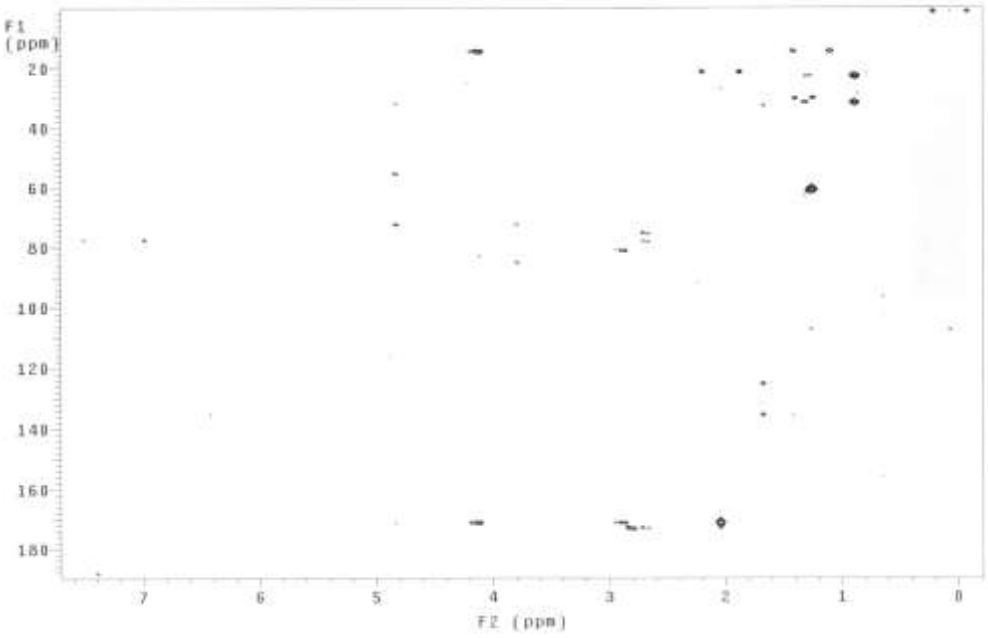

^{1}H NMR spectrum (500 MHz) (vinylic protons region) of aurantoic acid (**45**) in $CDCl_3$

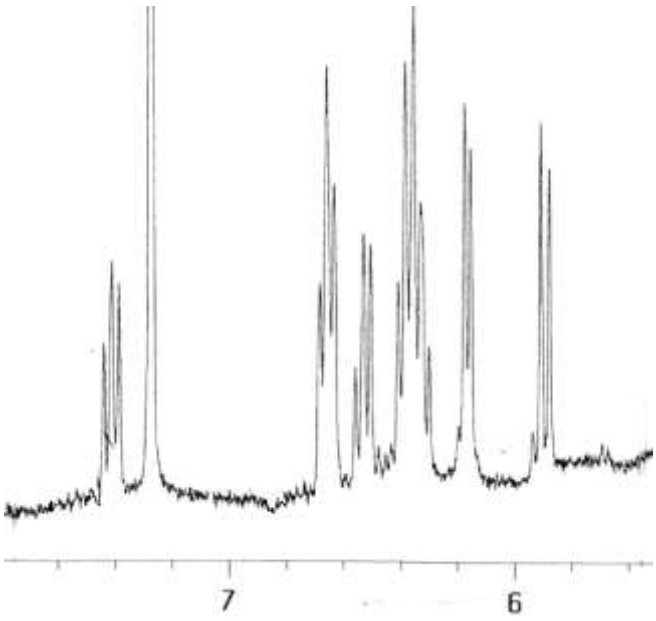

^{13}C NMR spectrum (500 MHz) of aurantoic acid (**45**) in $CDCl_3$

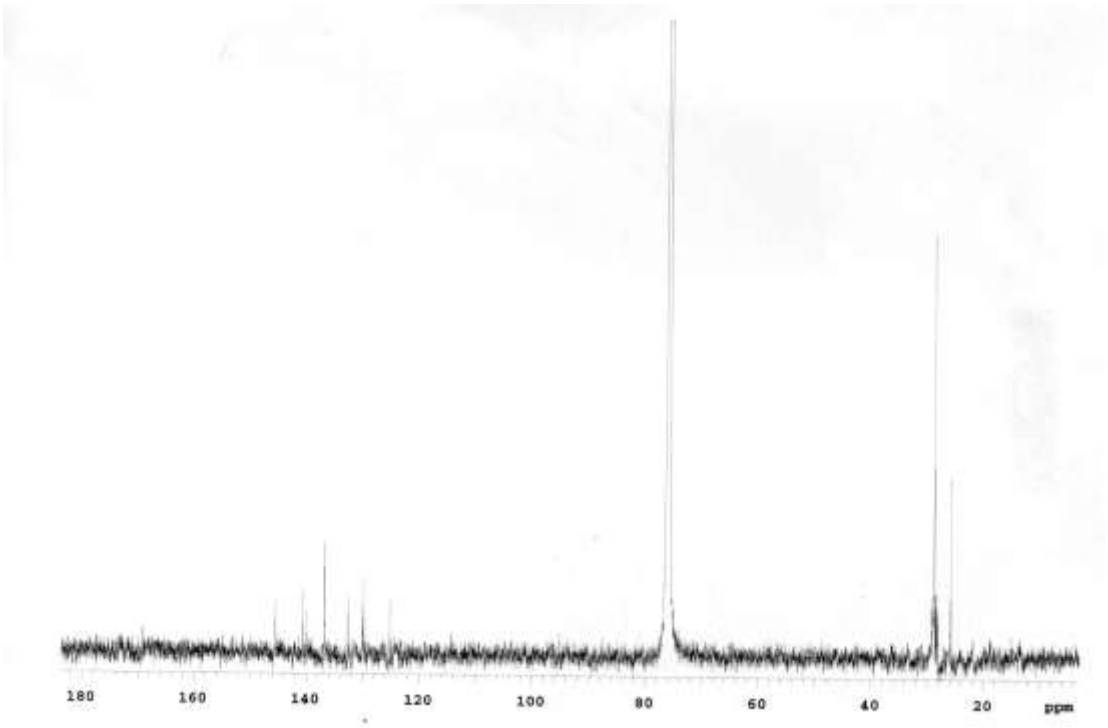

^{1}H NMR spectrum (700 MHz) of dehydroconicasterol (**46**) in $CDCl_3$

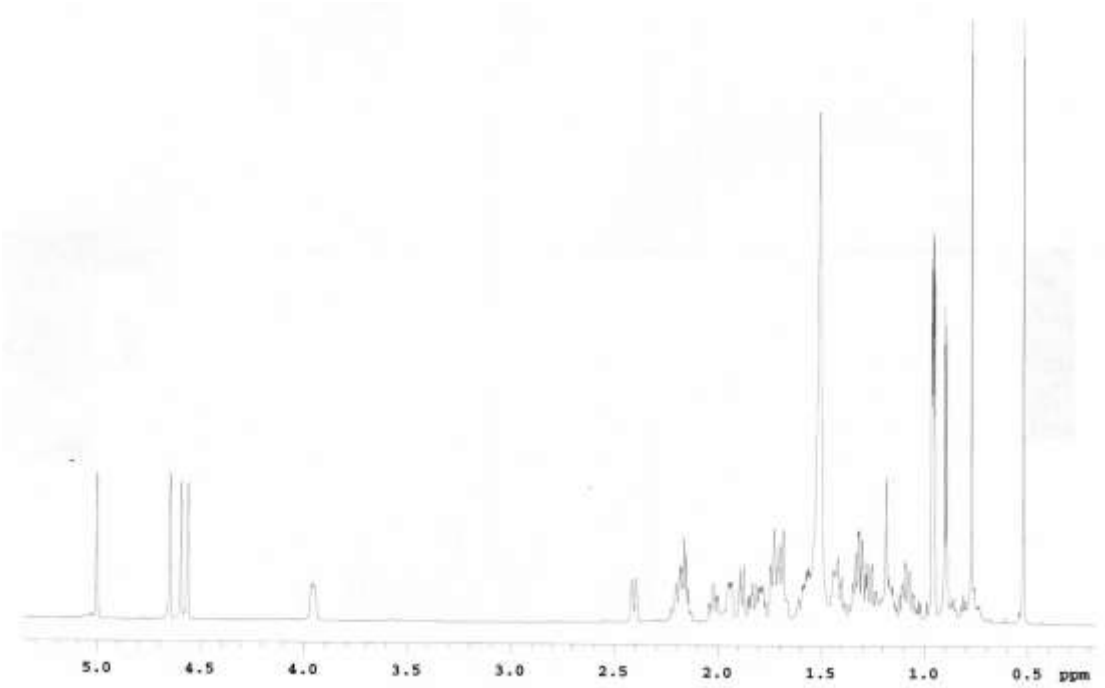

^{13}C NMR spectrum (500 MHz) of dehydroconicasterol (**46**) in $CDCl_3$

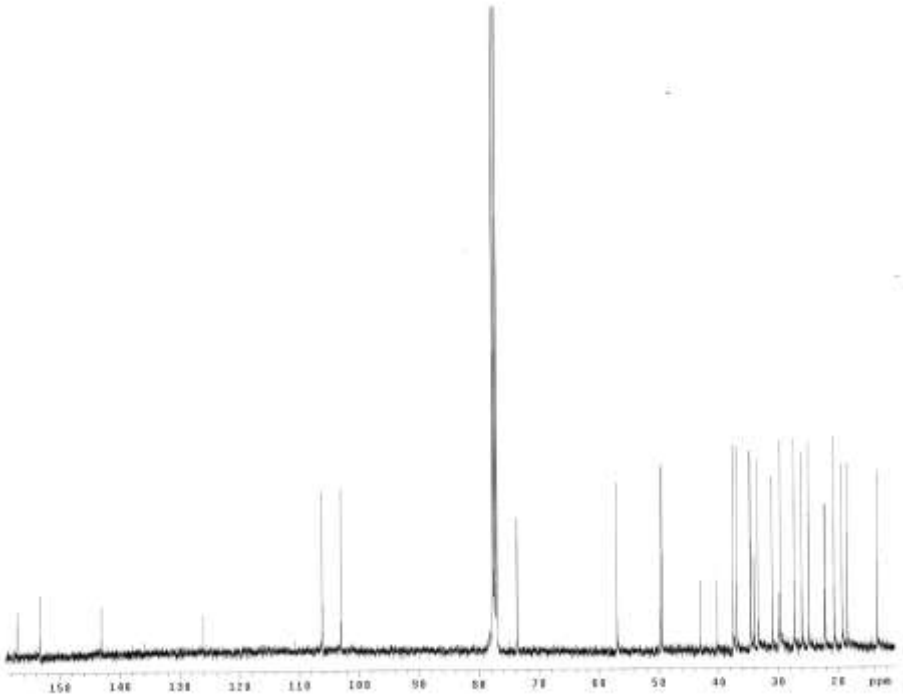

COSY spectrum (700 MHz) of dehydroconicasterol (**46**) in $CDCl_3$

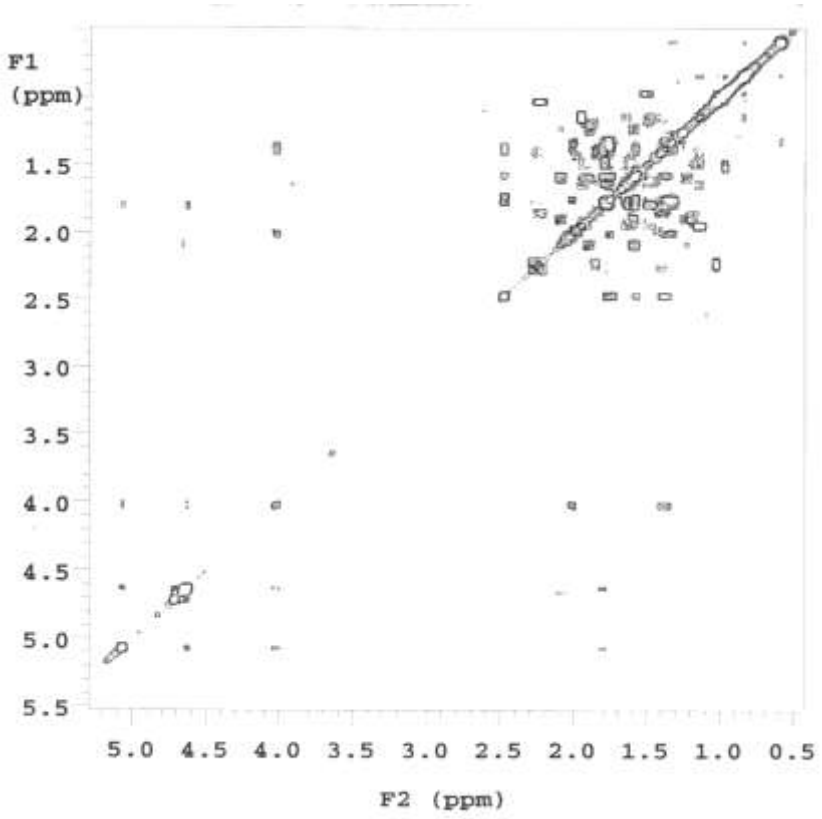

HMBC spectrum (700 MHz) of dehydroconicasterol (**46**) in $CDCl_3$

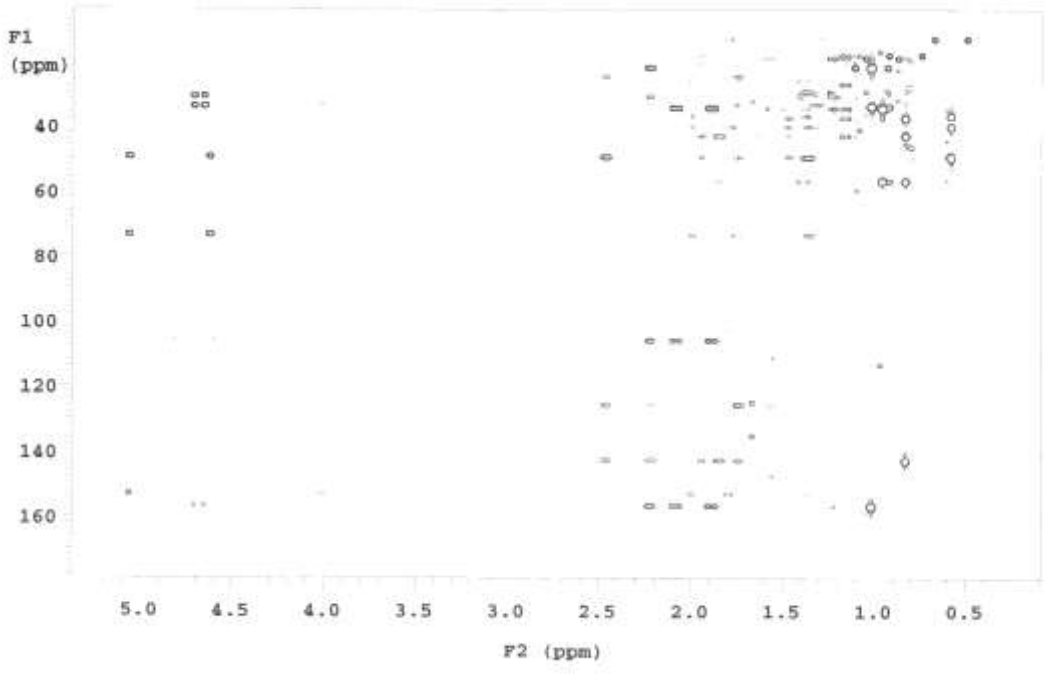

CHAPTER 7 - REFERENCES AND NOTES

(Papers published as result of the research carried out during the PhD course are in bold)

1. Fattorusso C., Campiani G., Catalanotti B., Persico M., Basilico N., Parapini S., Taramelli D., Campagnolo C., Fattorusso E., Romano A. and Tagliatatela-Scafati O.; *J. Med. Chem*. **2006,** *49,* 7088-7094.
2. Campagnolo C., Fattorusso E., Romano A., Tagliatatela-Scafati O., Basilico N., Parapini S., Taramelli D.; *Eur. J.Org. Chem*. **2005,** 5077-5083.
3. **Angawi RF., Calcinai B., Cerrano C., Dien H., Fattorusso E.,Scala F., Taglialatela Scafati O.; *J.Nat. Prod*., in press.**
4. Karplus M.; *J. Chem. Phys.*, **1959**, 11.
5. Dale, J.A., Mosher H.S.; *J. Am. Chem. Soc.*, **1968**, 3732.
6. Dale J.A., Dull D., Mosher H. S.; *J. Org. Chem.*, **1969**, 2543.
7. Matsumori N., Kaneno D., Murata, M.; *J. Org. Chem*, **1999**, 866.
8. Casteel D.A.; In *Burger's Medicinal Chemistry and Drug Discovery* 5; Wolff, M. E., Ed.; John Wiley and Sons, New York, **1997**; pp. 3-91.
9. Avery M.A., Chong W.K.M., Jennings-White C.; *J. Am. Chem. Soc*., **1992**, *114*, 974-9.
10. Cafieri F., Fattorusso E., Taglialatela-Scafati O., Ianaro, A.; *Tetrahedron,* **1999**, *55,* 7045-7056.
11. Fattorusso E., Parapini S., Campagnuolo C., Basilico N., Taglialatela-Scafati O., Taramelli D.; *J. Antimicrob. Chemother.,* **2002**, *50*, 883-888.
12. Yao G., Steliou K.; *Org. Lett.*, **2002**, *4*, 485-488.
13. Gochfeld D.J., Hamann M.T.; *J. Nat. Prod*., **2001**, *64*, 1477-1479.

14. Hu J., Gao H., Kelly M., Hamann M.T.; *Tetrahedron*, **2001**, *57*, 9379-9383.

15. Jimenez M.d.S., Garzon S.P., Rodriguez A.D.; *J. Nat. Prod.*, **2003**, *66*, 655-661. In this paper plakortides O and P were named plakortides M and N, respectively, but their names were later corrected.

16. Kobayashi M., Kondo K., Kitagawa I.; *Chem. Pharm. Bull*., **1993**, *41*, 1324-1326.

17. Murakami N., Kawanishi M., Itagaki S., Horii T., Kobayashi M.; *Bioorg. Med. Chem. Lett.*, **2002**, *12*, 69-72.

18. Murakami N., Kawanishi M., Mostaqul H.M., Li J., Itagaki S., Horii T., Kobayashi M.; *Bioorg. Med. Chem. Lett.*, **2003**, *13*, 4081-4084.

19. Quinoa E., Kho E., Manes L.V., Crews P.; *J. Org. Chem.*, **1986**, *51*, 4260-4264.

20. El Sayed K.A., Hamann M.T., Hashish N.E., Shier W.T., Kelly M., Khan A.; *J. Nat. Prod*., **2001**, *64*, 522-524.

21. Taglialatela-Scafati, O.; Fattorusso, E.; Romano, A.; Scala, F.; Barone, V.; Cimino, P.; Stendardo, E.; Catalanotti, B.; Persico, M.; Fattorusso C. *Org. Biomol. Chem*, in press; 2010, DOI: 10.1039/B918600J.

22. Jefford C.W.; *Curr. Med. Chem.,* **2001**, 15, 1803-1826 and references cited therein; Jefford C.W.; *Drug Discov. Today* **2007**, 12, 487-495; Robert A., Benoit-Vical F., Dechy-Cabaret O.; *Pure Appl. Chem.*, **2001**, 73, 1173–1188; Tang, Y., Dong, Y., Vennerstrom J.L.; *Med. Res. Rev*., **2004**, 24, 425-448.

23. Kannan, R., D. Sahal, D., Chauhan, V.S.; *Chem. Biol*., 2002; **9**, 321–332; b) Becker, K., Tilley R., Vennerstrom, J.L., Roberts,D., Rogerson, S., Ginsburg H.; *Int. J. Parasitol.,* **2004** , 34, 163-89.

24. O'Neill P. M., Posner G. H.;*J. Med. Chem.*, **2004**, 47, 2945-2964.

25. Arantes C., de Araujo M. T., Taranto A. G., Carneiro J.W.D.; *Int. J. Quantum Chem.*, **2005**, 103, 749-762; Drew M.G.B., Metcalfe J., Dascombe M., Ismail F.M.D.;, *J. Mol. Struct. (Theochem)*, **2007,** 823, 34–46.

26. Posner G. H., Wang D., Cumming J. N., Oh C. H., French A. N., Bodley A.L., Shapiro T. A.; *J. Med. Chem.*, **1995**, 38, 2273-2275.

27. Robert A., Dechy-Cabaret O., Cazelles J., Meunier B. ; *Acc. Chem. Res.*, **2002**, 35, 167-174.

28. Magri D.C., Workentin M.S.; *Chem. Eur. J.*, **2008**, 14, 1698-1709.

29. Donkers R.L., Workentin M.S.;*J. Phys. Chem. B*, **1998**, 102, 4061-4063; Donkers R. L., Workentin M.S.; *J. Am. Chem. Soc.,* **2004**, 126, 1688-1698.

30. Hu J.-F., Gao H.-F., Kelly M., Hamann M. T.; *Tetrahedron*, **2001**, 57, 9379-9383.

31. Haynes R.K., Vonwiller S. C.; *Tetrahedron Lett.*, **1996**, 37, 257-260.

32. Creek D.J., Chiu F.C.K., Prankerd R.J., Charman S.A., Charman W.N.; *J. Pharm. Sci.*, **2005**, 94, 1820-1829.

33. Posner G.H., Dowd H.; *Heterocycles,* **1998**, 47, 643-646.

34. Matsumori N., Kaneno D., Murata M., Nakamura H., Tachibana K.; *J. Org. Chem.*, **1999**, 64, 866-876.

35. Ciminiello P., Fattorusso E., Forino M., Poletti R.; *J. Org. Chem.*, **2001**, 66, 578-582.

36. Campagnuolo C., Fattorusso C., Fattorusso E., Ianaro A., Pisano B.,Taglialatela-Scafati O.; *Org. Lett.*, **2003**, 5, 673-676.

37. Campagnuolo C., Fattorusso C., Fattorusso E., Ianaro A., Pisano B., Taglialatela-Scafati O.; *Eur. J. Org. Chem.*, **2002,** 61-69.

38. Dalisay D.S., Quach T., Nicholas G.N., Molinski T. F.; *Angew. Chem. Intl. Ed.*, 48, 4367-4371.

39. Murakami N., Kawanishi M., Itagaki S., Horii T., Kobayashi M.; *Biorg. Med. Chem. Lett*. **2002**, 12, 69-72.

40. Murakami N., Kawanishi M., Itagaki S., Horii T., Kobayashi M.; *Bioorg. Med. Chem. Lett.*, **2004**, 14, 3513-3516.

41. Fattorusso, E.; Romano, A.; Taglialatela-Scafati, O.; Achmad, M. J.; Bavestrello, G.; Cerrano C. *Tetrahedron Letters*, **2008**, *49*, 2189-2192.

42. Fattorusso, E.; Romano, A.; Taglialatela-Scafati, O.; Achmad, M. J.; Bavestrello, G.; Cerrano C. *Tetrahedron*, **2008**, *64*, 3141-3146.

43. Kobayashi M., Kondo K., Kitagawa I.; *Chem. Pharm. Bull.*, **1993**, *41*, 1324-1326.

44. Ohtani I., Kusumi T., Kashman Y., Kakisawa H.; *J. Am. Chem. Soc*., **1991**, *113*, 4092-4096.

45. Ichiba T., Scheuer P.J., Kelly-Borges M.; *Tetrahedron*, **1995**, *51*, 12195-12202; see also corrigenda in *Tetrahedron*, **1996**, *52*, 14079.

46. Wegerski C. J., Hammond J., Tenney K., Matainaho T.; Crews, P. *J. Nat. Prod.*, **2007**, *70*, 89-94.

47. Freire F., Seco J. M., Quinoa E., Riguera R.; *J. Org. Chem.*, **2005**, *70*, 3778-3790.

48. Murakami N., Kawanishi M., Itagaki S., Horii T., Kobayashi M.; *Tetrahedron Lett.*, **2001**, *42*, 7281-7285.

49. Matsumoto M., Kondo K. ; *J. Org. Chem.,* **1975**, *40*, 2259-2260.

50. Clennan E.L., Mehrsheikh-Mohammadi M. E. ; *J. Am. Chem. Soc.*, **1983**, *105*, 5932-33.

51. Bobrowski M., Liwo A., Oldziej S., Jeziorek D., Ossowski T. ; *J. Am. Chem. Soc.*, **2000**, *122*, 8112-8119.

52. Matsumoto M., Kuroda K.; *Tetrahedron Lett.*, **1982**, *23*, 1285-1288.

53. Ragoussis N., Ragoussis V.; *J. Chem. Soc. Perkin Trans. I*, **1998**, 3529-3533.

54. Ragoussis V., Panopoulou M., Ragoussis N.; *J. Agric. Food Chem.*, **2004**, *52*, 5047-5051.

55. Robinson T. V., Taylor D.K., Tiekink E.R.T.; *J. Org. Chem.*, **2006**, *71*, 7236-7244.

56. Kepler J. A., Philip A., Lee Y.W., Morey M.C., Carroll F.I.; *J. Med. Chem.*, **1988**, *31*, 713-716.

57. Bloodworth A.J., Eggelte, H.J.; *J. Chem. Soc., Perkin Trans. 2*, **1984**, 2069-72.

58. Fattorusso E., Romano A., Taglialatela-Scafati O., Irace C., Maffettone C., Bavestrello G.;,Cerrano C.; *Tetrahedron*, **2009**, *65*, 2898-2904

59. Wegerski C. J., Hammond J., Tenney K., Matainaho C., Crews P.; *J. Nat. Prod*., **2007**, *70*, 89-94.

60. Matsunaga S., Fusetani N.; *J. Org. Chem*. **1995**, *60*, 1177–1181.

61. Hamada T., Matsunaga S., Yano G., Fusetani N.; *J. Am. Chem. Soc.* **2005**, *127*, 110–118.

62. Ford P. W., Gustafson K.R., McKee T.C., Shigematsu N., Maurizi L. K., Pannell L K., Williams D.E., de Silva E.D., Lassota P., Allen T.M.; van Soest R.W.M., Andersen R. J., Boyd M.R*J;. Am. Chem. Soc.* **1999**, *121*, 5899–5909.

63. (a) Carmely S., Kashman Y.; *Tetrahedron Lett.* **1985**, *26*, 511-514. (b) Kobayashi M., Tanaka J., Katori T., Kitagawa I.; *Tetrahedron Lett.* **1989**, *30*, 2963-2966.

64. Ratnayake A. S., Davis R.A., Harper M.K., Veltri C. A., Andjelic C.D., Barrows L.R., Ireland C.M.; *J. Nat. Prod*., **2005**, *68*, 104-107, and references cited therein.

65. Andrianasolo E.H., Gross H., Goeger D., Musafija-Girt M., McPhail K.P., Leal R.M., Mooberry S.L., Gerwick W.H.; *Org. Lett.* **2005**, *7*, 1375-1378.

66. Piel J., Hui D., Wen G., Buzke D., Platzer M., Fusetani N., Matsunaga S.; *Proc. Natl. Acad. Sci. U.S.A.* **2004**, *101*, 16222–16227

67. Cason J., Davis R., Sheehan M.H.; *J. Org. Chem*, **1971**, *36*, 2621-2625.

68. Sakemi S., Ichiba T., Kohmoto S., Saucy G., Higa T.; *J. Am. Chem. Soc.*, **1988**, *110*, 4851-4853.

69. Matsunaga S., Fusetani N., Kato Y.; *J. Am. Chem. Soc.*, **1991**, *113*, 9690-9692.

70. Kho E., Imagawa D.K., Rohmer M., Kashman Y., Djerassi C.; *J. Org. Chem.*, **1981**, *46*, 1836-1839.

71. Williams C.M., Mander L.N.; *Tetrahedron*, **2001**, *57*, 425-447.

72. Qureshi A., Faulkner D.J.; *J. Nat. Prod.*, **2000**, *63*, 841-842, and references cited therein.

73. On October 19th 2009, the database SciFinder® showed 68 entries reporting chemical studies with the isolation of new molecules from *Theonella swinhoei*.

74. Fattorusso, E.; Romano, A.; Scala, F.; Taglialatela-Scafati, O. *Molecules*, 2008, *13*, 1465-1471.

75. Costantino V., Fattorusso E., Menna M., Taglialatela-Scafati O.; *Curr. Med. Chem.*, **2004,** *11*, 1671-1692.

76. Laroche M., Imperatore C., Grozdanov L., Costantino V., Mangoni A., Hentschel U., Fattorusso E.; *Mar. Biol.*, **2007**, *151*, 1365-1373.

77. Costantino V., Fattorusso E., Mangoni A., Di Rosa M., Ianaro A.; *J. Am. Chem. Soc.*, **1997**, *119*, 12465-12470.

78. Costantino V., Fattorusso E., Mangoni A., Di Rosa M., Ianaro A.; *Bioorg. Med. Chem. Lett.,* **1999**, *9*, 271-276.

79. Cafieri F., Fattorusso E., Taglialatela-Scafati O., Ianaro A.; *Tetrahedron,* **1999**, *55*, 7045-7056.

80. Fattorusso E., Parapini S., Campagnuolo C., Basilico N., Taglialatela-Scafati O., Taramelli D.; *J. Antimicrob. Chemother*., **2002**, *50*, 883-888.

81. Campagnuolo C., Fattorusso E., Taglialatela-Scafati O. ; *Eur. J. Org. Chem*., **2003**, *2*, 284-287.

82. Borrelli F., Campagnuolo C., Capasso R., Fattorusso E., Taglialatela-Scafati O.; *Eur. J. Org. Chem*., **2004**, *15*, 3227-3232.

83. Campagnuolo C., Fattorusso C., Fattorusso E., Ianaro A., Pisano B., Taglialatela-Scafati O.; *Org. Lett.*, **2003**, *5*, 673-676.

84. Sciuto S., Chillemi R., Piattelli M.; *J. Nat. Prod.*, **1988**, *51*, 322-325.

85. Laville R., Thomas O.P., Berrue F., Reyes F., Amade P.; *Eur. J. Org. Chem.*, **2008**, 121-125.

86. Schmitz F.J., Hollenbeak K.H., Campbell D.C.; *J. Org. Chem.*, **1978**, *43*, 3916-3922.

87. Turk T., Frangez R., Sepcic K.; *Mar. Drugs*, **2007**, *5*, 157-167.

88. Kubanek J., Andersen R.J.; *Tetrahedron Lett.*, **1997**, *38*, 6327-6330.

89. Trager W., Jensen J.B.; *Science,* **1976**, *193*, 673-675.

90. Makler M., Hinrichs D.; *Am. J. Trop. Med. Hyg.*, **1993**, *48*, 205-210.

91. Parapini S., Basilico N., Mondani M., Olliaro P., Taramelli D., Monti D.; *FEBS Lett.*, **2004**, *575*, 91-94.